チョウの色模様形成に関する分子生理学的研究

Doctoral Thesis of Philosophy

Molecular physiological studies on butterfly wing color pattern formation

September 2013

by

Bidur Dhungel

Marine and Environmental Science

Graduate School of Engineering and Science

University of the Ryukyus

Doctoral Thesis of Philosophy

Molecular physiological studies on butterfly wing color pattern formation

September 2013

by

Bidur Dhungel

A dissertation submitted to the Graduate School of
Engineering and Science, University of the Ryukyus,
in partial fulfillment of the requirements for the degree of

Doctor of Philosophy

Marine and Environmental Science
Graduate School of Engineering and Science
University of the Ryukyus

Supervisor: Associate Professor Joji Otaki

We, the undersigned, hereby, declare that we have read this thesis and we have attended the thesis defense and evaluation meeting. Therefore, we certify that, to the best of our knowledge this thesis is satisfactory to the scope and quality as a thesis for the degree of Doctor of Philosophy under Marine and Environmental Science, Graduate School of Engineering and Science, University of the Ryukyus.

THESIS REVIEW & EVALUATION COMMITTEE MEMBERS

(**Chairman) Joji Otaki**

(**Committee) Soichi Nakamura**

(**Committee) Akihiro Takemura**

Abstract

Butterfly wings provide excellent materials for pattern formation and diversification study. Butterfly wings are composed of pattern elements that are idealized in the "nymphalid ground plan", and study of these element formation and diversification aids in the actual study of pattern formation and diversification.

Among the elements on butterfly wings, concentric rings of colored scales, eyespots, are widely studied elements. Immunohistochemistry and *in situ* hybridization studies showed a number of genes expressed in and around the presumptive focus during eyespot development. In the absence of reliable and reproducible functional assay system, the functional evidence of the candidate genes has been lacking. Several methods to transfer and express a foreign gene in butterfly wings have been reported, but they were suffering from low success rates or lower expression levels. I here developed a functional assay system using the blue pansy butterfly *Junonia orithya*. I obtained the successful expression of foreign gene *GFP* (Green fluorescence protein) in *J. orithya w*ith baculovirus injection followed by anti-gp64 antibody injection. The expression pattern of candidate gene *Distal-less* (*Dll)* at the center of the eyespot and later again at scale building cells around foci of the eyespot implicates its role in eyespot formation. However, the ectopic expression of *Dll* using baculovirus gene delivery tool did not produce any ectopic eyespot. I conclude that the expression of *Dll* is not sufficient for eyespot formation. Nevertheless, the baculovirus tool can be an invaluable tool to transfer, express, and functionally examine foreign genes in butterfly wings.

On the other hand, the DNA polymorphism in one of the candidate gene *Dll* is linked with eyespot size variation in *Bicyclus anynana*. Using *J. orithya*, I compared *Dll* cDNA sequence variations on one side of the wing with color pattern on the other side from the identical individual, as the butterfly has the identical wing color pattern on both sides. I found three different types of *Dll* variants in *J. orithya* wing however no clear relationship between *Dll* sequence and eyespot variation was observed. In the future, with the *in situ* hybridization technique, the precise location of the individual *Dll* variants can be traced and the molecular basis of morphological variation can be established.

To establish a standard rearing method, we reported various artificial diets for *J. orithya*. The modified Insecta F-II diet was used for rearing *J. orithya* larvae. Interestingly I

found, three diets AD-FZMUV, AD-FZM and AD-FBY produced homeotic transformed adults and diet AD-FBY kept larvae at longer time at an earlier stage. The modified artificial diet Insecta F-II was used to feed pharmacological agent sodium tungstate to compare with low temperature treatment, whether it can induce hardiness against tungstate and cold-shock treatment in terms of TS-type modification and fall-morph. The low temperature experience, but not consumption of tungstate during the larval stage, induced hardiness against cold-shock or tungstate treatment. Low temperature treatment at larval stage provided immunity against cold shock or tungstate treatment. Therefore, I speculate that the cold-shock or tungstate induced color-pattern pathway has a physiological relationship with the fall-morph-inducing pathway. The use of artificial diets can increase the use of a particular organism for experimental use.

In addition, using three nymphalid butterflies, *J. orithya*, *Vanessa cardui*, and *Danaus chrysippus*, the mechanism of tissue size determination during morphogenesis was studied by counting and measuring all the scales on one of the compartment of the wing. I found that, the butterfly wing tissue size is determined primarily by the number of scale cells and then by the size change of scale cells before or during the period of row arrangement. The putative morphogen signal is likely a ploidy signal that determined cell size and scale size. It also likely determines scale coloration and shape.

In summary, based on the current knowledge, I proposed an integrated model for the wing color pattern formation and modification.

Author's publication list

1) **Dhungel, B.,** Otaki J.M. (2009) Local pharmacological effects of tungstate on the color pattern determination of butterfly wings: a possible relationship between the eyespot and parafocal element. Zoological Science, 26, 758-764.

2) **Dhungel, B.,** Ohno, Y., Matayoshi, R., Otaki, J.M. (2013) Baculovirus-mediated gene transfer in butterfly wings *in vivo*: an efficient expression system with anti-gp64 antibody. BMC Biotechnology, 13, 27.

3) **Dhungel, B.,** Otaki, J.M. (2013) Morphometric analysis of nymphalid butterfly wings: number, size, and arrangement of scales, and their implications for tissue-size determination. Entomological Science. Advance online publication. doi: 10. 1111/ens. 12046.

4) **Dhungel, B.,** Otaki, J.M. (2013) Larval temperature experiences determines sensitivity to cold-shock-induced wing color pattern changes in the blue pansy butterfly *Junonia orithya*. Journal of Thermal Biology, 38, 427-433.

Acknowledgements

The writing of this thesis has been one of the most significant academic challenges. Without the support, patience and guidance of the following people, this study would not have been completed. It is to them that I owe my deepest gratitude.

First of all, I would like to express my gratitude to my research supervisor Associate Professor Joji Otaki whose inspiration, encouragement, valuable guidance, suggestions and support from the initial to the final level enabled me to develop this thesis. His trust, patient, and understanding have truly helped me to bring out this study in its current shape without which this work would not have seen the daylight.

I would also like to thank my committee members Professor Soichi Nakamura and Professor Akihiro Takemura for their analytical reading of the whole thesis and valuable suggestion.

I gratefully acknowledge the Ministry of Education, Culture, Sports, Science and Technology (MEXT) for providing funding to do my research in Japan. I would also like to express my immense pleasure and sincere gratitude to Faculty of Science, University of the Ryukyus for providing me the facilities for the smooth completion of my research.

I am very much thankful and indebted to all the members of BCPH unit of Molecular Physiology lab.

At last, but not least, my deepest and heartiest gratitude goes to my parents, sisters and brothers, relatives and friends for their love, support and encouragement to achieve this success.

Table of Contents

List of Figures

NO **Title** **Page**

List of Tables

NO **Title** **Page**

Chapter 1

General Introduction

1.1 The Nymphalid Groundplan

Butterfly wings are rich sources for pattern studies. The study of butterfly wing color pattern elements in general will help in understanding pattern development and evolution. The butterfly wing color pattern is a meeting point for development and evolutionary biology. The developmental biologists are interested in mechanisms of development of patterning elements and their diversifications are of interest to evolutionary biologist. Based on earlier work comparative data on wing patterns among Nymphalid butterflies, Nijhout (1990, 1991, 2001) proposed a general theme for wing color patterns and revised by Otaki (2012a). This ground plan is based on Nymphalid butterflies and can be useful in studying wing color patterns in other non-Nymphalid butterflies as well. This ground-plan is an ideal color pattern, and it cannot be applied to all real butterflies, but is helpful in studying wing color patterns of butterfly and moths.

The nymphalid groundplan can be broadly divided into symmetry systems running from anterior to posterior margin of the wing, namely wing root system towards the base, basal symmetry system, the central symmetry system is at the center of the wing, border symmetry system, and marginal band system towards the outer margin of the wing. The wing root band is independent from basal symmetry system, and marginal and submarginal bands are like a single system referred as the "marginal band system". Each symmetry system is composed of elements. Elements such as the discal spot, eyespots, parafocal element (PFE), marginal and submarginal bands and their size, shape, color and position on the wings are characteristic for each species. The central and basal symmetry system also has circular elements like eyespots and their developmental mechanism are similar to those of border symmetry system. The white bands are produced as a result of light colored space between the two symmetry systems. The butterfly wing color pattern is composed of elements on backgrounds. The real butterfly wing color pattern is supposed to be modified from these groundplan by changes in shape, size, color and position of elements in the overall wing in a systemic way. The overall study of element formation and evolution is the study of pattern development and evolution.

1.2 Wing color pattern origin

The scales are the basic unit of butterfly wings. Each scale has a color and final color pattern is the arrangement of these colored scales. The final color of the scale depends on the presence of chemical pigments. With the help of biochemical techniques, the molecular nature of these pigments is already known. The major types of pigments are melanin, ommochromes, pterins, and flavonoids (Nijhout, 1991). The melanin is derived from tyrosine amino acid and responsible for black, brown, tan, or

reddish brown. The ommochromes are derived from tryptophan and responsible for colors ranging from red to brown or yellow over red and brown to black. The pterins are derived from guanosine triphosphate and are responsible for yellow to red colors. The flavonoids are responsible for yellow or white color.

1.3. Molecular findings, gene mapping and genetic manipulation in butterfly wing pattern study

Using *in situ hybridization* and antibody staining, butterfly wing was studied for genes expressed in the developmental pathways that are involved in wing patterning (Carroll *et al*., 1994; Brakefield *et al*., 1996; Keys *et al*., 1999; Brunetti *et al*., 2001; Reed *et al*., 2004; Monteiro *et al*., 2006; Weatherbee *et al*., 1999; Saenko *et al*., 2011; Oliver *et al*., 2012; Shirai *et al*., 2012).

In an attempt to study linking between genotype with phenotype using butterflies, gene mapping has provided excellent help (Beldade *et al*., 2002). The search of the polymorphic gene in the genome and finally their segregation with various phenotypes can be examined. The search of the polymorphic gene could be one of the candidate genes revealed by gene expression pattern, or more appropriate one will be the genome wide searches and construction of linkage maps for various butterfly species.

The ability to manipulate genes whose expression pattern has been revealed will definitely help in understanding their involvement in wing pattern formation. There are several methods for genetic manipulation such as RNA interference, morpholinos and viral ectopic expression vectors. The viral ectopic expression vector is used in the butterfly pattern study with some success. In butterfly, Sindbis (Lewis *et al*., 1999) and vaccinia virus (Lewis *et al*., 2006) have been used in genetic manipulation and has limited success. For further research, search of the other virus system such as baculovirus or germ-line transformation will help in genetic manipulation of butterfly genes and wing color pattern study.

1.4. Wing color pattern formation

The color pattern formation can be divided into four sequential steps: signaling, reception, interpretation and expression. In normal wing color pattern formation, signals originate from organizing center and are received, interpreted, and expressed by nearby cells. For normal color pattern production, reception step starts once the signaling step is fully settled and gradient of the signal is established (Otaki, 2008).

The eyespot formation is determined in four sequential steps (Brakefield *et al*., 1996). The center of the eyespot or prospective focus acts as an organizing center, which releases a putative morphogen for color pattern determinations (Nijhout, 1980). Although the final color pattern is seen at adult stage

of the butterfly. However, the beginning of the color pattern begins in the mid-fifth instars larvae in an imaginal wing disc. The regulatory genes such as *Distal-less* (*Dll*) expression are seen at the wing margin that elongates towards the center of each subdivision (Carroll *et al*., 1994; Monteiro *et al*., 2006). Then foci are determined in particular wing subdivision at the end of the final stage of larvae. In early pupae, the morphogenic signals from the prospective foci are emitted and determine the fate of the nearby cells. In late pupal stage, the surrounding cells around foci differentiate into various colored scales according to the morphogenic signals they receive from the foci. Each scale synthesizes a single color pigment (Nijhhout, 1991) and form fully developed adult color pattern. The wing color pattern determination and pigment synthesis begin from pre-pupal and pupal stage and final color pattern is seen on the final day of eclosion (Koch *et al*., 1998, 2000).

There are various theoretical models to explain the wing color pattern formation in butterflies, such as the classical morphogen gradient model (Nijhout, 1978, 1981), heterochronic uncoupling model (Otaki, 2008), two morphogens model (Dhungel and Otaki, 2009), wave model (Otaki, 2008) and induction model. The induction model can explain most cases of butterfly wing color pattern (Otaki, 2011b, c; Otaki 2012 a, b) and further supported by mathematical modeling (Otaki, 2012b). However, uniform decelerated motion for long range signals are not known to developmental biologist yet and it also does not account for the molecular nature of the signals and receptors. However, the induction model is still a good model to explain most cases of butterfly wing color patterns.

1.5. Wing formation: Cell growth and cell proliferation

Genes and environment control organism's body size. Many organisms' traits are also isometric to the body size (Raff, 1996; Colon and Raff, 1999). The building blocks of each trait are the basic unit of life, i.e., cells. During development to maintain isometric structures, the cells get bigger (cell growth) or increase in number (cell proliferation).

In butterflies, wing size depends upon the adult body size. The main driving factor, either scales getting bigger or greater in number for maintaining isometric structure is still unclear. Furthermore, even in a single wing the shapes and sizes differ dependent upon the position of the scales in a wing and could be influenced by positional information from organizing centers (Kusaba and Otaki, 2009).

1.6 Temperature and chemical effects on butterflies

The butterfly wing color pattern can be changed by cold-shock application, and similar kind of effect has been also found with chemical injection of sodium tungstate. Both generate similar kinds of modifications of wing color patterns (Nijhout, 1984; Otaki and Yamamoto, 2004; Otaki *et al*, 2005; Otaki, 2008 Dhungel and Otaki, 2010; Mahdi et al., 2010, 2011; Hiyama *et al*, 2012). Therefore, the

changes are system's character rather than the character of each treatment. Tungstate is believed to be a chemical mimic of putative cold shock hormone (CSH). In color pattern determination, cold shock hormone and the tungstate might work as an inhibitor of a phophatase in a signal transduction pathway (Otaki, 1998).

These physiologically induced color patter changes can be interpreted as cases of phenotypic plasticity of the treated organism. The modification patterns are termed as TS type modification and follow two basic transformation principles, size change and positional changes (Otaki, 2008). The modification generated these physiological changes can be helpful in deciphering developmental determination and evolutionary diversification of the butterfly wing color patterns.

With the temperature (also photoperiod), there is another kind of phenotypic plasticity observed in butterflies known as seasonal polyphenism. *Arashnia levana, Precis octavia, B. anynana,* and, *J. orithya* show seasonal polyphenism. In seasonal polyphenism, for a given genotype depending upon temperature and photoperiod that were experienced during larval development, different phenotypes are produced and are regulated by ecdysteroid hormones (Koch and Bückmann, 1987; Rountree and Nijhout, 1995a; Nijhout, 1991, 1994; Koch *et al*, 1996). Furthermore, summer-morph-producing hormone (SMPH) also controls seasonal polyphenism in *Polygonia c-aureum* (Endo *et al*., 1988, 1990; Tanaka *et al*., 1997). These phenotypes provide excellent materials for studying interaction among development, gene expression, pigment synthesis, and environmental conditions.

Methodologically, the introduction of foreign materials such as tungstate to butterflies can be at pupal stage with a simple injection with a microsyringe (Otaki 1998, 2003, 2007; Otaki and Yamamoto 2004; Umebachi and Osanai, 2003; Otaki et al., 2005; Serfas and Carroll, 2005) or with the sandwich method (Dhungel and Otaki, 2010). But for the early introduction of chemicals, larvae have to be fed with artificial diet. Introduction of foreign materials is much easier with artificial diet compared with natural host plant leaves. However, artificial diet for few butterflies has only been reported such as *J. orithya* (Hirai *et al*., 2011), *J. coenia* (Bowers, 1984), *B. anynana* (Holloway, 1991), *Z. maha* (Hiyama *et al*., 2010). The use of artificial diet increases the horizon for the experimental use of a particular species. Many chemicals that might have an effect on the wing color pattern can be scanned with artificial diets and indirectly will aid in studies on butterfly wing color pattern development and evolution.

1.7. Significance of wing color pattern modifications

Butterfly wing color patterns have ecological or biological functions or no significant function. Regarding the ecological function, the ambiguous visual signals are used for predator avoidance. Camouflage and mimicry are examples showing the interaction of wing color patterns with nature.

Camouflage and mimicry help in butterfly survival in presence of predators (Jiggins *et al*., 2001). Furthermore, mimicry is an example of adaptive evolution and is also associated with speciation. Environmental factors such as temperature can act as a pressure of natural selection. Color patterns are more adaptive in presence of visually hunting predators that hunt animals for their wing color. These color patterns adaptive traits together with other adaptive traits might move a population towards forming a new species.

In nature, butterfly wing color pattern also has behavioral functions like mate selection and species recognition (Mallet *et al*., 1998; Kronforst *et al*., 2006). Clear visual signals are used for species recognition and mate selection (Oliver et al., 2009). The plasticity in mating behavior by changing in sex roles between males and females has been seen in butterfly *B. anynana* when the larvae were reared at different temperatures (Prudic *et al*., 2011). Furthermore, temperature induced modified phenotypes have been reproduced in the laboratory physiologically and genetically (Hiyama *et al*., 2010).

Physiologically and genetically induced butterfly color pattern is important in generating new color pattern in butterfly biology as well as in studies of experimental and theoretical pattern formation in biology (Nijhout, 1991; Nijhout *et al*., 2003; Otaki, 2008). The elemental changes in pattern elements of butterflies may collaborate with the process of species recognition, sexual and natural selection, mate choice, visual signaling, mimicry and camouflage. The color pattern modification induced by physiological changes could reveal significant information about development mechanism and diversification of butterfly wing color pattern.

1.8. Objective of the thesis

An eyespot has been widely studied in wing color pattern formation with surgical manipulation (Nijhout, 1991; Brakefield *et al*., 1995; French et al., 1995; Otaki *et al*., 2005; Otaki, 2011a), physiological treatments (Otaki, 2008), *in situ* hybridization histochemistry or immunohistochemistry (Carroll *et al*., 1994; Brakefield *et al*., 1996; Keys *et al*., 1999; Brunetti et al., 2001; Monteiro *et al*., 2006; Oliver et al., 2012; Shirai *et al*., 2012; Saenko *et al*., 2011), and morphological color pattern analysis (Kodandaramaiah, 2009; Otaki, 2011b; Otaki, 2011c). Gene expression studies have already revealed a series of candidate genes in eyespot development (Carroll *et al*., 1994; Brakefield *et al*., 1996; Keys *et al*., 1999; Brunetti *et al*., 2001; Monteiro *et al*., 2006; Oliver *et al*., 2012; Shirai *et al*., 2012; Saenko *et al*., 2011). However, because of lack of reliable and reproducible genetic manipulation system for functional study of genes, the function of these candidate genes remains elusive. Sindbis virus (Lewis *et al*., 1999) and vaccinia virus (Lewis *et al*., 2006) has been used in ectopic expression study in the wing color pattern study without much success. In chapter 2, a

baculovirus system was developed and showed the expression of reporter gene *GFP* on the wings of butterflies.

Among candidate regulatory genes, *Distal-less notch, engrailed, hedgehog, cubitus interruptus, patched,* and *spalt* expressed at prospective eyespot, the expression pattern of gene *Dll* is unique. Initially at the wing margin then at the center of the eyespot and finally around foci in a subset of epidermal cells, the scale building cells (Carroll *et al*., 1994; Brunetti *et al*., 2001; Monteiro et al., 2006). The expression pattern implicates its role in eyespot formation. However, without functional assay only the expression can neither prove nor deny *Dll'*s role in eyespot development. In Chapter 3, using a recently developed baculovirus tool, *Dll* gene was expressed ectopically.

Furthermore, the linkage between genotype with phenotype has been studied with model butterfly organism *B. anynana*. DNA polymorphism in *Dll*, one of the candidate genes related to eyespot development, has been studied. DNA polymorphism in *Dll* gene has been linked with various eyespot sizes (Beldade *et al*., 2002). The different eyespot sizes might be due to variation in *Dll* variation. We focused on variation of *Dll* sequence and observed the variation in phenotype in Chapter 4.

Butterfly wings are composed of scales. Different adult wing sizes can be achieved by either increasing the number of scales, or increasing sizes of scales, but the precise mechanism is not known till now. In this chapter 5, we tried to find the mechanism behind the tissue size determination. Furthermore, we also discussed the nature of putative morphogenic signal determining cell size, scale size, scale coloration and shape. In this particular chapter, three different species of nymphalid butterflies, *J. orithya*, *Vanessa cardui*, and *Danus chrysippus* were used.

Artificial diets have been already reported for few butterflies such as *J. orithya* (Hirai *et al*., 2011), *Junonia coenia* (Bowers, 1984), *Bicyclus anynana* (Holloway, 1991), *Z. maha* (Hiyama *et al*., 2010). We showed the use of artificial diet not only to standardize the laboratory conditions but also to study the wing color pattern formation. The use of artificial diet increases the horizon for the experimental use of a particular species. We prepared artificial diet for *J. orithya* in chapter 6. We found artificial diet AD-FZMUV, AD-FZM, and AD-FB produced homeotically transformed butterfly wings. Furthermore, diet AD-FBY was able to keep larvae at an earlier stage for longer time without growth. Finally, we modified artificial diet Insecta F-II that could be used in rearing *J. orithya* larvae for at least more than a week.

Using modified artificial diet Insecta F-II and physiological tools such as cold shock and tungstate, we studied physiological relationship between pathways that produce TS type modification (Nijhout, 1984; Otaki and Yamamoto, 2004; Otaki *et al*., 2005; Otaki, 2008 Dhungel and Otaki, 2010;

Mahdi *et al*., 2010, 2011; Hiyama *et al*., 2012) and seasonal polyphenism (Koch and Bückmann, 1987; Rountree and Nijhout, 1995; Nijhout, 1991, 1994; Koch *et al*., 1996) in butterfly in chapter 7.

The blue pansy butterfly *J. orithya* is abundant in Okinawa Island and has a very simple wing color pattern. Using three different species of nymphalid butterflies, mostly *J. orithya*, *Vanessa cardui*, and *Danus chrysippus*, butterfly wing color pattern formation was studied and summarized in this thesis. Finally, I incorporated finding in those studies with finding in other butterfly color pattern formation studies.

1.9. References

Beldade P, Brakefield PM, Long AD: Contribution of Distal-less to quantitative variation in butterfly eyespots. Nature 2002, 415: 315-318.

Bowers MD: Iridoid glycosides and host-plant specificity in larvae of the buckeye butterfly, *Junonia coenia* (Nymphalidae). Journal of Chemical Ecology 1984, 10: 11.

Brakefield PM, French V: Eyespot development on butterfly wings: the epidermal response to damage. Developmental Biology 1995, 168: 98-111.

French V, Brakefield PM: Eyespot development on butterfly wings: the focal signal. Developmental Biology 1995, 116: 103-109.

Brakefield PM, Gates J, Keys D, Kesbeke F, Wijngaarden PJ, Monteiro A, French V, Carroll SB: Development, plasticity and evolution of butterfly eyespot patterns. Nature 1996, 384:236-242.

Brunetti CR, Selegue JE, Monteiro A, French V, Brakefield PM, Carroll SB: The generation and diversification of butterfly eyespot color patterns. Current Biology 2001, 11:1578-1585.

Carroll SB, Gates J, Keys DN, Paddock SW, Panganiban GE, Selegue JE, Williams JA: Pattern formation and eyespots determination in butterfly wings. Science 1994, 265:109-114.

Conlon I, Raff M: Size control in animal development. Cell 1999, 96: 235-244.

Dhungel B, Otaki JM: Local pharmacological effects of tungstate on the color pattern determination of butterfly wings: a possible relationship between the eyespot and parafocal element. Zoological Science 2010, 26: 758-74.

Endo K, Masaki T, Kumagai K: Neuroendocrine regulation of the development of seasonal morphs in the Asian comma butterfly, *Polygonia c-aureum L.*: Difference in activity of summer-morph-

producing hormone from brain extracts of the long-day and short-day pupae. Zoological Science 1988, 5: 145-152.

Hirai N, Tanikawa T, Ishii M: Development, seasonal polyphenism and cold hardiness of the blue pansy, *Junonia orithya orithya* (Lepidoptera, Nymphalidae). Lepidoptera Science 2011, 62: 57-63.

Hiyama A, Iwata M, Otaki JM: Rearing the pale blue *Zizeeria maha* (Lepidoptera, Lycaenidae): Toward the establishment of a lycaenid model system for butterfly physiology and genetics. Entomological Science 2010, 13: 293-302.

Hiyama A, Taira W, Otaki JM: Color pattern evolution in response to environmental stress in butterflies. Frontiers in Genetics 2012, 3: 15.

Holloway GJ, Brakefield PM, Kofman S, Windig JJ: An artificial diet for butterflies, including *Bicyclus* species, and its effects on development period, weight and wing pattern. The journal of Research on the Lepidoptera 1991, 30: 121-128.

Jiggins CD, Naisbit RE, Coe RL, Mallet J: Reproductive isolation caused by color pattern mimicry. Nature 2001, 411: 302-305.

Keys DN, Lewis DL, Selegue JE, Pearson BJ, Goodrich LV, Johnson RL, Gates J, Scott MP, Carroll SB: Recruitment of a hedgehog regulatory circuit in butterfly eyespots evolution. Science 1999, 283:532-534.

Koch PB, Bückmann D: Hormonal control of seasonal morphs by the timing of ecdysteroid release in *Araschnia levana L*. (Nymphalidae: Lepidoptera). Journal of Insect Physiology 1987, 33: 823-829.

Koch PB, Brakefield, PM, Kesbeke F: Ecdysteroids control eyespot size and wing color pattern in the polyphonic butterfly *Bicyclus anynana* (Lepidoptera: Satyridae). Journal of Insect Physiology 1996, 42: 223-230.

Koch PB, Keys DN, Rocheleau T, Aronstein K, Blackburn M, Carroll SB, ffrench-Constant RH: Regulation of dopa decarboxylase expression during colour patten formation in wild-type and melanic tiger swallowtail butterflies. Development 1998, 125: 2303-2313.

Koch PB, Lorenz U, Brakefield PM, ffrench-Constant RH: Butterfly wing pattern mutants: development; heterochrony and co-ordinately regulated phenotypes. Development Genes and Evolution 2000, 210: 536-554.

Kronforst MR, Young LG, Kapan DD, McNeely C, O'Neil RJ, Gilbert LE: Linkage of butterfly mate preference and wing color preference cue at the genomic location of wingless. Proceeding of the National Academy of Sciences USA 2006, 103: 6575-6580.

Kusaba K, Otaki JM: Positional dependence of scale size and shape in butterfly wings: Wing-wide phenotypic coordination of colour-pattern elements and background. Journal of Insect Physiology 2009, 55: 174-182.

Mallet J, McMillan WO, Jiggins CD: *Mimicry and warning color at the boundary between races and species. In Endless Forms: Species and Speciation (eds. Howard DJ, Berlocher SH)pp 390-403* New York, USA: Oxford University press, 1998a.

Mallet J, McMillan WO, Jiggins CD: Estimating the mating behavior of a pair of hybridizing *Heliconius* species in the wild. Evolution 1998b, 52:503-510.

Monteiro A, Glaser G, Stockslager S, Glansdrops N, Ramos D: Comparative insights into questions of lepidopteran wing pattern homology. BMC Developmental Biology 2006, 6:52.

Lewis DL, Brunetti CR: Ectopic transgene expression in butterfly imaginal wing disc using vaccinia virus. Biotechniques 2006, 40:48-54.

Lewis DL, DeCamillis MA, Brunetti CR, Halder G, Kassner VA, Selegue JE, Higgs S and Carroll SB: Ectopic gene expression and homeotic transformation in arthropods using recombinant Sindbis viruses. Currently Biology 1999, 9:1279-1287.

Mahdi SHA, Gima S, Tomita Y, Yamasaki H, Otaki JM: Physiological characterization of the cold-shock-induced humoral factor for wing color pattern changes in butterflies. Journal of Insect Physiology 2010, 56: 1022-1031.

Mahdi SHA, Yamasaki H, Otaki JM: Heat-shock-induced color pattern changes of the blue pansy butterfly *Junonia orithya*: Physiological and evolutionary implications. Journal of Thermal Biology 2011, 36: 312-321.

Monteiro A, Glaser G, Stockslager S, Glansdrops N, Ramos D: Comparative insights into questions of lepidopteran wing pattern homology. BMC Developmental Biology 2006, 6:52.

Nijhout HF: Pattern formation in Lepidoptera: determination of an eyespot. Developmental Biology 1980, 80: 267-274.

Nihjout HF: Wing pattern formation in Lepidoptera: a model. Journal of Experimental Biology 1978, 206: 119-136.

Nihjout HF: The color patterns of butterflies and moths. Scientific America 1981, 245: 104-115.

Nijhout HF: Colour pattern modification by coldshock in Lepidoptera. Journal of Embryology and Experimental Morphology 1984, 81: 287-305.

Nijhout HF: A comprehensive model for colour pattern formation in butterflies. *Proc R Soc B* 1990, 239: 81-239.

Nijhout HF: The developmental and evolution of butterfly wing patterns Washington, USA: Smithsonian Institution Press; 1991.

Nijhout HF: Insect hormones Princeton, USA: Princeton University Press; 1994.

Nijhout HF: Elements of butterfly wing patterns. Journal of Experimental Zoology 2001, 291: 213-225.

Nijhout HF, Maine PK, Madzvamuse A, Wathen AJ, Sekimura T: Pigmentation pattern formation in butterflies: experiments and models. Comptes Rendus Biologies 2003, 326: 717-727.

Oliver JC, Robertson KA, Monteiro A: Accommodating natural and sexual selection in butterfly wing pattern evolution. Proceedings of the Royal Society B *2009*, 276: 2369-2375.

Otaki JM: Color pattern modifications of butterfly wings induced by transfusion and oxyanions. Journal of Insect Physiology 1998, 44: 1181-1190.

Otaki JM: Asymmetrical color pattern modification of *Vanessa cardui*: a case report of a field-caught individual and experimental pattern modification. Butterflies 2003, 35: 50-56.

Otaki JM: Reversed type of the color pattern modifications of butterfly wings: a physiological mechanism of the wing wide-color pattern determination. Journal of Insect Physiology 2007, 53: 526-537.

Otaki JM: Physiologically induced color pattern changes in butterfly wings: mechanistic and evolutionary implications. Journal of Insect Physiology 2008, 54:1099-1112.

Otaki JM: Artificially induced changes of butterfly wing colour patterns: dynamic signal interactions in eyespot development. Scientific Reports 2011a, 1:111.

Otaki JM: Color pattern analysis of eyespots in butterfly wings: a critical examination of morphogen gradients models. Zoological Science 2011a, 28: 403-413.

Otaki JM: Generation of butterfly wing eyespot patterns: a model for morphological determination of eyespot and parafocal element. Zoological Science 2011b, 28: 817-827.

Otaki JM: Color pattern analysis of Nymphalid butterfly wings: revision of the Nymphalid groundplan. Zoological Science 2012a, 29: 568-576.

Otaki JM: Structural analysis of eyespots: dynamics of morphogenic signals that govern elemental positions in butterfly wings. BMC Systems Biology 2012b, 6: 17

Otaki JM, Ogasawara T, Yamamoto H: Tungstate-induced color pattern modifications of butterfly wings are independent of stress response and ecdysteriod effect. Zoological Science 2005, 22: 635-644.

Otaki JM, Yamamoto H: Species-specific color pattern modifications of butterfly wings. Development, Growth and Differentiation 2004a, 46: 1-14.

Otaki JM, Yamamoto H: Color pattern modifications and speciation in butterflies of the genus *Vanessa* and its related genera *Cynthia* and *Bassaris*. Zoological Science 2004b, 21: 967-976.

Raff MC: Size control: The regulation of cell numbers in animal development. Cell 1996, 86: 173-175.

Reed RD, Serfas MS: Butterfly wing pattern evolution is associated with changes in a *Notch/Distal*-less temporal pattern formation process. Current Biology 2004, 14:1159-1166.

Rountree DB, Nijhout HF: Hormonal control of a seasonal polyphenism in *Precis coenia* (Lepidoptera: Nymphalidae). Journal of Insect Physiology 1995, 41: 987-992.

Saenko SV, Marialva MS, Beldade P: Involvement of the conserved Hox gene *Antennapedia* in the development and evolution of a novel trait. Evo Devo 2011, 2:9.

Shirai LT, Saenko SV, Keller RA, Jerónimo MA, Brakefield PM, Descimon H, Wahlberg N, Beldade P: Evolutionary history of the recruitment of conserved developmental genes in association to the formation and diversification of a novel trait. BMC Evolutionary Biology 2012, 12:21.

Tanaka D, Sakurama T, Mitsumasu, K, Yamanaka A, Endo K: Separation of bombyxin from a neuropeptide of *Bombyx mori* showing summer-morph-producing hormone (SMPH) activity in the Asian comma butterfly, *Polygonia c-aureum L*. Journal of Insect Physiology 1997, 43: 197-201.

Umebachi Y, Osanai M: Perturbation of the wing color pattern of a Swallow-tail butterfly, *Papilio xuthus*, induced by acid carboxypeptidase. Zoological Science 2003, 20: 325-331.

Weatherbee SD, Nijhout HF, Grunert LW, Halder G, Galant R, Selegue J, Carroll, S: *Ultrabithorax* function in butterfly wings and the evolution of insect wing patterns. Current Biology 1999, 9:109-115.

Chapter 2

Baculovirus-mediated gene transfer in butterfly wings *in vivo*: an efficient expression system with an anti-gp64 antibody

2.1. Introduction

Diverse color patterns of butterfly wings are excellent two-dimensional systems to investigate development and evolution of pattern formation (Nijhout, 1991). Most conspicuous among color patterns are probably eyespots, which are constructed by simple circular arrangements of colored scales. Eyespots are found in many nymphalid butterflies including the blue pansy *Junonia orithya*, athe buckeye *Junonia coenia*, and the squinting bush brown *Bicyclus anynana*, which are frequently used for experimental manipulations in butterfly biology. Developmental mechanism of eyespots in nymphalid butterflies has been studied using various methods including surgical manipulations (Nijhout, 1991; Brakefield *et al*., 1995; French *et al*., 1995; Otaki *et al*., 2005; Otaki, 2011a), physiological treatments (Otaki, 2008), *in situ* hybridization histochemistry or immunohistochemistry (Carroll *et al*., 1994; Brakefield *et al*., 1996; Keys *et al*., 1999; Brunetti *et al*., 2001; Monteiro *et al*., 2006; Oliver *et al*., 2012; Shirai *et al*., 2012), and morphological color pattern analysis (Kodandaramaiah, 2009; Otaki, 2011b; Otaki, 2011c). The expression patterns of candidate regulatory genes for color pattern formation such as *Distal-less*, *notch*, *engrailed*, *hedgehog*, *cubitus interruptus*, *patched*, and *spalt* in *B. anynana* and in *J. coenia* resemble a part of adult butterfly eyespots, implying their roles in eyespot formation (Carroll *et al*., 1994; Brakefield *et al*., 1996; Keys *et al*., 1999; Brunetti *et al*., 2001; Monteiro *et al*., 2006; Weatherbee *et al*., 1999; Reed *et al*., 2004). Recent addition to this list is *Antennapedia*, which showed the earliest and exclusive expression at the prospective eyespot foci in *B. anynana* (Saenko *et al*., 2011).

However, there is no direct evidence for the roles of any candidate genes in eyespot formation due to a lack of reproducible and reliable functional assay systems. Random mutagenesis experiments did not produce diverse phenotypes in *B. anynana* (Monteiro *et al*., 2003), and hence spontaneous mutants are still the best way to analyze eyespot development in this species (Monteiro *et al*., 2007; Saenko *et al*., 2010). The germline transformation in butterflies has been reported (Marcus *et al*, 2004), but its practicality is not entirely apparent despite its labor-intensive character. Likewise, use of *in vivo* electroporation of DNA has been limited due to physical damage on wings caused by the procedure (Golden *et al*., 2007). On the other hand, virus vectors have been employed to transfer and express foreign genes in lepidopteran insects. Recombinant Sindbis virus vectors have been used to study a homeotic gene *Ultrabithorax* (*Ubx*) during development of *J. coenia* (Lewis *et al*., 1999), but probably because it is an RNA virus, use of Sindbis virus vectors has not been pursued further.

Similarly, use of vaccinia virus vectors has been reported, but high level expression has not been achieved (Lewis *et al*., 2006).

Baculovirus vectors seem to be promising as they infect butterflies in natural environments. Recombinant baculovirus vectors are simple, safe, and inexpensive to engineer, can infect various cell types, and have a large capacity for DNA inserts (Lewis *et al*., 2006; Carbonell *et al*., 1985; Skuratovskaya *et al*., 1982). Recombinant baculovirus vectors have been used for ectopic expression in *Drosophila melanogaster* and in the flour beetle *Tribolium castaneum* (Oppenheimer *et al*., 1999) as well as in the silkworm *Bombyx mori* (Yamao *et al*., 1999; Mori *et al.*, 1995)

To our knowledge, use of baculovirus vectors for gene transfer *in vivo* has not been reported in butterflies. This may be largely due to its high cytotoxic effects of baculovirus vectors in butterflies. Baculovirus –infected cells are known to undergo apoptosis as a part of defense mechanism (Clakr and Clem, 2003; Clem, 2005; Clem, 2007). However, it may be possible to reduce the cytotoxic effects and develop a relatively efficient gene delivery method to butterfly wings using recombinant baculovirus vectors. Baculovirus-associated cytotoxic effects may originate from concentrated infection and subsequent cell death. To minimize these unwelcome effects, we administered anti-gp64 antibody. This antibody was raised against the baculovirus coat protein gp64, known as an envelope protein for cell-to-cell transmission of infection (Monsma *et al*., 1996). We hypothesized that this antibody may prevent unnecessary and excessive infection by baculovirus in developing cells. Using this "immunotherapy" for infected individuals, we successfully achieved high survival rate after infection and high-level expression of a foreign gene (in this case, a gene for green fluorescent protein, GFP) in butterfly wings *in vivo*.

Methodologically, pupae have been shown to be highly resistant against chemical injection (Otaki, 2008; Otaki, 1998; Serfas *et al*., 2005; Martin *et al*., 2012), which has contributed to our understanding of color pattern determination in butterfly wings. We here employed a microsyringe-assisted injection as a simple delivery method for baculovirus vector and antibody. We demonstrated that pupae were resistant against injections twice at the same injection point. This resistance against the double chemical injections allowed us to establish a reliable gene delivery system in butterfly wings.

2.2. Methods

2.2.1. Butterflies

Throughout this study, we used the blue pansy butterfly *Junonia orithya* (Linnaeus, 1758). Female adult individuals were caught in Okinawa-jima Island or Ishigaki-jima Island in the Ryukyu

Archipelago, Japan, and eggs were collected from these females. Alternatively, larvae were field-caught in these islands. Larvae were fed their natural host plants at ambient temperature.

2.2.2. Baculovirus vector, anti-gp64 antibody, and injection

Recombinant baculovirus vector containing the *Aequorea victoria* green fluorescent protein (GFP) gene under the control of the polyhedrin promoter was obtained from AB Vector (San Diego, CA, USA) at a viral titer of 1×10^8 pfu/mL. In the present study, we expressed titers using two digits based on dilution factors, but only one digit is significant, as in the non-diluted original titer. A mouse monoclonal antibody IgG_{2a} against baculovirus gp64 (AcV1) of extracellular nonoccluded AcNPV (*Autographa californica* nucleopolyhedrovirus) (200 µg/mL in PBS) was obtained from Santa Cruz Biotechnology (Santa Cruz, CA, USA). In the case of the 2.0 µL injection, pfu/mL can be converted to pfu/individual by the factor of x (2 x 10-^{3}). Pupae were injected with 2.0 µL (unless otherwise specified) of a solution containing the baculovirus in the abdomen within 24 hours after pupation, followed by an antibody injection at the same position in various volume and times as indicated, using an Ito microsyringe (Fuji, Shizuoka, Japan).

2.2.3. Visualization of GFP fluorescent signal

The whole pupae, whole adults, isolated pupal wings, or isolated adult wings were placed on the ATTO illuminator VISIRAYS-B (Tokyo, Japan), a blue-LED light unit with emission wavelengths λ = 440-500 nm and λ_{max} = 470 nm. Under this illuminator, the GFP fluorescence image for low magnifications was observed and recorded using a digital single-lens reflex camera Canon EOS 50D (Tokyo, Japan) with the ATTO filter SCF515. We used the following imaging system for high magnification images of GFP fluorescence: a Nikon inverted epifluorescence microscope Eclipse Ti-U (Tokyo, Japan) equipped with a Nikon Intensilight C-HGFI (a mercury pre-centered fiber illumination system), a Coherent Sapphire 488 nm lazer controller (Santa Clara, CA, USA), a Yokogawa Electric CSU-X1 confocal scanner unit (Tokyo, Japan), and a Hamamatsu Photonics ImagEM EM-CCD camera (Hamamatsu, Japan). This microscope hardware system was controlled with the Hamamatsu Photonics AQUACOSMOS/RATIO analysis system. We used a Nikkon GFP-B fluorescent cube (excitation filter: 460-500nm, dichroic mirror: 505nm, and emission filter 510-520 nm) for GFP detection. When confocal images are presented, they are designated as such in this paper. For bright-field low-magnification images, we used the digital single-lens reflex camera Canon EOS 50D (Tokyo, Japan) and Saitou Kougaku SKM-S30-PC (Yokohama, Japan). For bright-field high-magnification images, we used a Keyence high-resolution digital microscope VHX-1000 (Osaka, Japan) and the Nikon microscope system described above.

2.2.4. Degrees of GFP fluorescence in pupae

After the injection of the baculovirus vector, the treated pupae were evaluated for fluorescence everyday using the ATTO illuminator VISIRAYS-B. We visually classified the level of GFP fluorescence in the GFP-positive pupae into three categories, GI, GII, and GIII as follows. In G0, there was no fluorescence observed in wings. In GI, GFP fluorescence was seen in less than 50% of the pupal forewing area (right or left wings). In GII, about 50 % or more of the pupal forewing area (right or left wings) was covered with GFP fluorescence. In GIII, almost entire pupal wing area (and often the other parts of the body) was covered with GFP fluorescence. When GFP fluorescence was observed for the first time, that pupa was classified into one three categories (GI, GII, or GIII) based on visual inspection. The fluorescence level could be higher (if alive) or less (if dead) on subsequent days, but we did not evaluate these subsequent changes in the fluorescent levels. Pupae were examined for five days after the injection of the baculovirus vector, and if we did not observe any GFP fluorescence, that pupa was defined as G0 (no fluorescence, or GFP-negative).

2.2.5. Pupal wing dissection and immunohistochemistry

Pupal wings from four-day-old pupae after pupation were dissected following a published protocol with some modifications (Brakefield *et al*., 2009). The pupa was lightly anesthetized on ice, and the cuticle around the wing margin was cut using a scalpel and lifted up to cut through the trachea connecting the wings to the thorax. Dissected wing tissues were placed on glass slides. The tissues were then directly subjected to the fluorescent microscope to examine the GFP fluorescence. They were then air-dried and stored in a refrigerator until use for immunohistochemistry.

For immunohistochemical detection of GFP in pupal wings, we followed a modified protocol of the previous studies (Brunetti *et al*., 2001; Matayoshi *et al*., 2011). We used monoclonal anti-GFP antibody (mouse IgG_{2b}, clone 1E4) raised against recombinant full length GFP (246 amino acids) (Medical & Biological Laboratories, Nagoya, Japan) as the primary antibody at a 1:200 dilution in following solution: 50mM Tris (pH 6.8), 150 mM NaCl, 0.5% NP40, and 1 mg/mL BSA. For negative controls, we used a non-specific normal mouse IgG (Santa Cruz Biotechnology) at a 1:200 dilutions in the same solution. After incubating the dissected wings with anti-GFP antibody or normal mouse IgG, the wings were treated with the secondary anti-mouse IgG antibody (Santa Cruz Biotechnology) in phosphate-buffer saline (PBS) and the VectaStain Elite ABC Kit (Vector Laboratories, Burlingame, CA, USA). For chromogenic detection, the DAB (3, 3'-diaminobenzidine) Peroxidase Substrate Kit was employed (Vector Laboratories). The wings were mounted in Softmout (Wako, Osaka, Japan), and pictures were taken using a Keyence high-resolution digital microscope VHX-1000 (Osaka, Japan).

2.3. Results

2.3.1. GFP fluorescent signals in pupae

We injected the GFP-containing baculovirus vector at various titers into the segmental boundaries of pupae in 6-12 hours after pupation. Although the vector was injected on either right or left side of the abdomen, the GFP epifluorescence was observed in various parts of the pupal body. The degree of fluorescence varied, and infected parts were heterogeneous among individuals (Fig. 2.1A-H). In some individuals, the whole body fluoresced including wings, antennae, eyes, abdomen, and proboscis (Fig. 2.1G). It appears that wings were one of the tissues that showed GFP fluorescence relatively frequently. This may be simply due to the fact that wings occupy a relatively large surface area in a pupa. In other individuals, there was no sign of fluorescence at all (Fig. 2.1B). Autofluorescence from non-infected individuals was virtually negligible (Fig. 2.1B), and when present, it was yellowish (not shown), which was easily distinguishable from the green fluorescence of GFP. We never observed GFP-like green fluorescence from non-infected individuals ($n > 10$).

At high baculovirus titers (3.3×10^4 pfu/mL and higher), percentage of the GFP-positive individuals scored 100%, and with lower virus titers, it was as low as 4% (Fig. 2.2A). A sudden transition between high and low percentages of the GFP-positive individuals was detected between 1.0×10^4 pfu/mL (13%) and 3.3×10^4 pfu/mL (100%). Although an unexpected peak was observed at the titer of 2.0×10^3 pfu/mL, this would be due to sensitivity variation of larvae or technical inconsistency of injection procedure. In contrast to high percentages of the GFP-positive individuals in high titers, the percentages of eclosed individuals were very low at 5.0×10^3 pfu/mL or higher. At the lower titers, the percentages of eclosed individuals were higher with low percentages of the GFP-positive individuals.

We observed various levels of GFP fluorescence in the treated pupae including G0 (Fig. 2.1B), GI (Figs. 1C, D), GII (Fig. 2.1E), and GIII (Fig. 2.1F, G). As expected, the GI category was seen mostly with lower titers, whereas the GII and GIII categories were seen more frequently with higher titers (Fig. 2.2B).

Taken together, we demonstrated that injection of baculovirus vector can deliver a foreign gene (i.e., GFP reporter gene) in butterfly pupae. However, no GFP-positive pupae eclosed or developed color patterns. This means that the pupal development was halted by the lethal effects of the baculovirus vector. We failed to find out a range of titers that are suitable both for GFP expression and for eclosion or at least for color pattern development.

2.3.2. Antibody treatment increased the survival rate of infected pupae

The major problem of using a baculovirus vector was the high pupal mortality rate associated with infection. To circumvent this problem, we used anti-gp64 antibody. To evaluate the effect of this antibody, we hereafter used a titer of 2.0×10^4 pfu/mL that was found at the transition region between high and low percentages of the GFP-positive individuals (Fig. 2.2A).

We injected 0.5, 1.0, 2.0, and 3.0 μL of the antibody 24 hours after injection of the baculovirus vector (Fig. 2.3A). With an increase of antibody volume, percentage of the GFP-positive individuals decreased from 73% to 4%, but the percentage of individuals that eclosed successfully increased from 5% to 92% (Figure 2.3A). Importantly, in a range of 0.5-2.0 μL, significant proportions of the treated individuals successfully eclosed with GFP fluorescence. These results demonstrated that the "immunotherapy" with anti-gp64 antibody rescued significant proportion of infected pupae from death and at the same time reduced the GFP-positive individuals and that it is possible to obtain GFP-positive wings with the color pattern development completed (Fig. 2.4).

Fixing the injection volume at 2.0 μL, we injected the antibody at various time points, 6, 24, and 48 hours after the baculovirus treatment. Percentage of the GFP-positive individuals decreased from 80% to 50%, and percentage of individuals that eclosed successfully remained in the range of 20-30% (Fig. 2.3B). We classified the GFP-positive pupae into three categories, GI, GII, and GIII, based on the degrees of fluorescence (Fig. 2.3C). The GII and GIII levels were obtained despite relatively small proportions. Together, we conclude that post-6-24 hour treatments using 0.5-2.0 μL of a solution containing the baculovirus at a titer of 2.0×10^4 pfu/mL are optimal conditions for gene transfer and expression in pupae.

2.3.3. GFP fluorescent signals in developing cells in wings

We used a confocal microscope to identify the source of fluorescence in developing wings from the GFP-positive pupae treated with the baculovirus and the anti-gp64 antibody (n = 9) (Figure 4A-D). In a wing isolated from a pupa at the early stage of development, a few fluorescent parts were found, and fluorescent cells constituting a wing were observed. Most likely, they will differentiate to both socket and scale cells. We noticed that the fluorescent cells occasionally formed a circular pattern, and its central region was relatively dark, which may be caused by the cytotoxic effects of the baculovirus infection.

2.3.4. GFP fluorescent signals in adult tissues

Because of the therapeutic effects of anti-gp64 antibody, we obtained several individuals that developed color patterns inside the pupal case or that successfully eclosed to become adults with GFP

fluorescence (*n* = 6). In one successfully eclosed wing (Figs. 2.5A-D) and one fully developed wing in the pupal case (Fig. 2.5E-I), we confirmed that fluorescence signals originated from scales themselves (Fig. 2.5D, I). In most cases, however, GFP fluorescence originated from the basal membrane (only when scales were removed) but not from scales (*n* = 4; Figure 5J-M). In two cases, GFP fluorescence was observed from the entire area of the wing basal membrane. We confirmed that green fluorescence was not detected at all in non-infected wings before and after the scale removal (not shown). In adults, the GFP fluorescent signals were also observed in eyes, antennae, palpi, proboscis, and abdomen (*n* = 6; Figs. 2.5N-Q). Importantly, no aberrant change in color patterns was observed in the wings with GFP fluorescence (*n* = 6; Figs. 2.5A, E, J).

2.3.5. Immunohistochemical detection of GFP in pupal wings

To rigorously confirm that the green fluorescence we observed above was not autofluorescence but indeed originated from the ectopically expressed GFP, we here performed immunohistochemical staining of pupal wing tissues using anti-GFP antibody. We allowed infected pupae to develop until fourth day of post-pupation and then the wings were dissected and subjected to immunohistochemical staining. The chromogenic DAB signal for anti-GFP antibody (Figs. 2.6A-C) and the GFP fluorescence (Figs. 2.6D-F) from the identical wing tissue completely overlapped in four wing samples from different individuals. In these wing tissues, we noticed that the GFP signals sometimes formed circular structure, as seen in Fig. 2.4. Its central region might have been damaged by the baculovirus toxicity, although this circular pattern was not observed in the completed wings that were examined in Fig. 2.5.

When we employed normal IgG instead of anti-GFP antibody with other procedures being the same, we detected no chromogenic DAB staining for GFP in the green fluorescent area in the four GFP-fluorescence-positive wings from two individuals (not shown). These results demonstrated that the immunohistochemical DAB staining signals were not artifacts and that the green fluorescence in wings originated from the expressed GFP molecules.

2.4. Discussion

In this study, we demonstrated that the recombinant baculovirus vector was able to deliver a foreign gene to wings of *J. orithya* pupae. Pupae treated with high titers of the baculovirus vector without the subsequent antibody treatment showed GFP fluorescence but died at the pupal stage before the color pattern development. This fact has most likely prevented researchers from pursuing the baculovirus-mediated gene transfer method in butterfly wings.

We first examined the GFP fluorescent levels with various virus titers. Heterogeneous GFP expression was observed at various levels in various parts of pupae even at the same titer, which could

be due to individual variation (genetic heterogeneity) or random variation of the injection procedure (technical inconsistency). A similar type of infection variation has also been reported in the other virus system (Zhao *et al*., 1996; Zhao *et al*., 1998). Nonetheless, we obtained dose-dependent changes of fluorescence. That is, with high baculovirus titers, we were able to obtain high percentages of the GFP-positive individuals and of the GIII level of GFP fluorescence. However, the high-level expression was accompanied by a high mortality rate. This is because of the induction of apoptosis in the infected cells (Clarke and Clem, 2003; Clem, 2005; Clem, 2007). Reducing virus titer did not allow the wing color pattern to develop with GFP fluorescence. This suggests that minimum titer of baculovirus for GFP fluorescence can still induce cytotoxic effects sufficient to cause a pupal death. Therefore, the inhibition of baculovirus activity by anti-gp64 antibody is essential to obtain the color pattern development with GFP fluorescence.

To overcome the pupal death associated with the baculovirus infection, we used an antibody against the baculovirus coat protein gp64. Pupae tolerated double injection at the same injection point, and the therapeutic effect was dramatic. At high doses of anti-gp64 antibody, almost all pupae eclosed successfully. This result indicates that anti-gp64 antibody prevented cells from dying due to infection with the baculovirus vector. Although high doses of the anti-gp64 antibody weakened the GFP expression level, we achieved the eclosion rate of 10-40% and the GFP-positive rate of 50-60% in optimized conditions. Examining GFP-positive individuals that completed the color pattern development was now possible with the administration of the anti-gp64 antibody. We do not know the precise mechanism of how the immunotherapy with anti-gp64 antibody works. But it is likely that the antibody prevents further propagation of baculovirus by blocking the function of the coat protein gp64.

Mechanistically, F_c-receptor-mediated activations of immune cells, which are expected to work in mammals, may not be possible in insects, because insects are not equipped with the adaptive immune system. Nonetheless, the binding of the anti-gp64 antibody to baculovirus particle appears to be sufficient to block the virus infection efficiently. This treatment is often sufficient to allow the infected individual complete metamorphosis to adults. Using a mammalian antibody in insects for its therapeutic effect is most likely a new attempt. Additionally, double injection of chemicals into a pupa is a new attempt. These methodologically new aspects of this study may find applications in other fields of entomological research. For example, since a recombinant baculovirus vector is relatively easier to engineer, any non-model insects are now targets for the *in-vivo* gene transfer experiments. Furthermore, this immunotherapy may be able to rescue insects of commercial use such as the silkworm naturally infected with baculovirus.

GFP-positive fluorescent cells were clearly detected in developing pupal wings. GFP expression was not only seen in wings but also in other body parts such as eyes and antennae. The broad tissue

tropism was also reported in *J. coenia* using Sindbis virus (Lewis *et al*., 2006) and in *Xenopus laevis* using baculovirus (Oppenheimer, 1999). Interestingly, GFP fluorescence can be observed not only in pupal wings but also in adult wings. Although the scales are dry extracellular structures, it appears that GFP molecules are able to be incorporated into scale structures. Importantly, GFP expression did not change the normal color patterns of wings.

The ability of baculovirus vectors to transfer foreign genes to developing wing tissues without any color pattern changes in adults makes this system useful in investigating gene functions in butterfly wing color pattern development *in vivo*. There are precedent cases of virus-mediated *in vivo* expression systems for functional assays of candidate genes in insects (Lewis *et al*., 1999). A non-insect example is found in the functional proof for an odorant receptor gene using an adenovirus-mediated gene transfer system (Zhao *et al*., 1996; Zhao *et al*., 1998). We envision a similar *in vivo* functional assay system for the putative genes for the color pattern formation in butterfly wings.

Recently, a relatively simple method to generate somatic transgenic cells in various insect tissues has been reported (Ando and Fujiwara, 2013). This electroporation method maybe less toxic than our method, once a gene is integrated into host chromosome. Remarkably, the electroporation method achieved stable GFP expression in somatic cells in larvae and pupae (Ando and Fujiwara, 2013). However, the level of GFP expression in a pupal wing of the silkworm (Figure 2C in [Ando and Fujiwara, 2013]) was much less than that of our study, and no expression in adult tissues was demonstrated. Furthermore, the electroporation method appears to be more technically demanding than our method. Each method has strength and weakness, and it is favorable that researchers will have an opportunity to try different methods suitable for an insect system of interest.

2.5. Conclusions

The functional analysis of candidate genes for butterfly wing color pattern formation has been hampered by a lack of method to manipulate gene expression. We have developed a method to transfer a foreign gene to pupal wings of *J. orithya* using recombinant baculovirus. We were able to express GFP in the developing wings of pupae by the simple injection of a recombinant baculovirus vector followed by the second injection of anti-gp64 antibody. The method developed here can be used for a functional study of candidate genes for wing color pattern development. The baculovirus vector in conjunction with the anti-gp64 antibody could also be an invaluable tool to investigate gene functions in other non-model insects.

2.6. References

Beldade P: Evolutionary history of the recruitment of conserved developmental genes in association to the formation and diversification of a novel trait. BMC Evolutionary Biology 2012, 12:21.

Brakefield PM, Beldade PM, Zwaan BJ: Dissection of larval and pupal wings from the African butterfly *Bicyclus anynana*. Cold Spring Harbor Protocol 2009, 2009: pdb.prot5207.

Brakefield PM, French V: Eyespot development on butterfly wings: the epidermal response to damage. Developmental Biology 1995, 168: 98-111.

Brakefield PM, Gates J, Keys D, Kesbeke F, Wijngaarden PJ, Monteiro A, French V, Carroll SB: Development, plasticity and evolution of butterfly eyespot patterns. Nature 1996, 384:236-242.

Brunetti CR, Selegue JE, Monteiro, A, French V, Brakefield PM, Carroll SB: The generation and diversification of butterfly eyespot color patterns. Current Biology 2001, 11:1578-1585.

Carbonell LF, Klowden MJ, Miller LK: Baculovirus-mediated expression of bacterial genes in dipteran and mammalian cells. Journal of Virology 1985, 56:153-160.

Carroll SB, Gates J, Keys DN, Paddock SW, Panganiban GE, Selegue JE, Williams JA: Pattern formation and eyespots determination in butterfly wings. Science 1994, 265:109-114.

Clarke TE, Clem RJ: Insect defense against virus infection: the role of apoptosis. International Reviews of Immunology 2003, 22: 401-424.

Clem RJ: The role of apoptosis in defense against baculovirus infection in insects. Current Topic in Microbiology and Immunology 2005, 289: 113-129.

Clem RJ: Baculoviruses and apoptosis: a diversity of genes and responses. Current Drug Targets 2007, 8: 1069-1074.

Fraser MJ: Ultrastructural observations of virion maturation in *Autographa californica* nuclear polyhedrosis virus infected *Spodoptera frugiperda* cell cultures. Journal of Ultrastructure and Molecular Structure 1986, 95:189-195.

French V, Brakefield PM: Eyespot development on butterfly wings: the focal signal. Developmental Biology 1995, 168:112-123.

Golden K, Sagi V, Markwarth N, Chen B, Monteiro A: *In vivo* electroporation of DNA into the wing epidermis of the butterfly, *Bicyclus anynana*. Journal of Insect Science 2007, 7: 1-8.

Keys DN, Lewis DL, Selegue JE, Pearson BJ, Goodrich LV, Johnson RL, Gates J, Scott MP, Carroll SB: Recruitment of a *hedgehog* regulatory circuit in butterfly eyespots evolution. Science 1999, 283:532-534.

Kodandaramaiah U: Eyespot evolution: phylogenetic insights from *Junonia* and related butterfly genera (Nymphalidae: Junoniini). Evolution and Development 2009, 11:489-497.

Lewis DL, Brunetti CR: Ectopic transgene expression in butterfly imaginal wing disc using vaccinia virus. Biotechniques 2006, 40:48, 50, 52.

Lewis DL, DeCamillis MA, Brunetti CR, Halder G, Kassner VA, Selegue JE, Higgs S and Carroll SB: Ectopic gene expression and homeotic transformation in arthropods using recombinant Sindbis viruses. Current Biology 1999, 9:1279-1287.

Marcus JM, Ramos DM, Monteiro A: Germline transformation of the butterfly *Bicyclus anynana*. Proceedings of the Royal Society B (Suppl.) 2004, 271:S263-S265.

Martin A, Papa R, Nadeau NJ, Hill RI, Counterman BA, Halder G, Jiggins CD, Kronforst MR, Long AD, McMillan WO, Reed RD: Diversification of complex butterfly wing patterns by repeated regulatory evolution of a Wnt ligand. Proceedings of the National Academy of Sciences USA 2012, 109:12632-12637.

Matayoshi R, Otaki JM: Immunohistochemical detection of olfactory-specific sensory transduction proteins in olfactory neuroblastoma. Neuroscience Research 2011, 69: 258-262.

Monsma SA, Oomens AG, Blissard GW: The GP64 envelope fusion protein is an essential baculovirus protein required for cell-to-cell transmission of infection. Journal of Virology 1996 70: 4607-4616.

Monteiro A, Chen B, Scott LC, Vedder L, Prijs HJ, Belicha-Villanueva A, Brakefield PM: The combined effect of two mutations that alter serially homologous color pattern elements on the fore and hindwings of a butterfly. BMC Genetics 2007, 8:22.

Monteiro A, Glaser G, Stockslager S, Glansdrops N, Ramos D: Comparative insights into questions of lepidopteran wing pattern homology. BMC Developmental Biology 2006, 6:52.

Monteiro A, Prijs J, Bax M, Hakkaart T, Brakefield PM: Mutants highlight the modular control of butterfly eyespot patterns. Evolution and Development 2003, 5:180-187.

Mori H, Yamao M, Nakazawa H, Sugahara Y, Shirai N, Matsubara F, Sumida M, Imamura T: Transovarian transmission of a foreign gene in the silkworm, *Bombyx mori*, by *Autographa californica* nuclear polyhedrosis virus. Biotechnology 1995, 13:1005-1007.

Nijhout HF: Cautery-induced colour patterns in *Precis coenia* (Lepidoptera: Nymphalidae). Journal of Embryology and Experimental Morphology 1985, 86:191-203.

Nijhout HF: *The development and evolution of butterfly wing patterns* Washington, USA: Smithsonian Institution Press; 1991.

Oliver JC, Tong XL, Gall LF, Piel WH, Monteiro A: A single origin for nymphalid butterfly eyespots followed by widespread loss of associated gene expression. PLOS Genetics 2012, 8:e1002893.

Oppenheimer DI, MacNicol AM, Patel NH: Functional conservation of the wingless-engrailed interaction as shown by a widely applicable baculovirus misexpression system. Current Biology 1999, 9:1288-1296.

Otaki JM: Color pattern modifications of butterfly wings induced by transfusion and oxyanions. Journal of Insect Physiology 1998, 44:1181-1190.

Otaki JM, Ogasawara T, Yamamoto H: Morphological comparison of pupal wing cuticle patterns in butterflies. Zoological Science 2005, 22:21-34.

Otaki JM: Physiologically induced color pattern changes in butterfly wings: Mechanistic and evolutionary implications. Journal of Insect Physiology 2008, 54:1099-1112.

Otaki JM: Artificially induced changes of butterfly wing colour patterns: dynamic signal interactions in eyespot development. Science Reports 2011a, 1:111.

Otaki JM: Colour-pattern analysis of eyespots in butterfly wings: a critical examination of morphogen gradient models. Zoological Science 2011b, 28:403-413.

Otaki JM: Generation of butterfly wing eyespot patterns: a model for morphological determination of eyespot and parafocal element. Zoological Science 2011c, 28:817-827.

Reed RD, Serfas MS: Butterfly wing pattern evolution is associated with changes in a Notch/Distal-less temporal pattern formation process. Current Biology 2004, 14:1159-1166.

Saenko SV, Brakefield PM, Beldade P: Single locus affects embryonic segment polarity and multiple aspects of an adult evolutionary novelty. BMC Biology 2010, 8:111.

Saenko SV, Marialva MS, Beldade P: Involvement of the conserved *Hox* gene *Antennapedia* in the development and evolution of a novel trait. Evo Devo 2011, 2:9.

Serfas MS, Carroll SB: Pharmacologic approaches to butterfly wing patterning: sulfated polysaccharides mimic or antagonize cold shock and alter the interpretation of gradients of positional information. Developmental Biology 2005, 287:416-424.

Shirai LT, Saenko SV, Keller RA, Jerónimo MA, Brakefield PM, Descimon H, Wahlberg N, Beldade P: Evolutionary history of the recruitment of conserved developmental genes in association to the formation and diversification of a novel trait. BMC Evolutionary Biology 2012, 12:21.

Skuratovskaya IN, Fodor I and Strokovskaya LI: Properties of the nuclear polyhedrosis virus of the great wax moth: oligomeric circular DNA and the characteristic of the genome. Virology 1982, 120:465-471.

Weatherbee SD, Nijhout HF, Grunert LW, Halder G, Galant R, Selegue J, Carroll, S: *Ultrabithorax* function in butterfly wings and the evolution of insect wing patterns. Current Biology 1999, 9:109-115.

Yamao M, Katayama N, Nakazawa H, Yamakawa M, Hayashi Y, Hara S, Kamei K, Mori H: Gene targeting in the silkworm by use of a baculovirus. Genes and Development 1999, 13:511-516.

Zhao H, Otaki JM, Firestein S: Adenovirus-mediated gene transfer in olfactory neurons *in vivo*. Journal of Neurobiology 1996, 30:521-530.

Zhao H, Ivic L, Otaki JM, Hashimoto M, Mikoshiba K, Firestein S: Functional expression of a mammalian odorant receptor. Science 1998, 279:237-242.

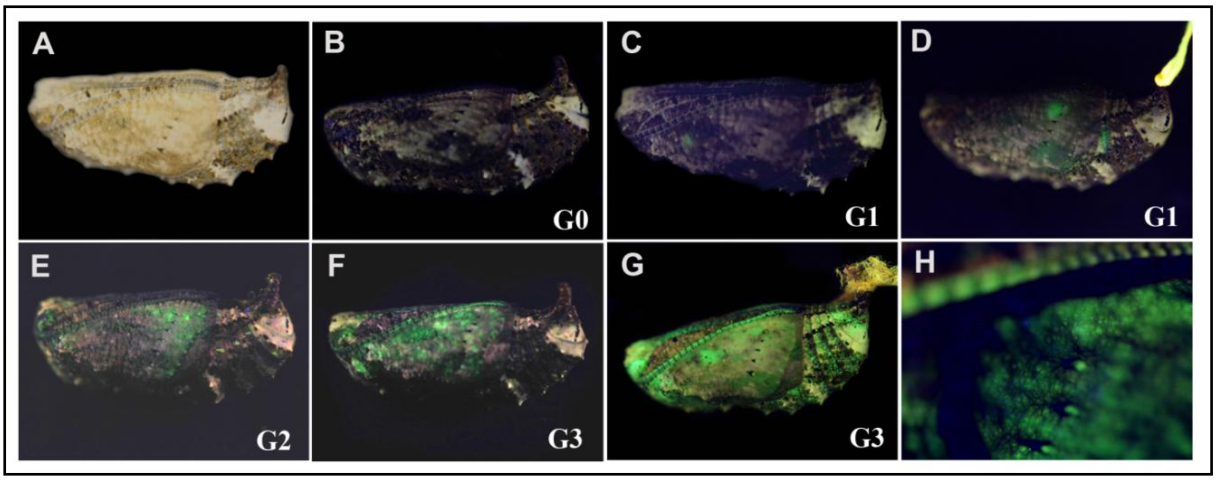

Fig. 2.1. Baculovirus-mediated GFP expression in *J. orithya* pupae. Baculovirus was injected at the pupal stage 6-12 hours after pupation. (**A**) A whole pupa under the bright field showing the GI level. The Injection consisted of 2.0 µL at 2.5×10^2 pfu/mL. This individual is identical to C. (**B-G**) Whole pupae under the blue light showing various GFP fluorescent levels. (**B**) G0. No injection (Normal pupa) (**C**) GI. (**D**) GI. The Injection consisted of 2.0 µL at 5.0×10^5 pfu/mL. (**E**) GII. The injection consisted of 2.0 µL at 2.0×10^5 pfu/mL. (**F**) GIII. The injection consisted of2.0 µL at 5.0×10^5 pfu/mL. The level of GFP fluorescence varied even if the same conditions were used in D and F. (**G**) GIII. The injection consisted of 2.0 µL at 1.0×10^7 pfu/mL. (**H**) Higher magnification of the wing region of the fluorescing pupa shown in D.

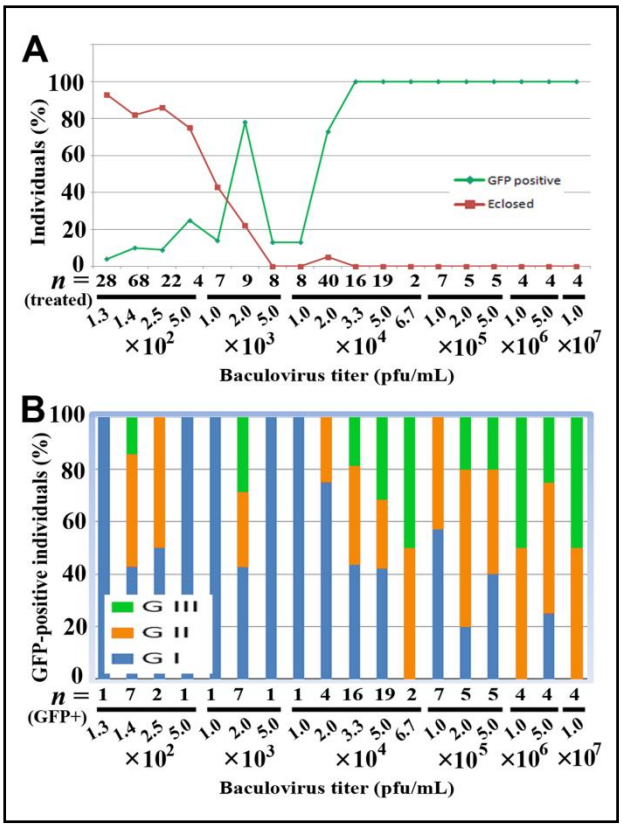

Fig. 2.2. Percentages of GFP-positive individuals, eclosed individuals, and the degrees of fluorescence in baculovirus-injected *J. orithya* pupae. Virus titre is shown in pfu/mL. Note that pfu/mL can be converted to pfu/individual by the factor of x ($2x10^{-3}$). (**A**) Percentages of GFP-positive pupae (green) and successfully eclosed individuals (red) at various baculovirus titers. Baculovirus (2 uL) was injected 24 hours post-pupation. (**B**) Proportions of GI, GII, and GIII levels of the GFP fluorescence in the fluorescent pupae at various baculovirus titers.

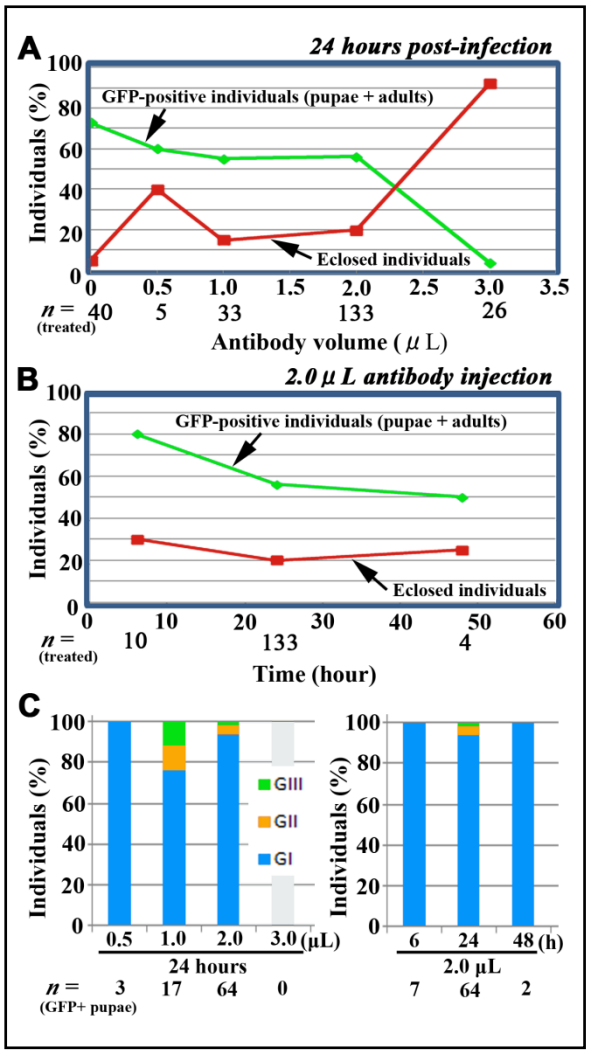

Fig. 2.3. Effects of the anti-gp64 antibody. Baculovirus vector was used at 2×10^4 pfu/mL. (**A**) Percentages of GFP-positive individuals and eclosed individuals at various antibody volumes. The antibody treatment was performed 18-24 hours post-infection. (**B**) Percentages of GFP-positive individuals and eclosed individuals at various time points of the antibody treatment (6 hours, 24 hours, and 48 hours). The antibody volume used was 2.0 μL. (**C**) Degrees of GFP fluorescence (GI, GII, and GIII) in the GFP-positive individuals. The left panel shows the results of various antibody volumes 18-24 hours post-infection, and the right panel shows the results of various treatment times using 2.0 μL antibody.

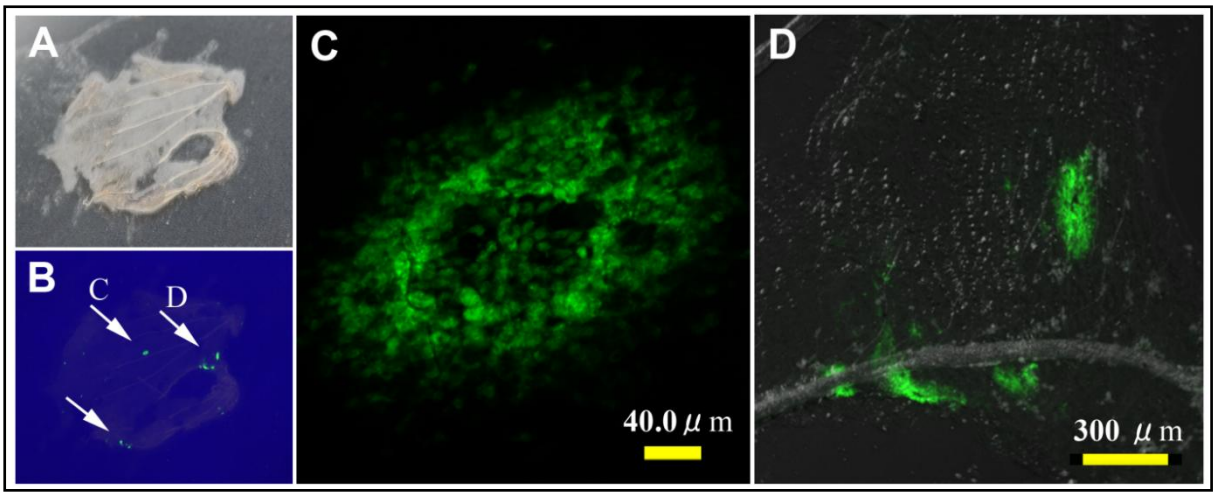

Fig. 2.4. GFP fluorescence in a developing *J. orithya* pupal wing at the cellular level. The baculovirus vector was injected at 1.0×10^6 pfu/mL (2.0 μL) 18-24 hours post-pupation, followed by anti-gp64 antibody injection (2.0 μL) 18-24 hours post-infection. Pupal wings were dissected 24 hours post-antibody treatment. (**A**) A whole wing under the bright field. (**B**) A whole wing identical to A under the blue light. Three major fluorescent clusters are indicated by arrows, two of which are shown in C and D. (**C**) Confocal image of a fluorescent region shown in B. A circular arrangement of the fluorescent signals is seen. (**D**) Confocal image of another fluorescent region shown in B, superimposed on the bright-field picture.

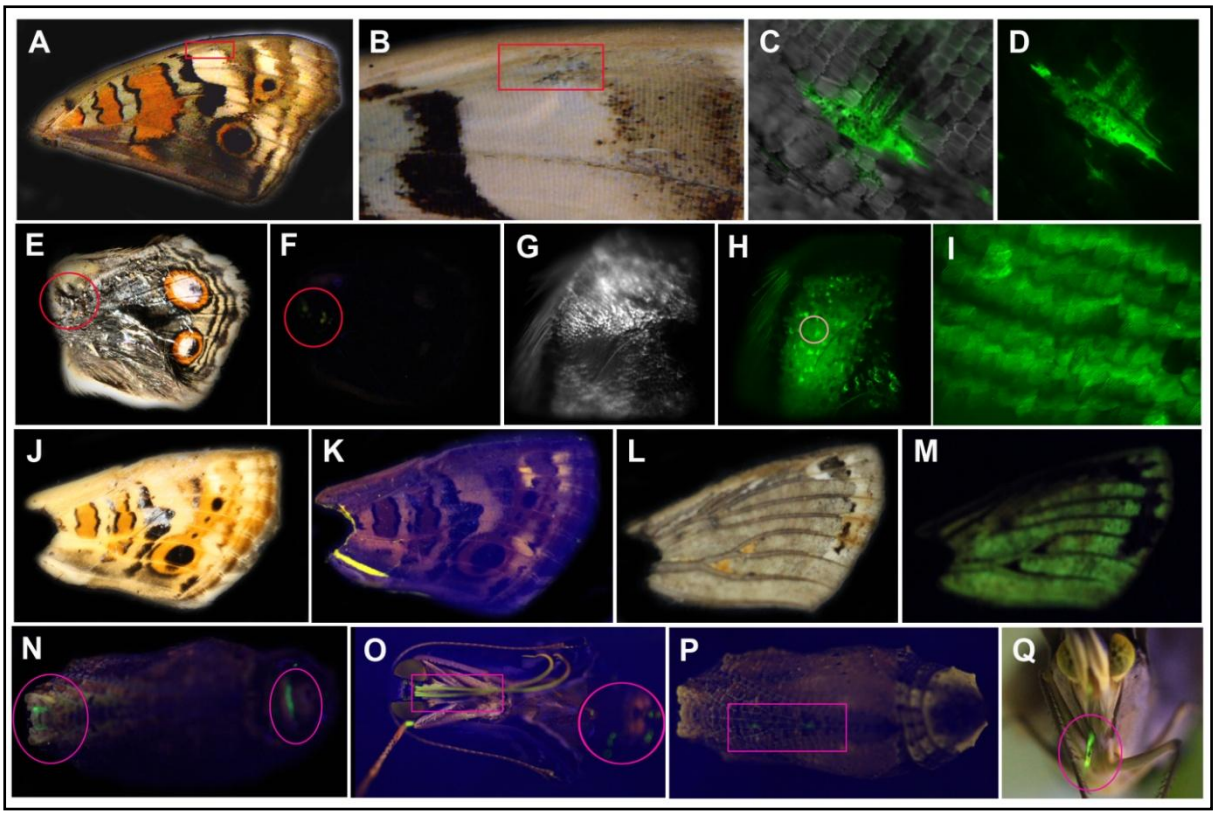

Fig. 2.5. Baculovirus-mediated GFP expression in *J. orithya* pupae and adults from baculovirus-injected and antibody injected individuals. In all cases, 2.0 μL of a solution containing the baculovirus at a titer of 2.0×10^4 pfu/mL was injected 18-24 hours post-pupation. (**A**) An adult ventral forewing with normal color pattern that was obtained from a baculovirus-injected and antibody-injected (2.0 μL, 6 hours post-infection) individual. The boxed region is enlarged in B. (**B**) High magnification of A. The boxed region is enlarged in C and D. (**C**) High magnification of B under the blue light and a small degree of the white light. Intense fluorescence was observed in regions where no scales were found, but some scales also fluoresced. (**D**) High magnification of C under the blue light. (**E**) An adult dorsal hindwing, isolated from a pupal case due to eclosion failure. This wing was obtained from a baculovirus-injected and antibody-injected (1.0 μL, 18-24 hours post-pupation) individual. The circled region is enlarged in G and H. (**F**) The same wing in E under the blue light. A few clusters of green fluorescence were observed, as indicated by circles. (**G**) High magnification of E. (**H**) The same region as G. Extensive GFP fluorescence was observed. The circled region is further magnified in I. (**I**) High-magnification confocal image of H. Intense fluorescence was seen in scales. (**J**) An adult ventral forewing, isolated from a pupal case due to eclosion failure. This wing was obtained from a baculovirus-injected and antibody-injected (2.0 μL, 6 hours post-infection) individual. (**K**) The same wing as J under the blue light. No green fluorescence was detected. (**L**) The same wing as J after the removal of scales. (**M**) The same wing as L, with scales removed, under the blue light. Green fluorescence was observed throughout the wing. (**N**) A pupa with fluorescence from a part of the proboscis and abdomen (circled). The wing shown in E was obtained from this pupa. (**O**) An eclosed

adult from the pupa in N. A section of the proboscis (boxed) and abdomen (circled) showed green fluorescence as predicted at the pupal stage. (**P**) A pupa with green fluorescence in a part of a leg (boxed). This pupa is a baculovirus-injected and antibody-injected (2.0 μL, 18-24 hours post-infection) individual. (**Q**) An eclosed adult from the pupa in P. A part of a leg shows fluorescence, as predicted at the pupal stage.

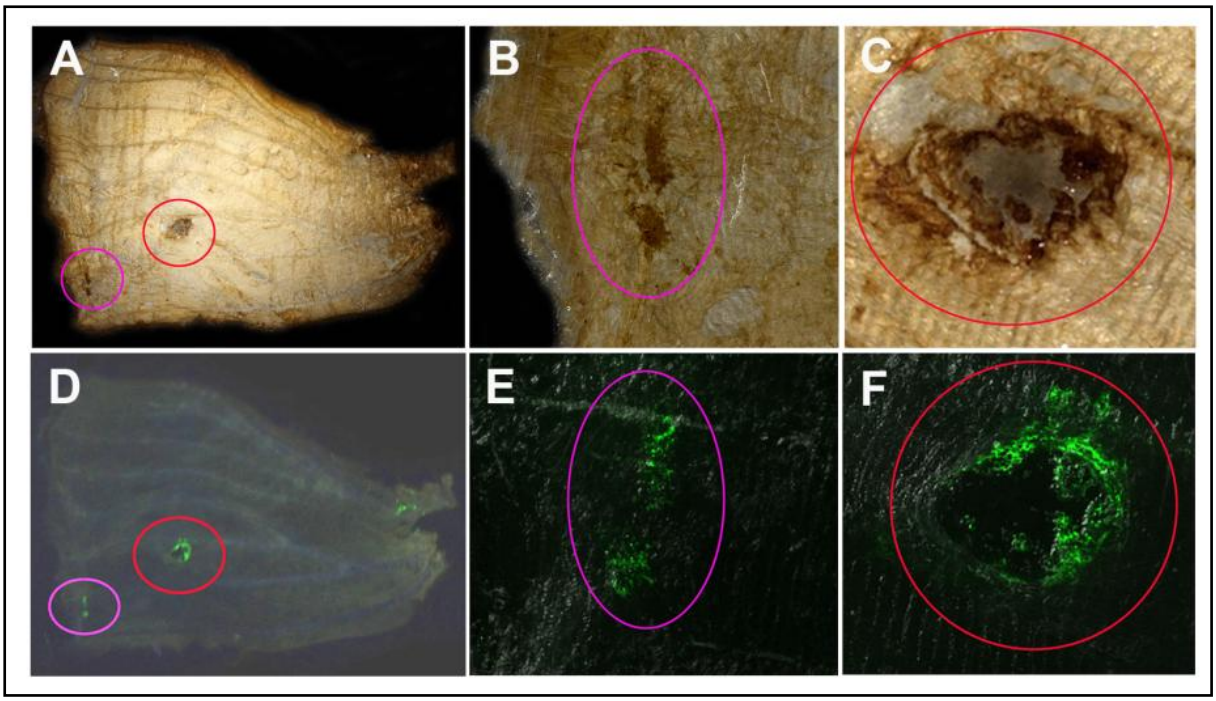

Fig. 2.6. Immunohistochemical detection of GFP on developing *J.orithya* pupal wings with anti-GFP antibody. A fourth day pupal wing infected with 2.0×10^4 pfu/mL baculovirus vector (2.0 μL, 18-24 hours post-pupation) and treated with anti-gp64 antibody. Immunohistochemical DAB staining and GFP fluorescent signals overlapped with each other. (**A-C**) Immunohistochemical DAB staining using anti-GFP antibody. Two major regions indicated by circles were stained in A, and they are magnified in B and C. (**D-F**) GFP fluorescence signals from the same in A-C. Two major regions indicated by circles showed fluorescence, and they are magnified in E and F.

Chapter 3

Baculovirus-mediated over-expression of *Dll* and *inv* gene in *Junonia orithya* pupae

3.1. Introduction

Butterfly wings are extraordinary resources of pattern elements. Butterfly wing color pattern study actually helps with study of the development and evolution of pattern elements (Nijhout, 1991). An eyespot is a simple circular arrangement of colored scales. It is a widely studied pattern element of butterfly wings. Many nymphalid butterfly wing color pattern consists of eyespots, such as the blue pansy *Junonia orithya*, the buckeye *Junonia coenia*, and squinting bush brown *Bicyclus anynana.* Eyespots are also believed to play roles in predator's interactions. The developmental mechanism of these eyespots has been studied in nymphalid butterflies. The results of *in situ* hybridization and immunohistochemistry have shown that several genes that also makes the wing of *Drosophla melanogaster* such as *Distal-less (Dll), Notch (N), invected (inv), hedgehog (hh), cubitus interruptus (ci), patched (patch), spalt (sal)* might be involved in eyespot development. Recently, in *B. anynana* another gene *Antennapedia* expression was shown to be the earliest and exclusive at the foci (Saenko *et al*., 2011). *Dll, Inv,* and *Sal* are all expressed at larval wing at eyespot center and present even at the pupal stage. Later, at pupal stage, their expression could still be seen in a group of epidermal cells, the scale building cells, around foci together with other genes pMad, Wg. Furthermore, the expression region of these developmental genes also resembles eyespot in the adult's wings (Carroll *et al*., 1994; Brakefield *et al*., 1996; Keys *et al*., 1999; Weatherbee *et al*., 1999; Brunetti *et al*., 2001; Reed *et al*., 2004; Monteiro *et al*., 2006). Together, the unique expression pattern of these genes in eyespot formation, first at the eyespot foci and later again around foci in the scale building cells and also its resemblance with adult eyespot implicate their role in eyespot development.

Sindbis virus (Lewis *et al*., 1999) has been used in homeotic gene *Ultrabithorax* function during development using a species of butterfly *J. coenia* but with limited success. Furthermore, baculovirus has also been used in ectopic gene expression in other species the fruit fly *Drosophila melanogaster*, the beetle *Tribolium castaneum*, and a vertebrate *Xenopus laevis* (Oppenheimer *et al.*, 1999). Recently, baculovirus-mediated transfer of foreign gene in *J. orithya* has been reported (Dhungel *et al*., 2013). The expression of reporter gene *gfp* has been shown without any color pattern modification. This new reliable and reproducible baculovirus tool in a butterfly system opened a gateway for functional studies of candidate gene in wing color pattern study.

Among the various genes expressed at the prospective eyespot foci and scales building cells around the prospective foci, *Dll* is unique. *Dll* gene has been cloned and studied in two different butterflies *J. coenia* (Panganiban *et al*., 1994) *and B. anynana* (Beldade *et al*., 2002). In *J. coenia,*

*Dll'*s role in the development and evolution of insect limbs has been studied (Panganiban *et al*., 1994). However, in *B. anynana,* polymorphism in *Dll* has been linked with different eyespot sizes. The difference in sizes of eyespot in *B. anynana* has been contributed by DNA polymorphism in *Dll* gene (Beldade *et al*., 2002). *Dll* could be responsible for eyespot formation and evolution.

Virus-mediated *in vivo* expression system has been used for functional assay of candidate genes *wingless* (Oppenheimer *et al*., 1999) and *Ultrabithorax* (Lewis *et al*., 1999) in insects. Similarly, in this chapter, baculovirus tool was used for ectopic expression of candidate genes *Dll* and *inv* whose role in eyespot development has been implicated. Earlier, the expression of reporter gene *gfp* was already shown with baculovirus mediated *in vivo* functional assay system. *Dll* and *inv*-baculovirus construct were designed and *J. orithya* pupae were infected with Dll and Inv-baculovirus. Currently, we are lacking *Dll* and *inv* sequences from *J. orithya*. So in designing *Dll* (Panganiban *et al*., 1994) and *inv* (Carroll *et al*., 1994) baculovirus construct, we used the already reported sequence from related species *J. coenia*.

The purpose of this chapter is to examine the functional role of candidate genes *Dll* and *inv* in butterfly eyespot formation using the blue pansy *J. orithya* as an experimental organism using the baculovirus tool.

3.2. Methods

3.2.1. Butterflies

We used the blue pansy butterfly *Junonia orithya* (Linnaeus, 1758). Female adult individuals were field-caught in Okinawa-jima Island or Ishigaki-jima Island in the Ryukyu Archipelago, Japan. Eggs were collected from these females. Alternatively, larvae were field caught in these islands. Larvae were fed their natural host plants at ambient temperature.

3.2.2. Distal less-baculovirus, Invected-baculovirus and anti-gp64 antibody

Two recombinant baculovirus vectors, Distal less-baculovirus (Dll-baculovirus) and Invected baculovirus (Inv-baculovirus) vector containing the *Aequorea victoria* green fluorescent protein (*GFP*) gene under the control of the polyhedrin promoter was obtained from AB Vector (San Diego, CA, USA). We designed a recombinant Dll-baculovirus vector, which contains expression unit for *Dll* (based on *J. coenia Dll* sequence). The construct contains *Dll*-Spacer-*gfp*-His6-Stop. Similarly, Inv-baculovirus (based on *J. coenia inv* sequence) was designed and obtained from WAKO (Osaka, Japan). Dll-baculovirus can express Dll and GFP as two separate functional proteins. Furthermore, Inv-baculovirus can express two separate functional proteins Invected and GFP.

A mouse monoclonal antibody IgG_2a against baculovirus gp64 (AcV1) of extracellular nonoccluded AcNPV (*Autographa californica nucloepolyhedrovirus*) was obtained from Santa Cruz Biotechnology (Santa Cruz, CA, USA).

3.2.3. Injection

Pupae were injected with 2.0 μL of a solution containing the recombinant baculovirus construct through the cuticle of abdomen within 18-24 hours after pupation, followed by 2.0 μL of anti-gp64 antibody after 6 hours post-infection at the same position, using an Ito microsyringe (Fuji, Shizuoka, Japan).

3.2.4. Visualization of GFP fluorescent signal, pupal wing dissection and immunohistochemistry

The detail procedures are described in Dhungel *et al*., (2013) and Chapter 2.

3.2.5. *Distal less-gfp and invected-gfp* construct detection

Pupae were injected with Dll or Inv-baculovirus followed by anti-gp64 antibody. After 3 days of anti-gp64 antibody injection, pupal wings were dissected. Isolated wings were readily frozen at -80 °C. RNeasy kit was used for RNA isolation and *Dll-gfp* construct was detected by PCR using a part of *Dll* sequence as an upstream primer (designed form *Dll* sequence from *J. coenia*) and a part of *gfp* sequence as a downstream primer. Similarly, *inv-gfp* construct was detected using a part of *inv* sequence as an upstream primer and a part of *gfp* sequence as a downstream primer.

3.2.6. Semi-quantification of *Distal-less* and *invected* in infected and non-infected individuals using RT-PCR

Total RNA from dissected wings of treated and non-treated pupae were isolated. *Dll* and *inv* mRNA in treated and non-treated individuals was measured and compared using RT-PCR and Image analysis software.

Agarose gel images were taken with Image Quant LAS 400 (GE Healthcare Life Sciences, Japan) with following parameters: precision exposure type; 1/8 exposure time; standard sensitivity/resolution; epi illumination fluorescence (EtBr) and UV (Trans-UV) Light method; 2 tray position with 605DF40 filter and F2.8 Iris.

For PCR band measurement, the image taken with Image Quant LAS 400 was used for image analysis in Image Quant TL 7.0 400 (GE Healthcare Life Sciences, Japan). First, the lanes were created manually in the image based on the number of bands on an agarose gel (3 lanes in this case),

followed by background subtraction with rubber band method, and finally, bands were detected. Each detected band was provided with a volume and we used the volume for our analysis.

For comparision between *Dll* and *inv* gene expression levels in infected and non-infected individuals, we used fourth-day pupae in both cases, infected and non-infected. For normalization, we used data from non-infected first-day pupae.

3.3. Results

3.3.1. Expression of *Dll-gfp* using recombinant Dll-baculovirus in pupae

Originally, GFP-baculovirus were diluted in 1/5000 and injected within 18-24 hours of pupation followed by anti-gp64 antibody 18-24 hours post-infection (Dhungel *et al*., 2013). But with new virus Dll-baculovirus, different dilutions were tried, although the GFP rate was 50-100 %, eclosion rate was 0 % except in 1/10000 dilution (Table 3.1). The expression of the *deal* was verified with the presence of GFP fluorescence from the wings and other body parts of infected pupae. GFP fluorescence was seen in pupal wing (Figs. 3.1C-G), apart from the wings, GFP fluorescence was frequently observed from antennae (Fig. 3.1H).

Surprisingly, even with the use of anti-gp64 antibody we were still having problem of high pupal mortality of 100% associated with baculovirus injection. Later different dilutions for Dll-baculovirus and timing for anti-gp64 antibody injection was tried. In two dilutions, 1/100 and 1/500, and anti-gp64 antibody injection 6 hours post-infection, we were able to obtain adults with GFP fluorescence from adult wings (Table 3.2).

Pupal wings infected with Dll-baculovirus followed by anti-gp64 antibody were isolated and developing cells were checked for fluorescence (n = 5) with a confocal microscope. The fluorescence was detected in the developing cells of wings (Figs. 3.2C, D)

For Inv-baculovirus, new optimized conditions as Dll-baculovirus were used. Dilution conditions 1/100 and 1/500 followed by anti-gp64 antibody 6 hours post-infection were used.

3.3.2. Expression of *Dll-gfp* using recombinant Dll-baculovirus in adults

Expression of *Dll-gfp* (n = 11, Figs. 3.3A-Q) and *Inv-gFP* (n = 2, Figs. 3.4 A-H) was detected with GFP fluorescence. The adults were screened for GFP signals or any wing color-pattern modifications.

Dll-baculovirus was able to produce a wing color pattern modification (Fig. 3.3). It was able to induce some pattern changes together, and in addition GFP fluorescence was also recorded from the identical locations (Figs. 3.3B, C, F, G, J, and K n = 3). But the damage associated with Dll-baculovirus was

inevitable. Damaged location in wings together with GFP fluorescence were seen (Figs. 3.3O, Q, n=8). Furthermore, color pattern modification was seen without GFP signals (Figs. 3.3R-U, V-Y, *n* = 2).

Inv-baculovirus was able to produce a wing color pattern modification (Fig. 3.4). It was able to induce some pattern changes together, and in addition GFP fluorescence was also recorded from the identical locations (Figs. 3.4C, G, K, O, *n* = 11). But the damage associated with Dll-baculovirus was inevitable. Damaged location in wings together with GFP fluorescence were seen (Figs. 3.3S, W, n=3). Furthermore, color pattern modification was seen without GFP signals (Figs. 3.5A-C, *n* = 2).

Both Dll and Inv-baculovirus were able to modify the wing color-pattern. *Dll* and *inv* were able to generate small spot-like structure but not a full ectopic eyespot.

3.3.3. Immunohistochemical detection of Distal less and Invected in pupal wings

The GFP signal from the developing pupae was easily seen. This could also be the probable location of *Dll* expression site. We used DAB staining for the Dll gene product detection. The spatial location of chromogenic DAB signal for anti-Dll antibody (Figs. 3.6 A-C, Fig. 3.7 A-C) and the GFP fluorescence (Figs. 3.6 D-F, Fig. 3.7 D-F) were completely overlapped (*n* = 5).

3.3.4. Detection of *Distal-less-gfp* and invested-*gfp* gene transcript in the pupal wing by RT-PCR

Wings from pupae treated with Dll-baculovirus and Inv-baculovirus were isolated and subjected for RNA isolation. The *Dll-gfp* and *inv-gfp* gene construct were detected by RT-PCR. The size of *Dll-gfp* construct was around 2000 base pairs (Figure 3.8A) and that of *inv-gfp* was around 450 base pairs (Fig. 3.8B).

3.3.5. Semi-quantification of *Dll* and *inv* gene in infected pupae

Total *Dll* and *inv* the gene transcript was semi-quantified by PCR and gene quant software. The *Dll* (Fig. 3.8C) and i*nv* (Fig. 3.8D) PCR products from the wings of baculovirus infected pupae on the fourth day and control pupae from the first and fourth day.

In Dll-baculovirus, we found 3.84 (Fig. 3.8E, $p = 0.005$, *t*-test) fold increases compared to control pupae. We obtained 2.14 (Fig. 3.7 F, $p = 0.03$, *t*-test) fold increase with Inv-baculovirus. Baculovirus were able to over-express *Dll* and *inv* gene in infected pupae.

3.4. Discussion

After the successful use of the baculovirus tool in gene function study of butterflies with reporter gene *gfp,* two candidate genes *Dll* and *inv* were tested whose functions were implicated in eyespot formation. However, the new baculovirus titer and also timing of antibody injection post-baculovirus injection was optimized first. Usual injection time of antibody 18- 24 hours post-infection caused 100% pupal mortality. It seems *Dll* expression is more toxic than *gfp* expression. The original protocol was slightly modified, by injecting anti-gp64 antibody 6 hours post-infection and was able to get adult buttery wings with modified color patterns.

As expected, heterogeneous infection in various parts of pupae was seen even at the same titer. Such variation has been observed with baculovirus (Dhungel *et al*., 2013) as well as other viral systems (Zhao *et al*., 1996; Zhao *et al*., 1998). We designed the baculovirus construct with general promoter polyhedron, and the GFP expression was seen throught out the body. The pupal wings together with other parts of pupa such as antennae, legs were infected. Such broad tissue tropism was also observed with baculovirus in *J. orithya* (Dhungel *et al*., 2013) and *Xenopus* larvae (Oppenheimer *et al.,* 1999) and Sindbis virus in *J. coenia* (Lewis *et al*., 1999). In future, to target the expression of candidate gene only to the wings, we need to use wing specific promoter rather than general promoter polyhedron. However, at the moment no such promoter that is specific to butterfly wing is known to us. Although, the expression is throught the pupal body mostly the expression of foreign gene is from the wings. Currently, we are getting the desired expression at the wing even with the polyhedron promoter; it can be used until another promoter specific to wing is found.

Candidate genes *Dll* and *inv* were tested for deciphering their possible role in eyespot development. The ectopic expression of *Dll* in both pupae and adults were verified with marker protein GFP. The green fluorescence signal was seen in both pupae and adult wings with Dll-baculovirus but only in adult wings with Inv-baculovirus. GFP fluorescence from Inv-baculovirus was too faint to be detected under the whole mount detection system. GFP fluorescence has been reported earlier, from pupal wings of silkworm and butterfly and adult scales of butterfly (Ando and Fujiwara, 2013; Lewis *et al*., 1999; Dhungel *et al*., 2013). Previously, another candidate gene *Ubx* role in homeotic transformation was deciphered using recombinant Sindbis viruses and *J. coenia. Ubx* expression in forewing had hindwing like characteristic (Lewis *et al*., 1999).

Individuals with the modified color pattern were obtained. When the precise location of the modified color pattern on the wings was observed for GFP signals, we were able to get GFP signals from some only. The expression of neither *gfp* nor the virus only can modify the normal color pattern (Dhungel *et al*., 2013; Lewis *et al*., 1999). We can thus conclude that the wing color pattern modifications are due to the candidate genes *Dll* and *inv*. However, no ectopic eyespot was developed

with the over-expression of the candidate gene *Dll* and *inv*. They were able to induced ectopic black spot but no eyespots are induced, the possibility is that no downstream genes are upregulated with the expression of *Dll* or *inv* only. These transcription factors can generate structure like black spots alone but together might be responsible for eyespot formation. Others candidate genes such as *sal* and *notch* are also equally important for eyespot development together with *Dll* and *inv*.

Similar color pattern modifications with both *Dll* and *inv* gene were found. The modified wings often had many small ectopic spots and an unorganized scale arrangement in the center of the ectopic spots. Spots with organized scales with damage and no GFP signals were also obtained. However, without the GFP signal it is very difficult to confirm if those color pattern changes are due to *Dll* or *Inv.*There is also the possibility that, the modifications are caused by *Dll* or *Inv* gene at the pupal stage but the GFP signals degraded or too weak to detect when they became adults. The GFP fluorescence from adult wing scales are difficult to observe.GFP signal was relatively very stronger in control baculovirus compared to GFP from Dll and Inv-baculovirus. *Dll* and *inv* are nuclear DNA, the signal from GFP in Dll-baculovirus and Inv-baculovirus is comparatively weaker than control GFP-baculovirus.

At the center of the eyespot *Dll, inv and sal* are expressed together (Keys *et al*., 1999). In the future, we could make recombinant baculovirus with candidate genes *Dll, inv and sal* in one construct and see if the combined effect of these genes is enough for eyespot formation. Possibly, a single gene is not enough for eyespot formation but they could generate some color pattern modifications like spots only. If we could express these genes together in the same cell or nearby cells then the cell or group of cells can themselves act as focus and guide in the development of eyespot as in native eyespot development.

Furthermore, the timing of ectopic gene expression is very critical. These candidate genes are expressed at prospective focus at late larval stage or early pupal stage 16-36 hours (Keys *et al*., 1999; Brunetti *et al*., 2001; Monteriro *et al*., 2006). With the recently developed baculovirus tool, we were able to express *Dll* and *Inv* only after they have already been pupae. If we are able to express the candidate genes earlier, there is a possibility of obtaining ectopic eyespots.

The over-expression of the candidate gene is one way of finding the functional proof for the gene. There are other mehods of functional analysis by silencing of the gene is also available, such as RNAi and morpholinos. Unfortunately, at present there are no reliable and reproducible tools for silencing gene in butterfly. In future reliable tools for RNAi and morpholinos have to be established and see the effect of silenced gene in wing color pattern formation. Together the ectopic expression of candidate gene and silencing of the candidate genes will be helpful in wing color pattern formation study.

In summary, the candidate genes *Dll* and i*nv* can generate some wing color pattern changes but not the eyespot formation. These genes are responsible but not sufficient for eyespot formatation.

3.5. Conclusions

With the baculovirus tool, it is now feasible for testing a candidate gene in functional study. We tried candidate genes *Dll* and *inv* regarding their functional role in eyespot development. Modified wing color patterns were produced, however, did not produce any eyespots when candidate genes were expressed ectopically by baculovirus. It seems that they are responsible but not sufficient for eyespot formation. Possibly, other gene s*al* or all genes *Dll*, *inv* and s*al* together can induce eyespot formation. Furthermore, this baculovirus tool can also be used in gene functions study in other non-model insects.

3.6. References

Ando T, Fujiwara H: Electroporation-mediated somatic transgenesis for rapid functional analysis in insects. Development 2013, 140: 454-458.

Beldade P, Brakefield PM, Long AD: Contribution of *Distal-less* to quantitative variation in butterfly eyespots. Nature 2002, 315-318.

Brakefield PM, Gates J, Keys D, Kesbeke F, Wijngaarden PJ, Monteiro A, French V, Carroll SB: Development, plasticity and evolution of butterfly eyespot patterns. Nature 1996, 384:236-242.

Keys DN, Lewis DL, Selegue JE, Pearson BJ, Goodrich LV, Johnson RL, Gates J, Scott MP, Carroll SB: Recruitment of a hedgehog regulatory circuit in butterfly eyespots evolution. Science 1999, 283:532-534.

Brunetti CR, Selegue JE, Monteiro, A, French V, Brakefield PM, Carroll SB: The generation and diversification of butterfly eyespot color patterns. Current Biology 2001, 11:1578-1585.

Carroll SB, Gates J, Keys DN, Paddock SW, Panganiban GE, Selegue JE, Williams JA: Pattern formation and eyespot formation in butterlfly wings. Science 1994, 265:109-114.

Dhungel B, Ohno Y, Matayoshi R, Otaki JM: Baculovirus-mediated gene transfer in butterfly wings in vivo: an efficient expression system with anti-gp64 antibody. BMC Biotechnology 2013, 13:27

Lewis DL, DeCamillis MA, Brunetti CR, Halder G, Kassner VA, Selegue JE, Higgs S and Carroll SB: Ectopic gene expression and homeotic transformation in arthropods using recombinant Sindbis viruses. Current Biology 1999, 9:1279-1287.

Monteiro A, Glaser G, Stockslager S, Glansdrops N, Ramos D: Comparative insights into questions of lepidopteran wing pattern homology. BMC Developmental Biology 2006, 6:52.

Nijhout HF: The development and evolution of butterfly wing patterns Washington, USA: Smithsonian Institution Press; 1991.

Oppenheimer DI, MacNicol AM, Patel NH: Functional conservation of the wingless-engrailed interactions as shown by a widely applicable baculovirus misexpression system. Current Biology 1999, 9: 1288-1296.

Panganiban G, Nagy L, Carroll SB: The role of the *Distal-less* gene in the development and evolution of insect limbs. Current Biology 1994, 8: 671-675.

Reed RD, Serfas MS: Butterfly wing pattern evolution is associated with changes in a *Notch/Distal-less* temporal pattern formation process. Current Biology 2004, 14:1159-1166.

Saenko SV, Marialva MS, Beldade P: Involvement of the conserved Hox gene *Antennapedia* in the development and evolution of a novel trait. Evo Devo 2011, 2:9.

Weatherbee SD, Nijhout HF, Grunert LW, Halder G, Galant R, Selegue J, Carroll, S: *Ultrabithorax* function in butterfly wings and the evolution of insect wing patterns. Current Biology 1999, 9:109-115.

Zhao H, Otaki JM, Firestein S: Adenovirus-mediated gene transfer in olfactory neurons in vivo. Journal of Neurobiology 1996, 30:521-530.

Zhao H, Ivic L, Otaki JM, Hashimoto M, Mikoshiba K, Firestein S: Functional expression of a mammalian odorant receptor. Science 1998, 279:237-242.

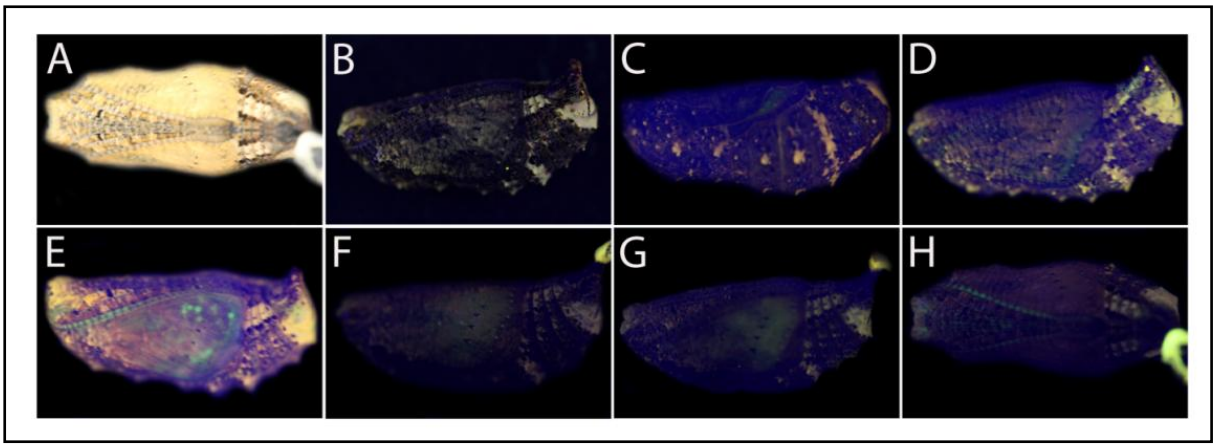

Fig. 3.1. Baculovirus-mediated *gfp/Dll* expression in *J. orithya* pupae. Baculovirus was injected at the pupal stage 18-24 hours post-pupation followed by anti-gp64 antibody injection (2.0 µL) 18-24 hours post-infection, except G in which anti-gp64 antibody was injected post 6 hours post-infection. (**A**) A whole pupa under the bright field. This individual is identical to H. The injection consisted of 2.0 µL at 1/5 dilutions. (B-H) Whole pupae under blue light showing GFP fluorescence. (**B**) No injection (normal pupae) and no GFP fluorescence. (**C-E**) GFP fluorescence from wings. The injection consisted of 2.0 µL at 1/10 dilutions. (**F**) GFP fluorescence from the wings. The injections consisted of 2.0 µL at 1/5 dilutions. (**G**) GFP fluorescence from the wings. The injection consisted of 2.0 µL at 1/5 dilutions. (**H**) GFP fluorescence from antennae. This individual is same as A.

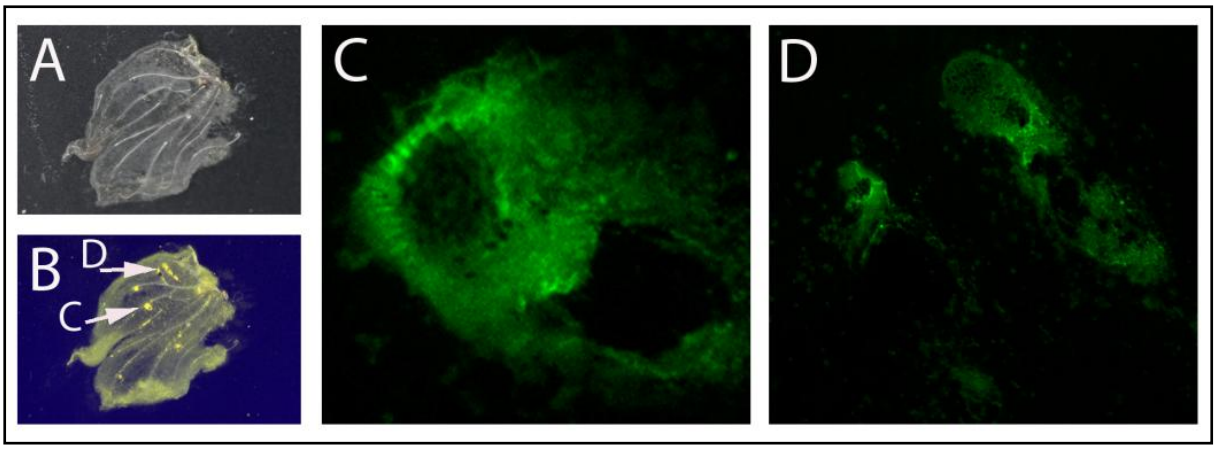

Fig. 3.2. *Dll* expression/GFP fluorescence in developing *J. orithya* pupal wing at the cellular level. The baculovirus-Dll-GFP vector of 2.0 µL was injected at 1/500 dilutions 18-24 hours post-pupation, followed by anti-gp64 antibody injection (2.0 µL) 6 hours post-infection. Pupal wings were dissected 24 hours post-antibody treatment. (**A**) A whole wing under bright field. (**B**) A whole wing identical to A under blue light. No GFP fluorescence was seen at low magnification. (**C**) High magnification fluorescent region, probable location is shown in B with an arrow. (**D**) High magnification of another fluorescent region, probable location is shown in B with an arrow.

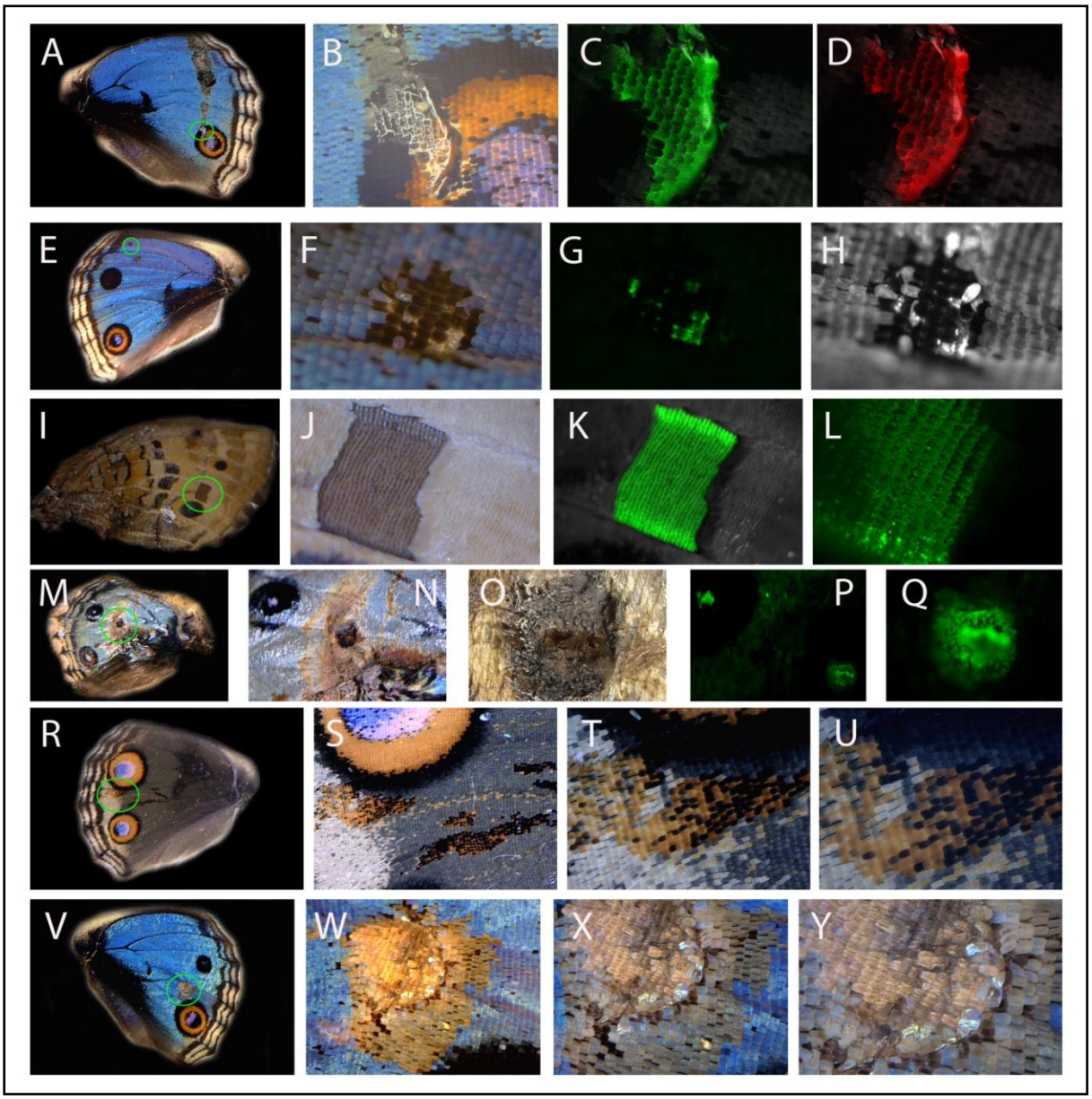

Fig. 3.3. Baculovirus-Dll-GFP vector mediated GFP/DLL expression in *J. orithya* adults obtained from baculovirus-injected and antibody-injected individuals. In all cases, injection containing 2.0 µL baculovirus-Dll-GFP at 1/500 dilutions except R (1/100 dilutions) was made 18-24 hours post-pupation followed by antibody injection (2.0 µL) 6 hours post-infection. (**A**) An adult dorsal hindwing. Encircled region is enlarged in B. (**B**) High magnification of A. (**C**) High magnification of B under blue light. Green fluorescence was observed in the region with ectopic structures. (**D**) High magnification of B under green light. Red fluorescence was observed in the region. The fluorescence was seen from the scales. (**E**) Another adult dorsal hindwing, with modified color pattern with small black spot. Encircled region is enlarged in F. (**F**) High magnification of E. (**G**) The same wing as F under blue light showing green fluorescence from location beneath the scales of basal region. No fluorescence is observed from the scale. (**H**) The same wing as G under bright light. (**I**) An adult ventral forewing. Encircled region enlarged in J. (**J**) High magnification of I, showing a region of

immature scales. (**K**) The same wing as J under blue light. Green fluorescence observed from immature scales. (**L**) High magnification of K. (**M**) Another modified dorsal hindwing. Encircled region is enlarged in N. (**N**) High magnification of M with ectopic spot. (**0**) High magnification of N. The center of the ectopic spot is blackened and no scales present. (**P**) The same wing as N under blue light. Green fluorescence at the center of the spot and eyespot center. (**Q**) High magnification of P showing green fluorescence at the center of the ectopic spot. (**R**) Another modified dorsal hindwing. Encircled region is enlarged in S. (**S**) High magnification of R. Group of colored scales, similar to eyespot. However, no green fluorescence was detected. (**T**) High magnification of S. (**U**) High magnification of T. (**V**) Another modified dorsal hindwing. Encircled region is enlarged in W. (**W)** High magnification of V. Yellow like spot with organized scales. No green fluorescence was seen from yellow like spot. (**X**) High magnification of W. (**Y**) High magnification of X. Yellow like spot is composed of yellow and black scales.

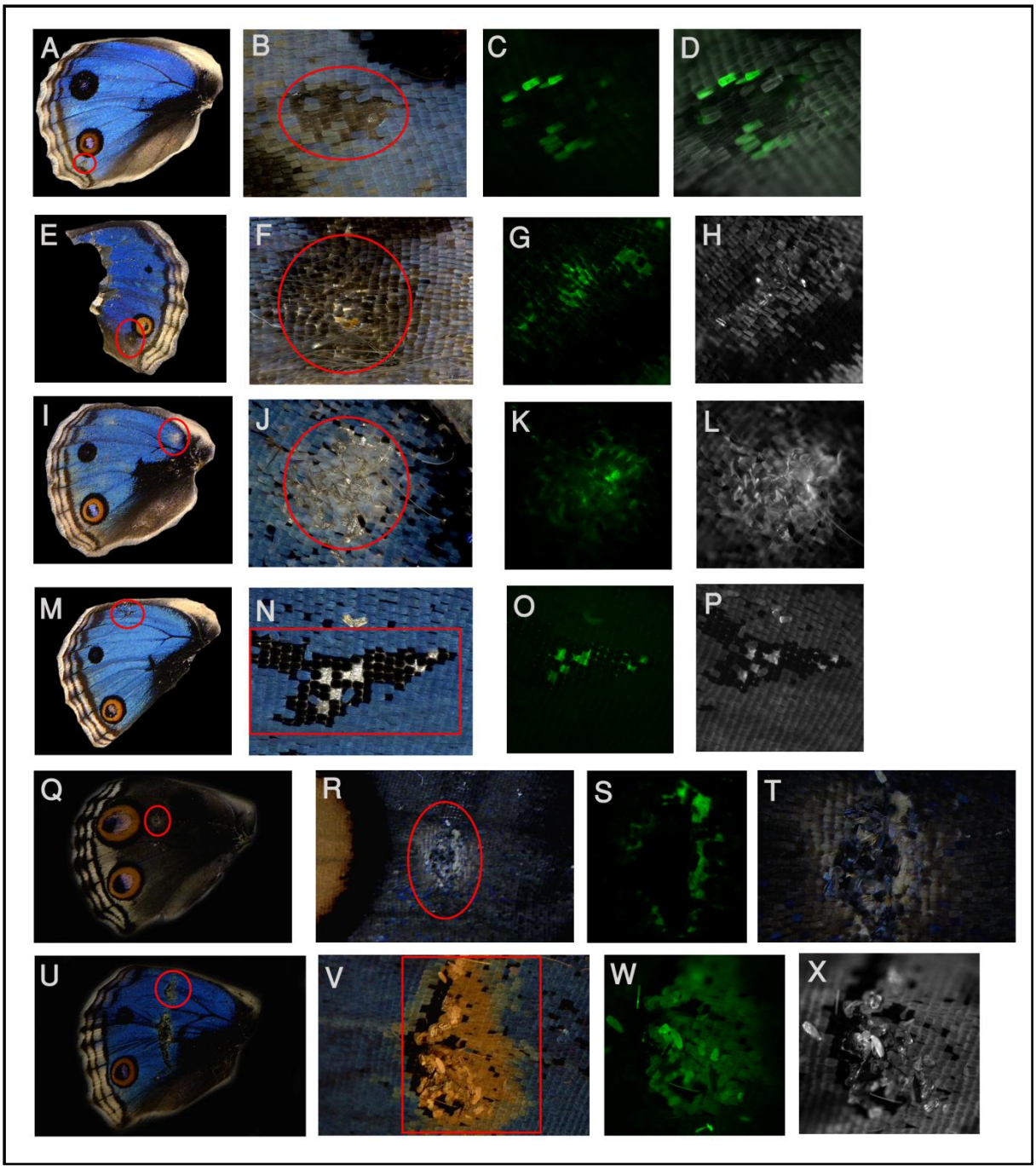

Fig.3.4. Baculovirus-Inv-GFP mediated Inv/GFP expression in *J. orithya* adults obtained from baculovirus-injected and antibody injected individuals. The injection consisted of 2.0 µL baculovirus-Inv-GFP vector 18-24 hours post–pupation, followed by 2.0 µL anti-gp64 antibody injections 6 hours post-infection. (**A**) A modified adult dorsal hindwing. The infection was at 1/100 baculovirus-Inv-GFP dilutions. Encircled region is enlarged in B. (**B**) High magnification of A. A spot is induced. (**C**) The wing similar to C under blue light. Green fluorescence at the scales. (**D**) A composite picture of C in bright field (**E**) Another modified adult dorsal hindwing. An injection at 1/100 diluted baculovirus-Inv-GFP was made. Encircled region enlarged in F. (**F**) High magnification of E. (**G**) The wing similar as F under blue light. Green fluorescence from the scales at the spot. (**H**) The wing same as G

under bright light. (**I**) An adult dorsal modified hindwing. Encircled region enlarged in J. An injection at 1/100 diluted baculovirus-Inv-GFP was made. (**J**) High magnification of I (**K**) The same wing as J under blue light. Green fluorescence observed from basal area where scales are removed. (**L**) The same wing as K under bright light. (**M**) Another modified dorsal hindwing. Encircled region is enlarged in N. An injection was made at 1/10 diluted baculovirus-Inv-GFP. (**N**) High magnification of M with ectopic spot. (**O**) The same wing as N under blue light. Green fluorescence at from the area where scales have been removed (**P**) The same wing as O under bright light. (**Q**) Another modified dorsal hindwing. The infection was at 1/100 baculovirus-Inv-GFP dilutions Encircled region is enlarged in R (**R**) High magnification of Q. A spot is induced. (**S**) The same wing as R under blue light, showing GFP from damaged site. (**T**) The same wing as S under bright light. (**U**) Another modified adult dorsal hindwing. An injection at 1/1000 diluted baculovirus-Inv-GFP (**V**) High magnification of U. A spot with yellow scale at periphery and disorganized scales at the center. (**W**) The wing similar as V under blue light. Green fluorescence from the scales at the spot.(**X**) The wing same as G under bright light.

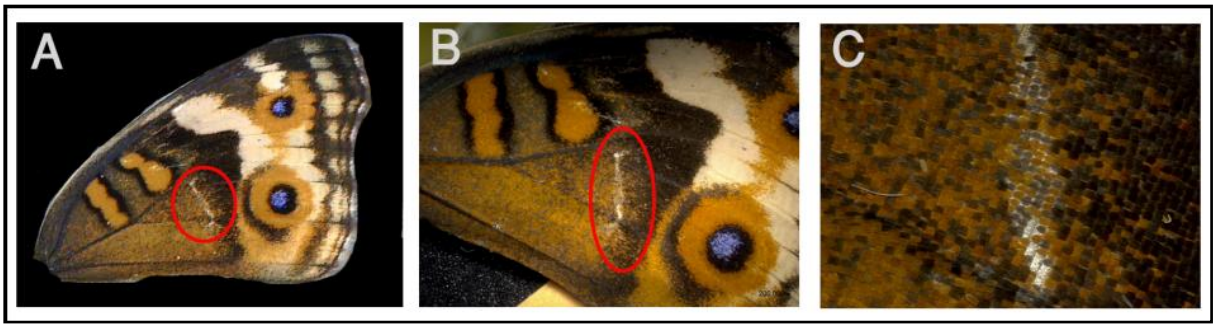

Fig. 3.5. Baculovirus-Inv-GFP mediated Inv/GFP expression in *J. orithya* adults obtained from baculovirus-injected and antibody injected individuals. The injection consisted of 2.0 µL baculovirus-Inv-GFP vector 18-24 hours post–pupation, followed by 2.0 µL anti-gp64 antibody injections 6 hours post-infection. The infection was at 1/10 baculovirus-Inv-GFP dilutions. (**A**) A modified adult dorsal forewing. A spot is induced but no GFP is seen from the spot. Encircled region is enlarged in B. (**B**) High magnification of A. (**C**) High magnification of encircled region of B.

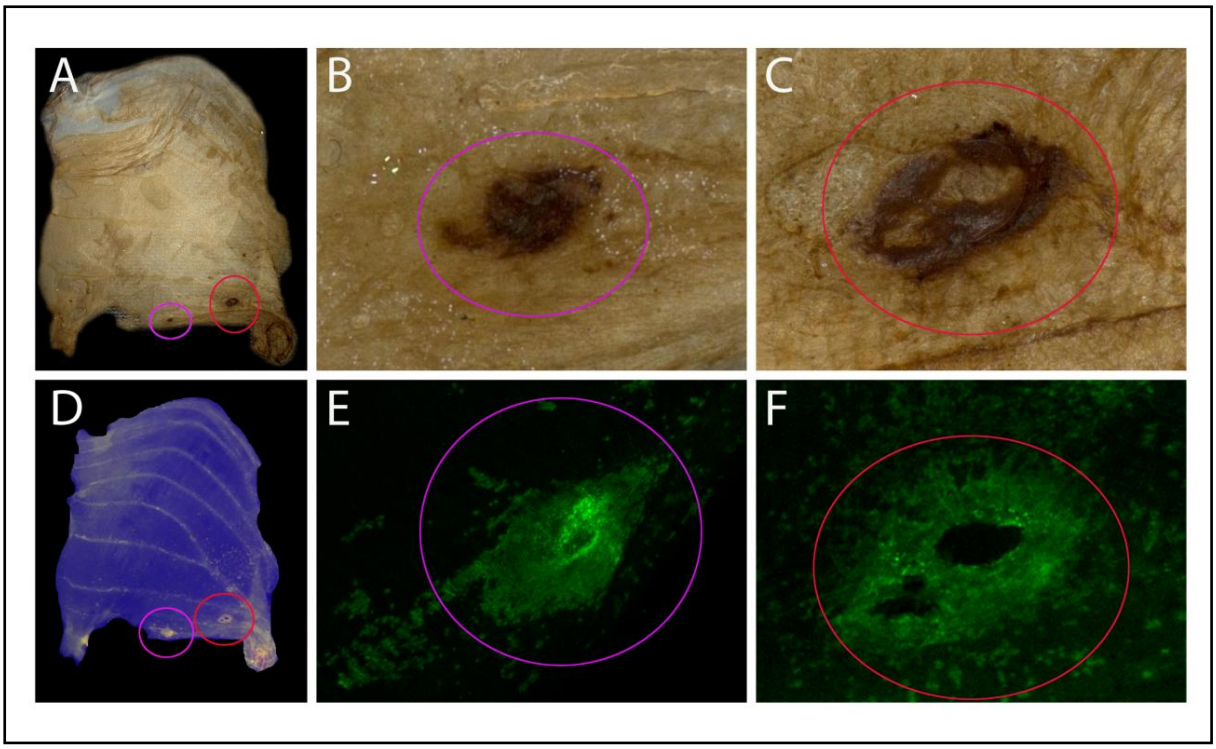

Fig. 3.6. Immunohistochemical detection of Dll in developing *J. orithya* pupal wings with anti-Dll antibody. A fourth day pupal wing infected with 1/500 diluted Dll baculovirus vector post (2.0 µL, 18-24 hours post-pupation) and treated with anti-gp64 antibody (2.0 µL, 6 hours post-infection) is shown. Immunohistochemical DAB staining for anti-Dll antibody and GFP fluorescent signals overlapped with each other. (**A-C**) Immunohistochemical DAB staining using anti-Dll antibody. Two major regions indicated by circles were stained in A, and they are enlarged in B and C. (**D-F**) GFP fluorescence signals from the same wing in A-C. Two major regions indicated by circles showed fluorescence, and they are magnified in E and F.

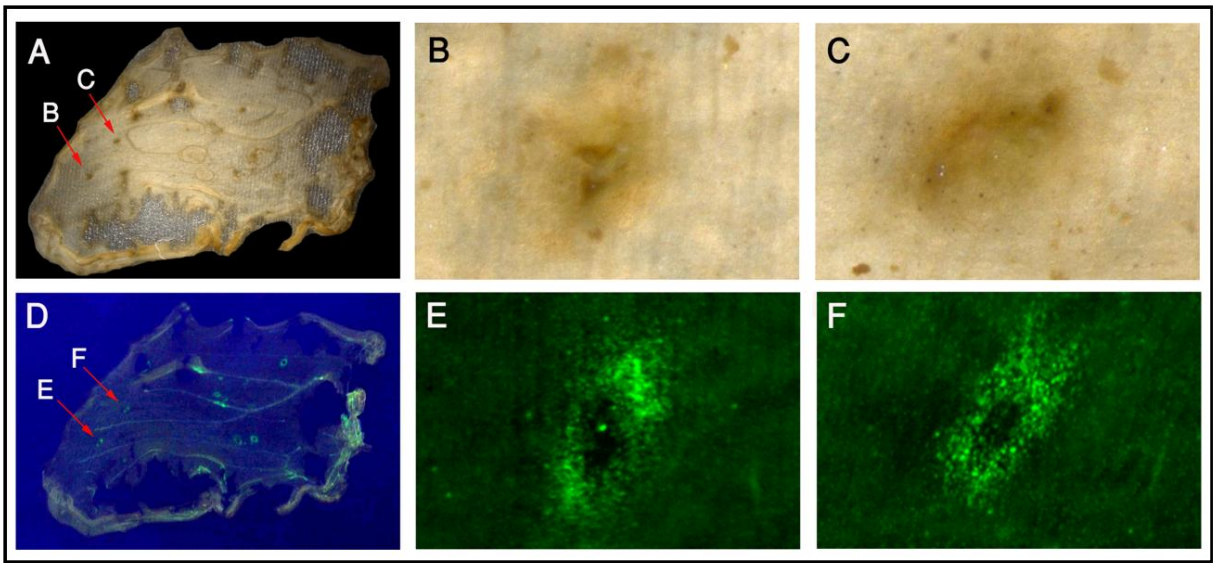

Fig. 3.7. Immunohistochemical detection of Dll in developing *J. orithya* pupal wings with anti-Dll antibody. A fourth day pupal wing infected with 1/10 diluted Dll baculovirus vector post (2.0 µL, 18-24 hours post-pupation) and treated with anti-gp64 antibody (2.0 µL, 6 hours post-infection) is shown. Immunohistochemical DAB staining for anti-Dll antibody and GFP fluorescent signals overlapped with each other. (**A-C**) Immunohistochemical DAB staining using anti-Dll antibody. Two major regions indicated by red arrows were stained in A, and they are enlarged in B and C. (**D-F**) GFP fluorescence signals from the same wing in A-C. Two major regions indicated by red arrows showed fluorescence, and they are magnified in E and F.

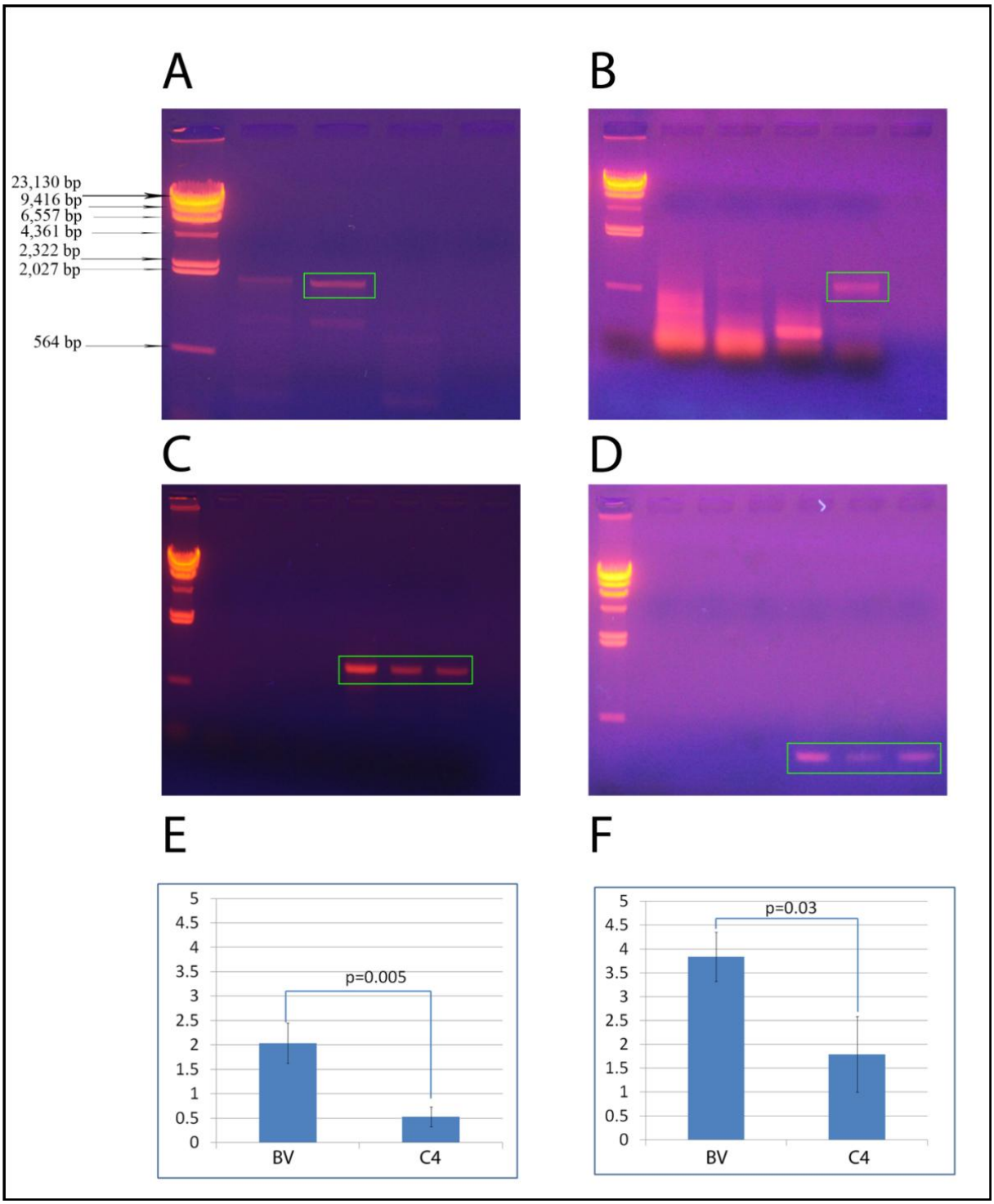

Fig. 3.8. Detection of Dll-GFP and Inv-GFP constructs in developing *J. orithya* pupal wings with PCR and semi-quantification of *Dll* and *Inv* gene in treated and non treated pupae. RNA from a fourth day pupal wing infected with baculovirus-Dll (1/100) and baculovirus-Inv (1/500) independently was isolated and used for further experiments. Using RT-PCR, *Dll-GFP* and *Inv-Dll* were detected. *Dll* and *Inv* gene expression level were semi quantified using PCR and gene quant software, and compared between fourth day baculovirus infected and fourth day control pupae. (**A**) An agarose gel. The *Dll-GFP* band is shown in the green rectangular box. The marker size is given in base pair and

applies to panel B, C, and D also. (**B**) Another agarose gel with *Inv-GFP* constructs shown in the green rectangular box. (**C)** Another agarose gel with PCR product of *Dll* from Dll baculovirus infected fourth day pupae (BV), first day (C1) and fourth day (C4) control pupae. Shown in green rectangular box. (**D**) Another agarose gel with PCR products of *Inv* from Inv-baculovirus infected fourth day pupae (BV), first (C1) and fourth day (C4) control pupae. Shown in green rectangular box. (**E**) Comparison of *Dll* expression in Dll-baculovirus infected pupae and controlled fourth day pupae. p = 0.05 from t-test. (**F**) Comparison of *Inv* expression in Inv-baculovirus infected pupae and controlled fourth day pupae. p = 0.03 from *t*-test.

Table 3.1. Baculovirus-Dll-GFP injection followed by an anti-gp64 antibody in *Junonia orithya.*

Dilution Factor	Number of pupae injected	Number of GFP positive individuals (%)	Number of non-GFP individuals (%)	Number of individuals eclosed successfully (%)
Undiluted	20	1 (5)	19 (95)	0 (0)
1/2	20	1 (5)	19 (95)	0 (0)
1/5	23	11 (47.83)	12 (52.17)	0 (0)
1/10	72	15 (20.83)	57 (79.17)	0 (0)
1/100	19	0 (0)	19 (100)	0 (0)
1/1000	20	0 (0)	20 (100)	0 (0)
1/10000	22	0 (0)	22 (100)	2 (9.09)

*Baculovirus-Dll-GFP (2 µL) injected at 18-24 hours post- pupation. Anti-gp64 antibody (2 µL) injected at 18-24 hours post-infection.

Table 3.2. Baculovirus-Dll-GFP injection followed by anti-gp64 antibody in *Junonia orithya.*

Dilutions, Volumes, Times	Number of pupae injected	Number of GFP positive pupae	Number of pupal wing	Number of GFP positive pupal wing	Pupal wing with GFP at wing	Adult wing	Adult wing with GFP	Adult wing with GFP at wing	Number of GFP positive individuals	Number of individuals eclosed successfully
1/10, 2uL, 3hr	19	7 (36.84)	1 (5.26)	0 (0)	NA	0	NA	NA	7 (36.84)	0 (0)
1/10, 2uL, 6hr	22	13 (59.09)	0 (0)	NA	NA	0	NA	NA	13 (59.09)	0 (0)
1/10, 2uL, 12hr	20	13 (65)	0 (0)	NA	NA	0	NA	NA	13 (65)	0 (0)
1/10, 2uL, 24hr	72	15 (20.83)	6 (8.3)	NA	NA	0	NA	NA	15 (20.83)	0 (0)
1/10, 3uL, 12hr	20	16 (80)	0 (0)	NA	NA	0	NA	NA	16 (80)	0 (0)
1/100, 2uL, 6hr	126	12 (9.52)	52 (41.27)	6 (11.53)	6 (100)	12 (9.52)	2 (16.67)	2 (100)	19 (15.07)	12 (9.52)
1/500, 2uL, 6hr	163	8 (4.90)	65 (39.88)	5 (7.7)	5 (100)	61 (37.42)	10 (16.39)	10 (100)	21 (12.88)	61 (37.42)

*Dilutions are for Baculovirus-Dll-GFP, however, volumes and times are for anti-gp64 antibody.

Table 3.3. Baculovirus-Inv-GFP injection followed by an anti-gp64 antibody in *Junonia orithya.*

Dilution Factor	Number of pupae injected	Number of GFP positive adults (%)	Number of non-GFP adults (%)	Number of individuals eclosed successfully (%)
Undiluted	5	0 (0)	5 (100)	0 (0)
1/5	7	0 (0)	7 (100)	1 (14.28)
1/10	57	1 (1.75)	56 (98.25)	48 (84.21)
1/20	8	0 (0)	8 (100)	6 (75)
1/100	78	7 (8.97)	71 (91.03)	58 (74.35)
1/500	30	0 (0)	30 (100)	3 (10)
1/1000	28	1 (3.57)	27 (96.43)	9 (32.14)

*Baculovirus-Inv-GFP (2 µL) injected at 18-24 hours post- pupation. Anti-gp64 antibody (2 µL) injected at 6 hours post-infection.

Chapter 4

Distal-less sequence variations in *Junonia orithya.*

4.1. Introduction

Butterfly wings are rich sources for pattern studies (Nijhout, 1991). Among the wing pattern elements, eyespots are concentric rings of different colored scales, easy for experimental manipulation, and might have functions in predator avoidance (Brakefield *et al*., 1999). Eyespots have been widely studied with surgical manipulation (Nijhout, 1985; Brakefield and French, 1995; French and Brakefield, 1995; Otaki *et al*., 2005; Otaki, 2011) and gene expression. Gene expression studies showed that, series of gene that patterns wings of *D. malanogaster* are also observed in the wings of butterflies. Gene expression patterns showed *apterous* on dorsal side only (Carroll *et al*., 1994), *wingless* and *Distal-less* (Brakefield *et al*., 1996, Carroll *et al*., 1994) along wing margin, *engrailed* on the posterior part only (Keys *et al*., 1999), and *cubitus interruptus* on anterior part only (Keys *et al*., 1999). In butterflies, these genes are redeployed again in a specific region of wings as in eyespots. *Distal-less, engrailed, and spalt* are expressed together in the center or focus of the eyespot and later again in the surrounding region around the eyespot (Brunetti *et al*., 2001) together with other patterning genes *patched*, *hedgehog* (Carroll *et al*., 1994, Keys *et al*., 1999), *decapentaplegic*, *wingless* (Carroll *et al*., 1994), and *ultrabithorax* (Weatherbee *et al*, 1999). A recent study showed that another gene *Antennapedia* expression is the earliest event and it is expressed exclusively in the center of the eyespots in butterfly *Bicyclus anynana* (Saenko *et al.*, 2011). The expression pattern of these candidate genes in eyespot foci and surrounding area and also resemblance with an adult eyespot implicate their roles in eyespot development. Various eyespots have different expression patterns of these candidate genes (Brakefield *et al*., 1996; Brakefield *et al*., 1999; Brunetti *et al*., 2001). This also implicates the role of these candidate genes in diverse morphological characters. However, the direct roles of these genes during development have been lacking.

The expression pattern of *Distal less* (first towards the wing margin, then again in center of eyespot followed by its expression around scale building cells around the center of eyespot) implies its role in eyespot formation. The expression pattern of *Distal-less* is also in accordance with eyespot variants (Brakefield *et al*., 1996). Furthermore, in *B. anynana*, the contribution of *Distal-less* to quantitative variation in butterfly eyespots has been reported (Beldade *et al*., 2002). *Distal-less* has been associated with within-species variation in eyespot patterns.

Junonia orithya, *Junonia coenia* and *Bicyclus anynana* are nymphalid butterflies with eyespots in their wings. *J. orithya* are sexually dimorphic and has different wing color patterns on dorsal and ventral wing surfaces. Females of *J. orithya* have two almost equal sizes of anterior and posterior

eyespots on dorsal side of the hindwing. However, eyespots in males are different in sizes. In males, anterior eyespot is often reduced to either black dot, or small black spot. Probably, the eyespots size variations in *J. orithya* might be due to *Distal-less* gene variation as suggested in the case of *B. anynana*.

However, *Distal-less* gene sequence from *J. orithya* butterfly has not yet been reported. Nevertheless, complete cDNA *Distal-less* sequence of 1146 bp and 4171 bp have already been reported from butterflies *J. coenia* (Panganiban *et al*., 1994) and *B. anynana* (Beldade *et al*., 2002), respectively. Based on already published sequences of *J. coenia* and *B. anynana* we tried to get complete cDNA *Distal-less* sequence from *J. Orithya* using the simple technique of polymerase chain reaction (PCR) followed by rapid amplification of complementary DNA ends (RACE).

With a simple experimental design, a pupal forewing from one side was excised and the wounded pupa was readily sealed with melted paraffin. *Distal-less* was cloned from the excised wing. Wing on the other side of the pupa was saved as a control. Sealed pupa was able to develop as a normal adult with normal wing color pattern on the other side. This experimental manipulation made it possible to compare the *Distal-less* sequence obtained experimentally from wing on one side with the phenotype on the other side. This chapter will help in understanding the molecular basis of morphological variation within a species using the blue pansy butterfly *J. orithya*.

4.2. Materials and methods

4.2.1. Wing excision and RNA isolation

Throughout the experiments, the blue pansy butterfly *J. orithya* was used. Immediately after pupation, all the wings from *J. orithya* pupae were excised and used immediately or readily frozen at -80˚C. For one side wing experiment, only a forewing from one side of a pupa was excised immediately after pupation and the pupa was readily sealed with melted paraffin. For total RNA isolation, RNeasy Mini Kit (QIAGEN, Marryland, USA) was used.

4.2.2. PCR, cloning, and sequencing

Based on sequence from *J. coenia*, primers for *Distal-less* were designed (Table 1). Recipes for RT-PCR and nested PCR are in Table 2 and 3. The cycling parameters for RT-PCR and nested PCR can be found in Table 4. The PCR products or gel purified PCR bands (MinElute Gel Extraction Kit, QIAGEN, Marryland, USA) were cloned with pCR 2.1-TOPO or pCR 4-TOPO vector, and their sequences were obtained from Invitrogen Haneda Laboratory.

4.2.3. Sequence analysis and alignment

Obtained sequences were analyzed and amino acid sequences were predicted using BioEdit Sequence Alignment Editor 7.0.9.0. The alignment was performed using ClustalX 2.0.11.

4.2.4. Rapid amplification of complementary DNA ends (RACE)

For RACE, GeneRACER Kit (Invitrogen, California, USA) was used. The gene specific primers (GSP) were designed from partial *Distal-less* sequence obtained experimentally from *J. orithya* (Table 5 and 6). Recipes for RT-PCR and nested PCR for RACE can be found in Table 7 and 8. The cycling parameters for RT -PCR and nested PCR for RACE can be found in Table 9.

4.3. Results

4.3.1. *Distal-less* complementary DNA (cDNA) sequences variations

With the primers designed based on *J. coenia* sequence, two bands around 861 and 459 bp (Fig. 4.1) were obtained. The BLAST result from the sequence obtained experimentally showed the alignment's Query coverage of 100% and E vale of 0 with both *J.coenia* and *B. anynana*. Finally, partial gene transcript of *Distal-less* was cloned from *J. orithya*.

In total, we cloned 64 cDNA sequences of *Distal-less* from *J. orithya*. Based on sequences variations of the experimentally obtained *Distal-less* sequences, we classified them into three major types, Type 1 (T1), Type 2 (T2) and Type 3 (T3). T1 is the longest of the all sequences and has 861 bp. T2 has 852 bp, missing 9 bp from position 699 to 707. T3 has 459 bp sequences and missing 402 bp in between from position 391 to 792 (Fig. 4.2). Out of 64 sequences, T1, T2 and T3 cover 71, 19 and 10% respectively (Fig. 4.3). We predicted amino acid sequences from the *Distal-less* cDNA sequences obtained. Total of 64 sequences could be divided into 5 different types, T1, T2, T3, T4, and T5. T1 has 286 amino acids. T2 has 283 amino acids, missing in between 3 amino acids from position 233 to 235. T3 has 152 amino acids missing in between 134 amino acids from position 130 to 263. T4 has 128 amino acids missing amino acids from position 128 onwards. Similarly, T5 has 168 amino acids and missing amino acids from 168 position onwards (Fig. 4.4). Out of 64 predicted amino acids sequences from *Distal-less* cDNA, T1, T2, T3, T4 and T5 covers 69, 19, 8, 2, and 2 % respectively (Fig. 4.3).

4.3.2. *Distal-less* cDNA sequence variations within an individual

Based on cDNA sequence, we obtained 3 different types of cDNA sequences T1, T2, and T3. However, we could not clearly identify any correlation between cDNA sequence variations and phenotype variations (Fig. 4.5A).

Based on amino acids sequences predicted from cDNA sequences of *Distal-less*, we obtained 5 different types, T1, T2, T3, T4, and T5. Here, also we were not able to identify any clear linkage between amino acids sequence variations and phenotype variations (Fig. 4.5B).

We tried to clone *Distal-less* cDNA sequences from one side of the wing and compare the sequence differences of *Distal-less* with phenotype of wings on other side. We had 7 individuals J1, J4, J5, J6, J8, J13, and J17. Four individuals J1, J4, J5, and J6 were blue females of *J. orithya*. J8, J13 and J17 were males with various eyespot sizes. Comparatively, J8 had small, J17 had medium, and J17 had big eyespots. The figures of all male and female individuals are shown in Figure 4. 6.

4.3.3. Rapid amplification of 5' and 3' cDNA ends (RACE)

Four different primer sets and four nested primers sets each were designed to find 5' end and 3' end sequences. We obtained PCR bands with the designed primers but we were not able to obtain the sequence of either 5' or 3' end. It seems difficult to find out 3' as well as 5' end sequences of *Dll* gene.

4.4. Discussion

Based on sequences from *J. coenia* (Panganiban *et al*., 1994) and *B. anynana* (Beldade *et al*., 2002), primers for *Distal-less* gene for *J. orithya* were designed. Initially, degenerate primers based on already published *Distal-less* cDNA sequences were designed. Unfortunately, we were not able to obtain any positive bands with those designed primers.

Furthermore, primers based on *J. coenia Distal-less* sequence were designed. Finally, we obtained positive bands in PCR. The PCR products or gel purified PCR bands were cloned and sequenced; those sequences were highly aligned with *Distal-less* cDNA of *J. coenia and B. anyana*. The match was more with *J. coenia* than *B anynana*. This is reasonable as *J. orithya and J. coenia* belong to the same genus *Junonia.*

However, in terms of *Distal-less* sequences, we obtained three different versions of *Distal-less* cDNA sequences. This could be because of alternate pre-messenger RNA splicing. The alternate splicing plays a role in physiology and development by creating protein diversity. In *D. melanogaster*, alternative splicing and RNA editing of sodium channel gene (*para*) is responsible for tissue/cell specific functional variants of *para* gene (Tan *et al*., 2002; Song *et al.,* 2004; Liu *et al*., 2004; Olson *et al*., 2008). Similar mechanism may be possible in butterfly wing color patterns and could be a reason behind the diversity of eyespots in *J. orithya*. However, the exact function of *Distal-less* in wing color pattern in not known and the exact function of the variants is also difficult to understand. The answers to these basic questions why and where these diverse variants of *Distal-less* gene is expressed in the

butterfly wings will provide valuable information in butterfly wing color pattern formation and diversification.

From one side wing experiment we were not able get strong correlation with type of *Dll* length variants we got and diverse phenotype of *J. orithya* that exists in nature. We suggest that there are only two variants per individuals except F1. The T3 type of *Dll* found in F1 could be pseudogene. Thus, two functional genes are found in an individual and indicate two alleles. However, the variants found in amino acids sequences may be real or simply PCR mistakes. For this we need to have a whole genomic DNA sequence of *Dll* to see whether the difference is form allele or alternative splicing of *Dll*.

Contrastingly, only a single *Distal-less* cDNA sequence has been reported in both cases of *J. coenia and B. anynana*. *J orithya* is a polymorphic and sexually dimorphic butterfly. The color pattern of *J. orithya* is more complex than that of *J. coenia and B. anynana*. This may be a reason that, in *J. orithya* variants of *Dll* were obtained. At the fisrt glance of the Dll sequence allignment, the sequences variation of *Dll* at the nucleotide suggest that this is not a single species however, these sequence variation are also seen in the *Dll* sequences from single individual.

Furthermore, developmental genes are involved in morphological character variations. In *D. melanogaster*, the number of bristles has been associated with development genes *Achaete-scute Complex* and *Delta* genes (Mackay, 2001). In *D. melanogaster*, *Ultrabithorax* plays a key role in patterning of trichomes on legs (Stern, 1998). *In B. anynana, Distal-less* has been implicated in eyespot size variation. DNA polymorphism in *Distal-less* in relation with different eyespot size in *B. anynana* (Beldade *et al*., 2002) has been shown but different sequences of the gene has not been reported yet. In this chapter, I found three different types of *Dll* gene from *J. orithya.* The eyespot variation in *J. orithya* might be due to *Distal-less* polymorphism.

Furthermore, experimentally obtained three different *Distal-less* variants are only partial cDNA sequences and we need to obtain full length cDNA to get the clear picture of the variants of *Distal-less*. However, the difficulty of getting sequences on both ends of *Distal-less* cannot be neglected. We tried to find the sequence on both ends with RACE but we were not able to succeed.

In addition, we also do not know if all the *Distal-less* variants cloned from *J. orithya* are functional. With the recently developed baculovirus tool (Dhungel *et al.*, 2013), it is possible to use all of these three variants of *Distal-less* and try to find out the functions of each variants of *Distal-less* in *J. orithya* wing color pattern development.

Alternatively, designing probes against the three different types of *Distal-less* gene and performing *in situ* hybridization histochemistry or immunohistochemistry of the pupal wing of *J.*

orithya might show the precise location of the individual *Distal-less* in the wing of *J. orithya*. It is possible that each *Distal-less* sequence is responsible for the different eyespots present in butterfly wings. Although the eyespot cannot be seen on pupal wings, their precise location could be traced out without any difficulties.

However, at this point, the possible role of other candidate genes *decapentaplegic* (Carroll *et al*., 1994), *engrailed* (Brunetti *et al*., 2001, Keys *et al*., 1999), *spalt* (Brunetti *et al*., 2001 and *Ultrabithorax* (Weatherbee *et al*, 1999) in linkage with eyespot size variation cannot be ruled out.

4.5. Conclusions

In a single individual, wing on one side has been excised and *Distal-less* sequence has been cloned. The *Distal-less* sequence variations were compared with phenotype on the other side. Three different types of *Distal-less* length variants T1, T2, and T3 were found, but a possible relationship with phenotype could not be established. Further experiments increasing sample sizes or using the baculovirus tool for ectopic expression of all these variants or *in situ* hybridization histochemistry or immunohistochemistry of the pupal wing could help understand the *Distal-less* gene variations and phenotype variations in *J. orithya*.

4.6. References

Beldade P, Brakefield PM: The genetics and evo-devo of butterfly wing patterns. Nature Reviews Genetics 2002, 3: 442-452.

Brakefield PM, French V: Eyespot development on butterfly wings: the epidermal response to damage. Developmental Biology 1995, 168, 98-111.

Brakefield PM, Gates J, Keys D, Kesbeke F, Wijngaarden PJ, Monteiro A, French V, Carroll SB: Development, plasticity and evolution of butterfly eyespot patterns. Nature 1996, 384: 236-242.

Brakefield PM and French V: Butterfly wings: the evolution of development of color patterns. Bioessays 1999, 21: 391-401.

Brunetti CR, Selegue JE, Monteiro A, French V, Brakefield PM, Carroll SB: The generation and diversification butterfly eyespot color patterns. Current Biology 2001, 11: 1578-1585.

Carroll SB, Gates J, Keys DN, Paddock SW, Panganiban GEF, Selegue JE, Williams JA: Pattern formation and eyespot determination in butterfly wings. Science 1994, 265: 109-114.

Dhungel B, Ohno Y, Matayoshi R, Otaki JM: Baculovirus-mediated gene transfer in butterfly wings in vivo: An efficient expressin system with anti-gp64 antibody. BMC Biotechnology 2013, 13:27.

French V, Brakefield PM: Eyespot development on butterfly wings: the focal signal. Developmental Biology 1995, 168: 112-123.

Keys DN, Lewis DL, Selegue JE, Pearson BJ, Goodrich LV, Johnson RL, Gates J, Scott MP, Carroll SB: Recruitment of a hedgehog regulatory circuit in butterfly eyespots evolution. Science 1999, 283: 532-534.

Liu Z, Song W, Dong K: Persistent tetrodotoxin-sensitive sodium current resulting from U-to-C RNA editing of an insect sodium channel. Proceedings of National Academy of Science USA 2004, 101: 11862-11867.

Mackay TFC: Quantitative trait loci in Drosophila. Nature Reviews Genetics 2001, 2: 11-20.

Nijhout HF: Cautery-induced colour patterns in *Precis coenia* (Lepidoptera: Nymphalidae). Journal of Embryology and Experimental Morphology 1985, 86: 191-203.

Nijhout HF: The development and evolution of butterfly wing patterns. Washington, USA Smithsonian Institution Press; 1991.

Olson RO, Liu Z, Nomura Y, Song W, Dong K: Molecular and functional characterization of voltage-gated sodium channel variants from *Drosophila melanogaster*. Insect Biochemistry and Molecular Biology 2008, 38: 604-610.

Otaki JM, Ogasawara T, Yamamoto H: Morphological comparison of pupal wing cuticle patterns in butterflies. Zoological Science 2005, 22:21-34.

Otaki JM: Artificially induced changes of butterfly wing colour patterns: dynamic signal interactions in eyespot development. Scientific Reports 2011, 1:111.

Panganiban G, Nagy L, Carroll SB: The role of the *Distal-less* gene in the development and evolution of insect limbs. Current Biology 1994, 8: 671-675.

Saenko SV, Marialva MS, Beldade P: Involvement of the conserved Hox gene *Antennapedia* in the development and evolution of a novel trait. Evo Devo 2011, 2:9.

Song W, Liu Z, Tan J, Nomura Y, Dong K: RNA editing generates tissue-specific sodium channels with distinctive gating properties. Journal of Biological Chemistry 2004, 279: 32554-32561.

Stern DL: A role of *Ultrabithorax* in morphological differences between *Drosophila* species. Nature 1998, 396: 463-466.

Tan J, Liu Z, Nomura Y, Goldin AL, Dong K: Alternative splicing of an insect sodium channel gene generates pharmacologically distinct sodium channels. Journal of Neuroscience 2002, 22: 5300-5309.

Weatherbee SD, Nijhout HF, Grunert LW, Halder G, Galant R, Selegue J, Carroll SB: *Ultrabithorax* function in butterfly wings and the evolution of insect wing patterns. Current Biology 1999, 9: 109-115.

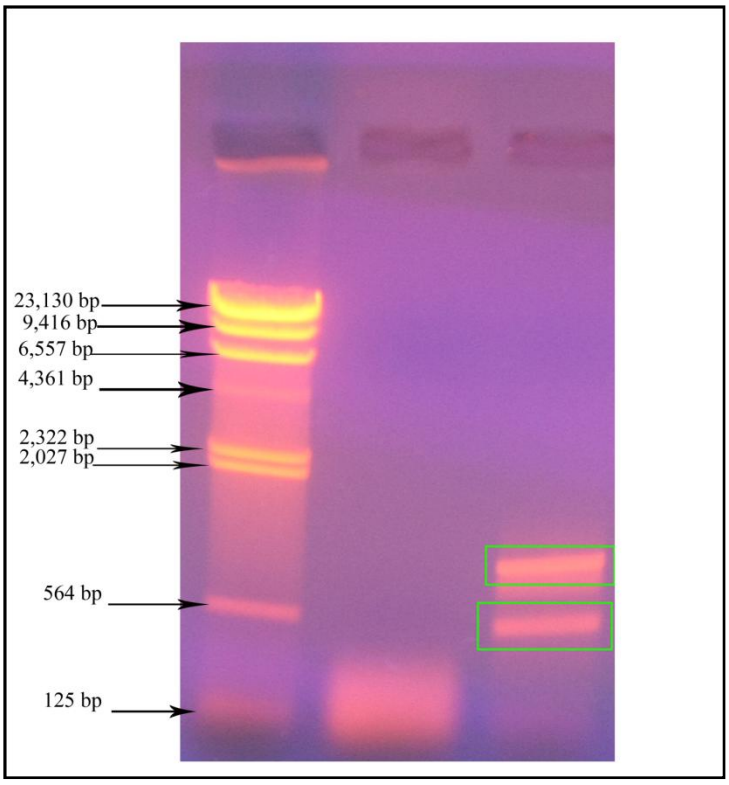

Fig. 4.1. PCR products of *Distal-less* gene transcript shown on agarose gel. The bands of two different sizes are shown with green rectangular boxes. Molecular marker sizes are indicated by arrows in base pairs (bp).

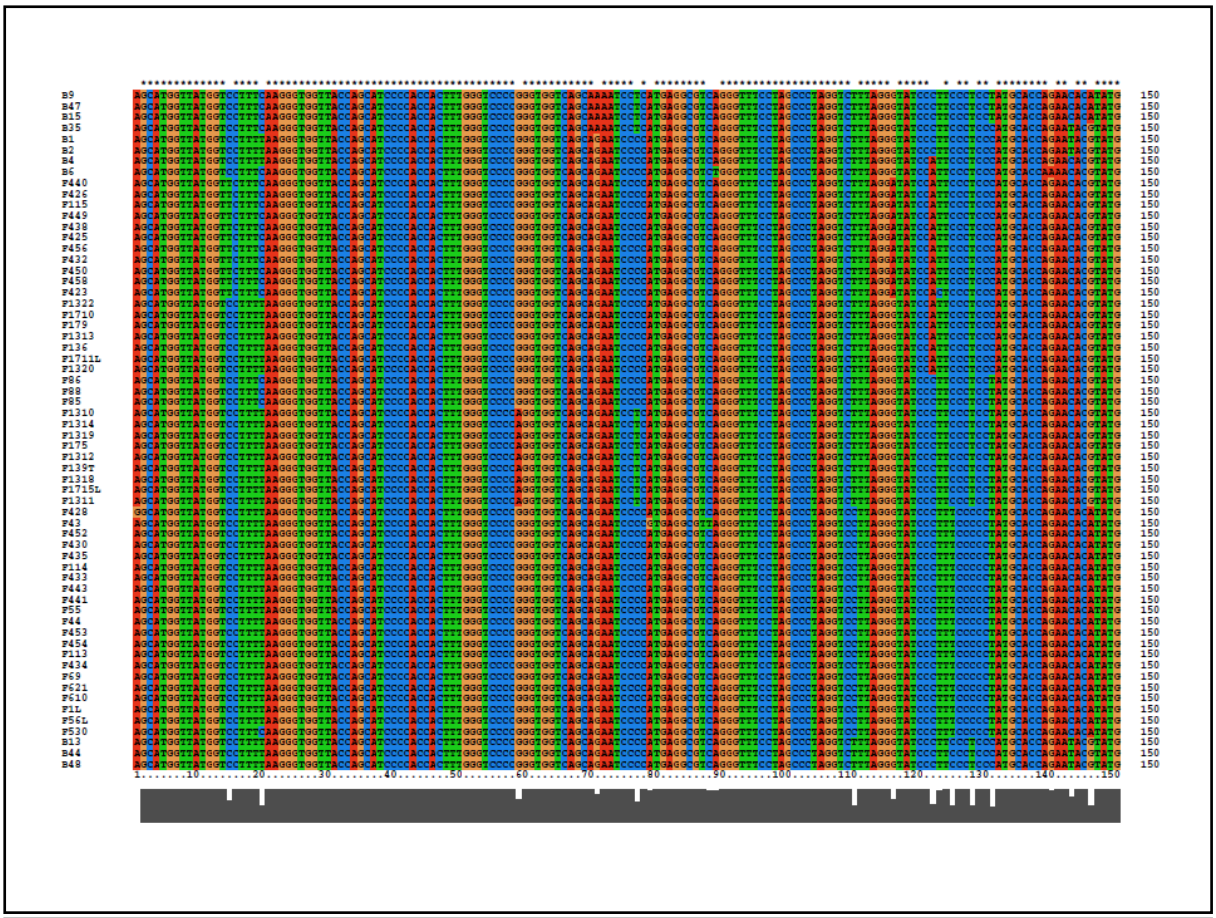

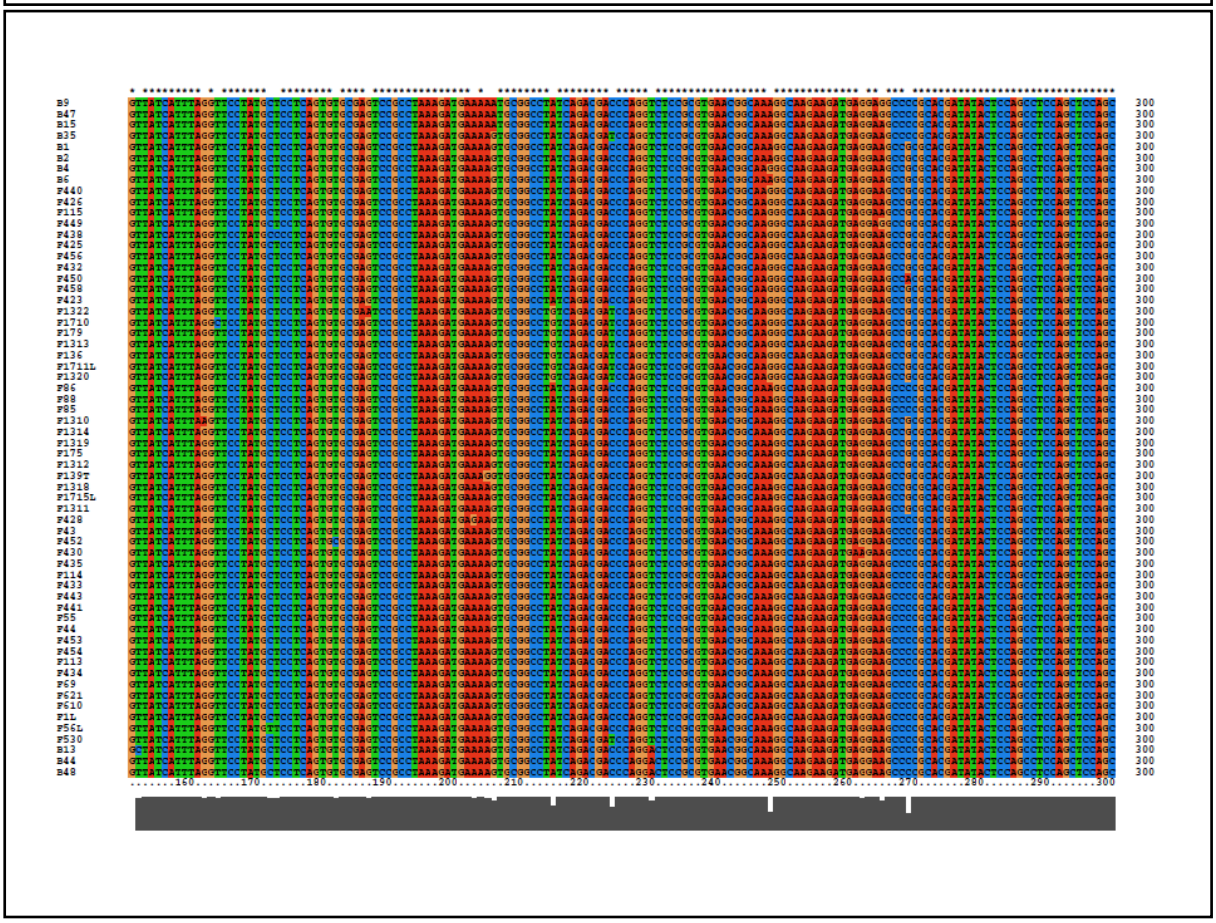

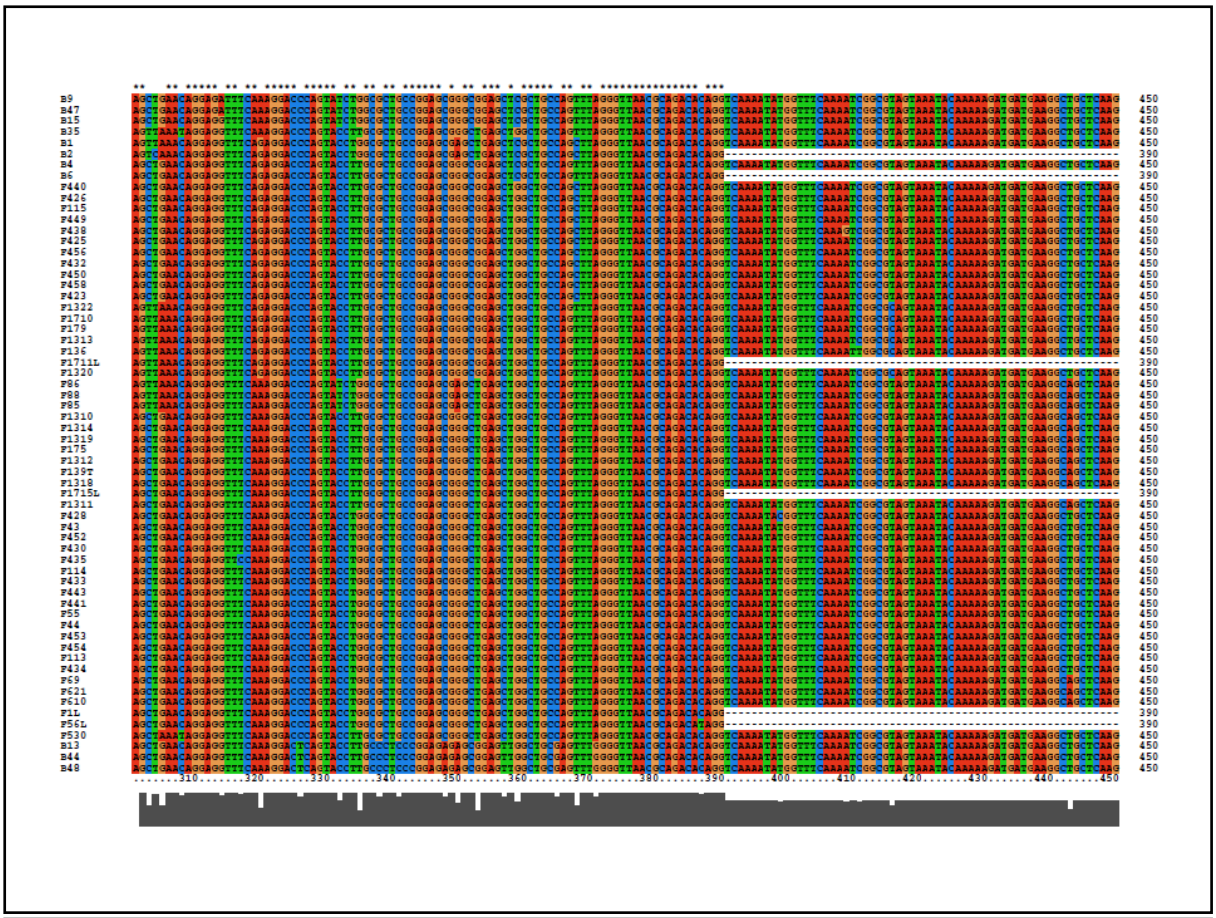

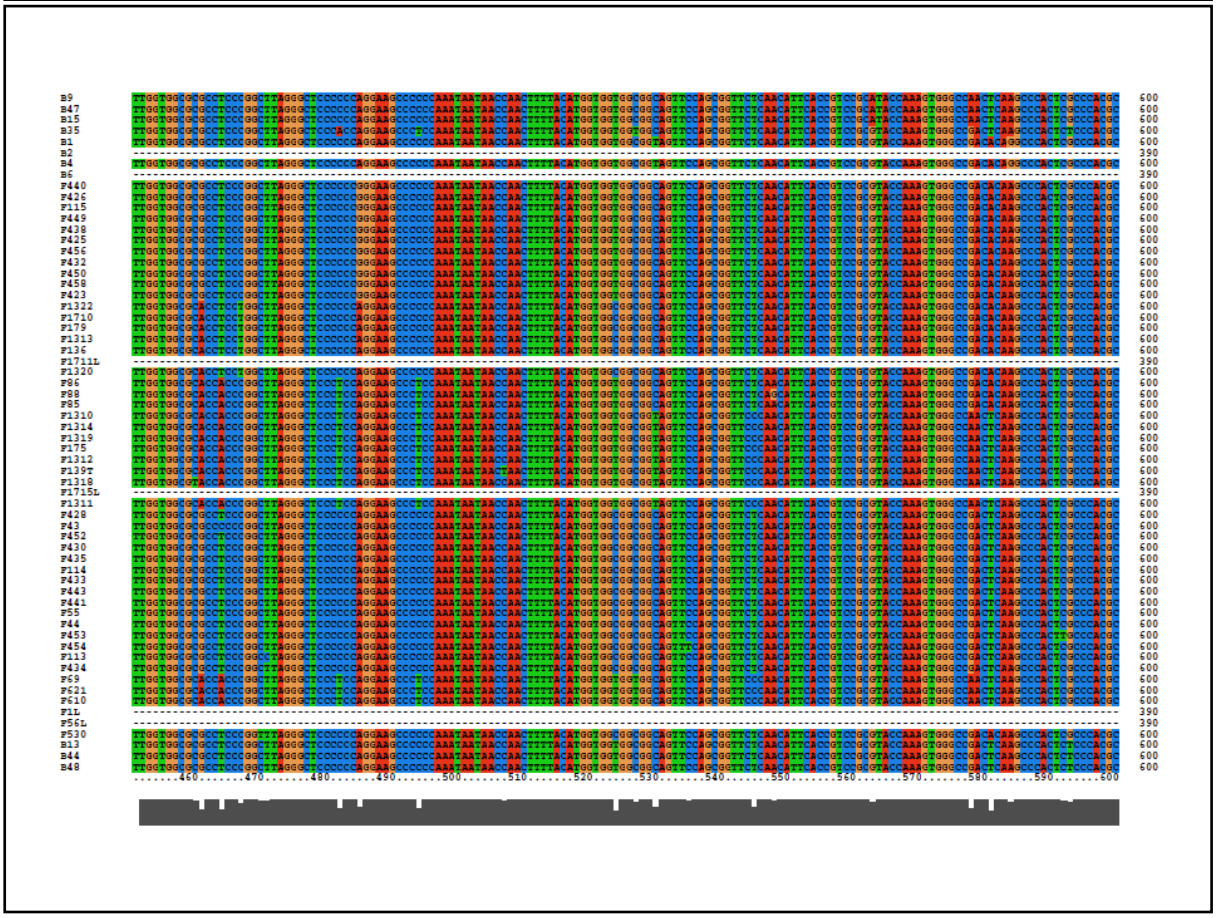

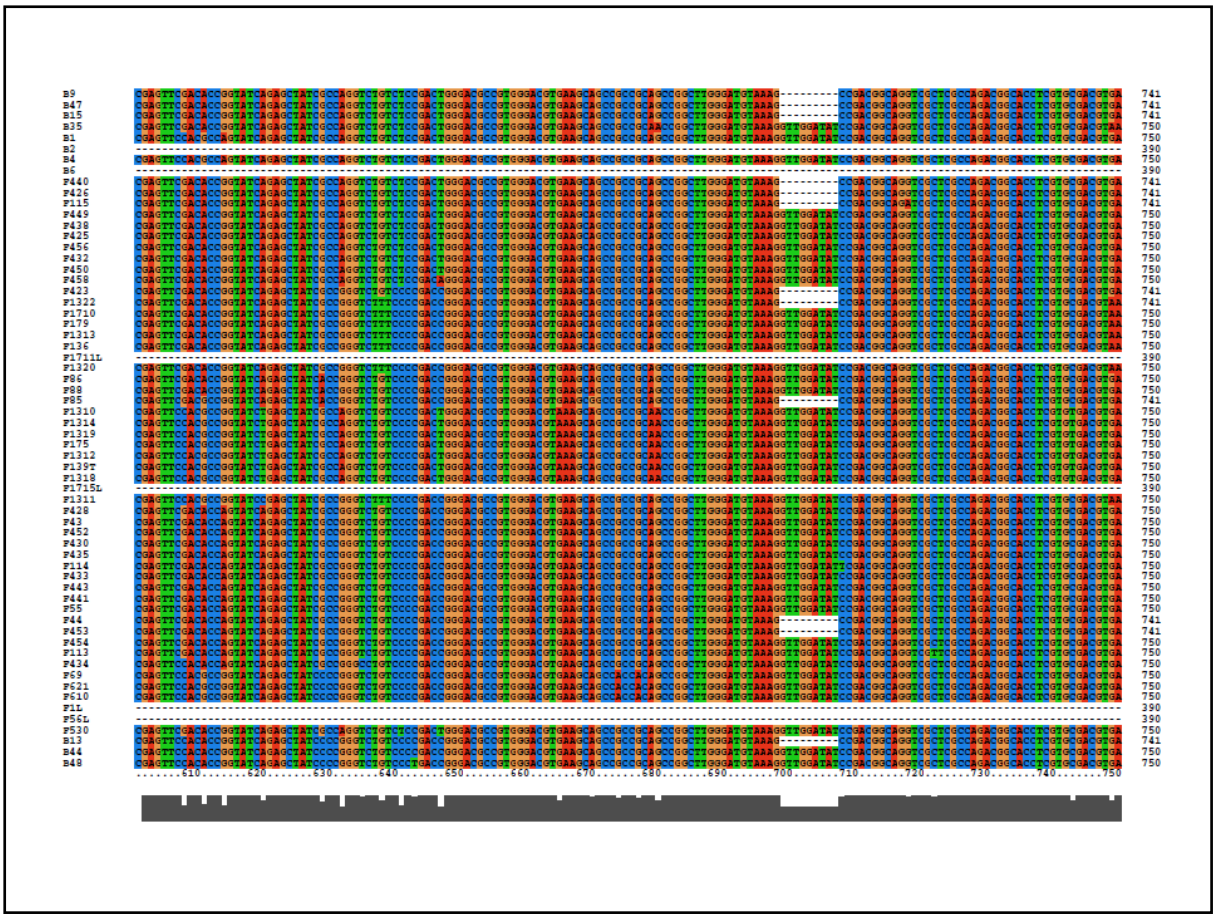

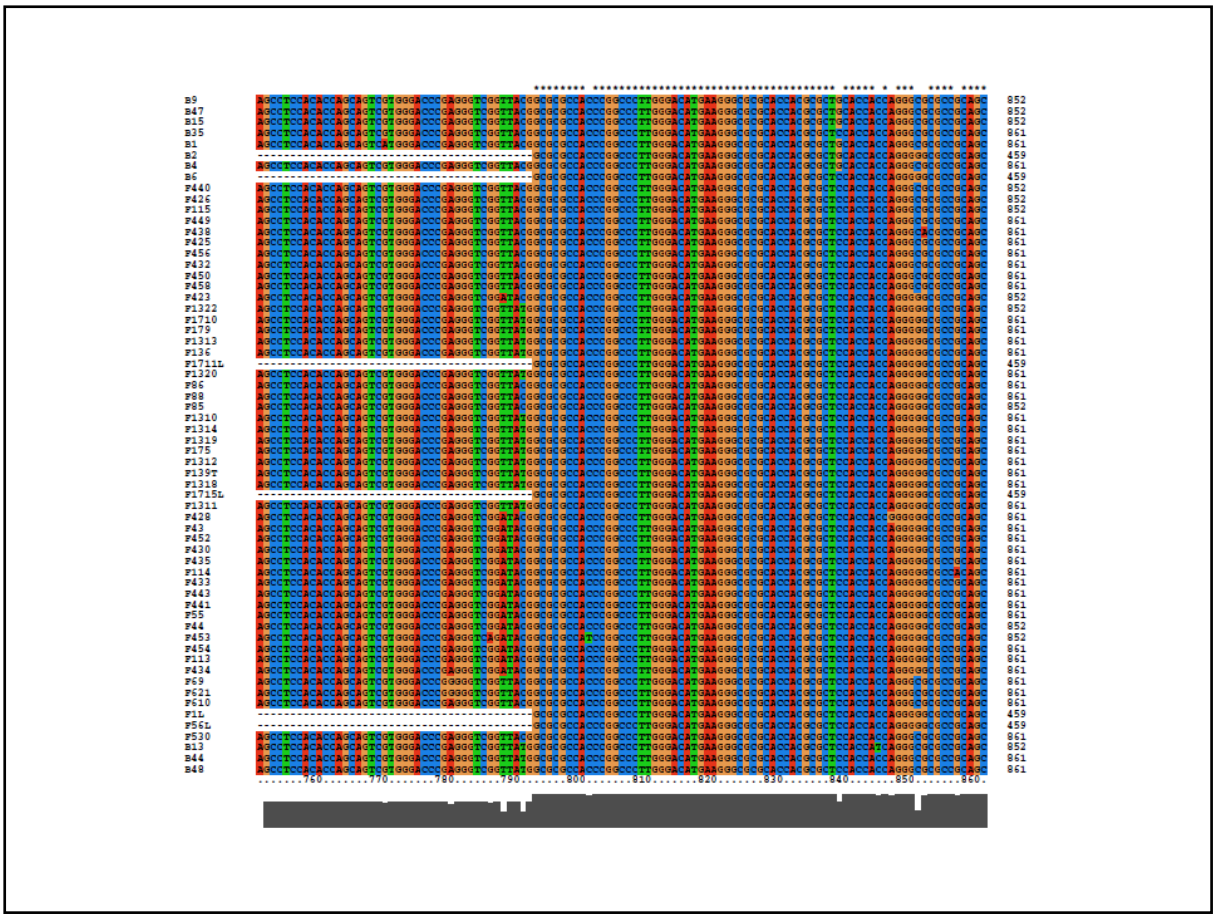

Fig. 4.2. Sequence alignment of cDNA sequences of *Distal-less* gene transcription products obtained experimentally. Three different types of *Distal-less* sequences were obtained, 861, 852, and 459 bp. The alignment was generated with Clustal X2 software.

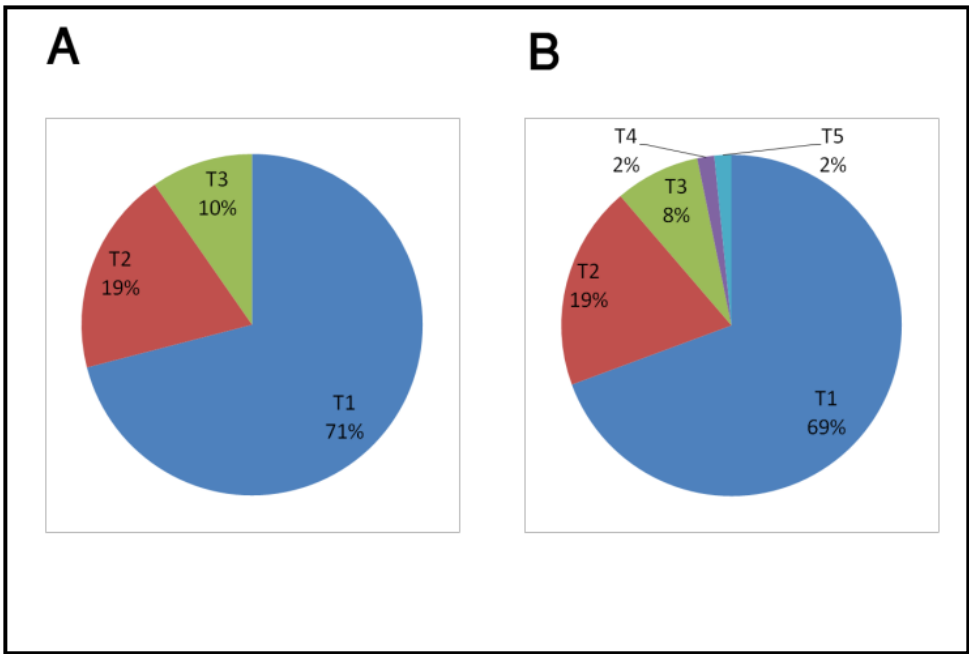

Fig. 4.3. Pie charts of percentage of total clones obtained experimentally and predicted amino acid sequences. (**A**) Different types of *Distal-less* cDNA sequences, T1 (861 bp), T2 (852 bp), and T3 (459 bp). (**B**) Predicted *Distal-less* amino acid sequences, T1 (286 amino acids), T2 (283 amino acids), T3 (152 amino acids), T4 (128 amino acids), and T5 (168 amino acids).

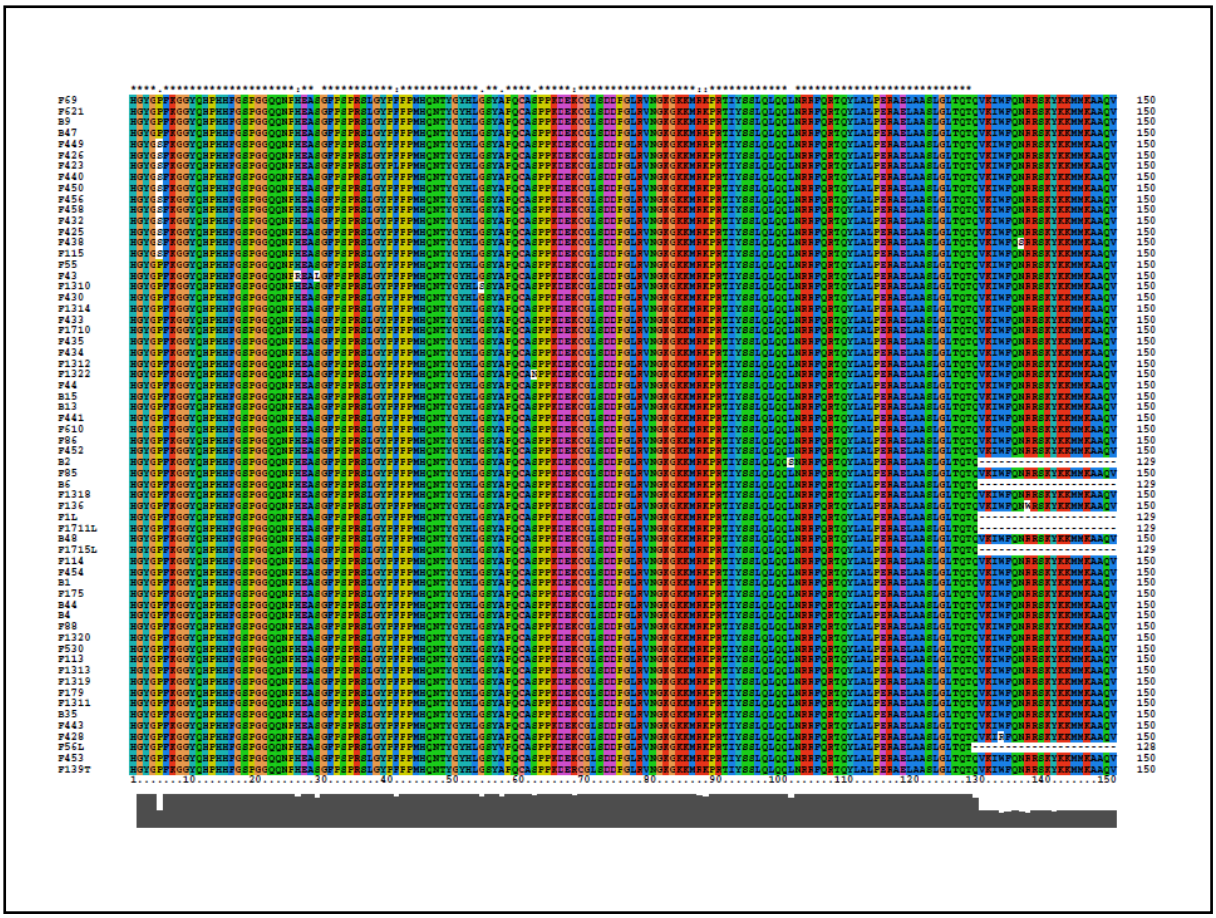

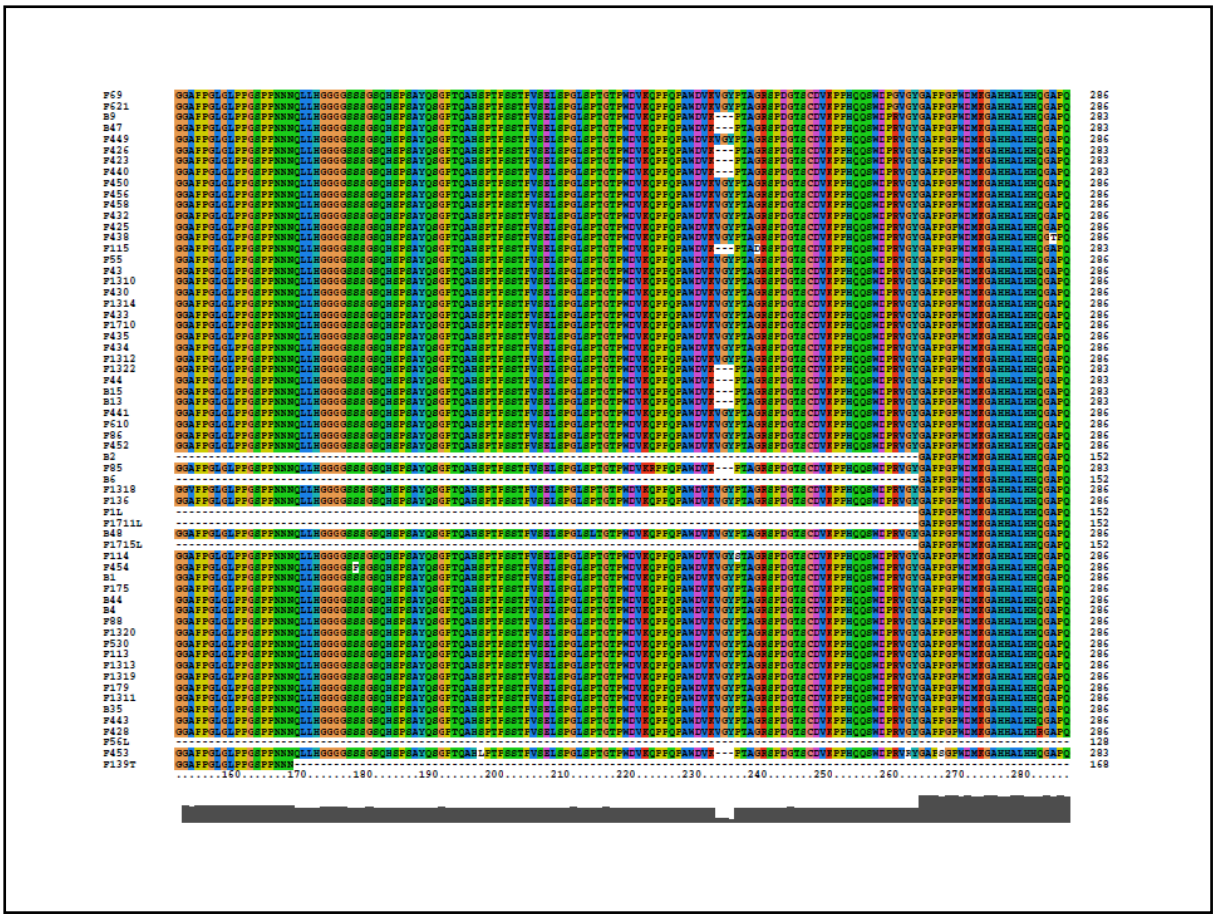

Fig. 4.4. Distal-less amino acids sequences predicted from cDNA sequences obtained experimentally. Five different types of *Distal-less* amino acids sequences were found, 286 amino acids, 283 amino acids, 152 amino acids, 128 amino acids, and 168 amino acids. The alignment was generated with Clustal X2 software. The amino acid sequences were predicted by Bioedit software.

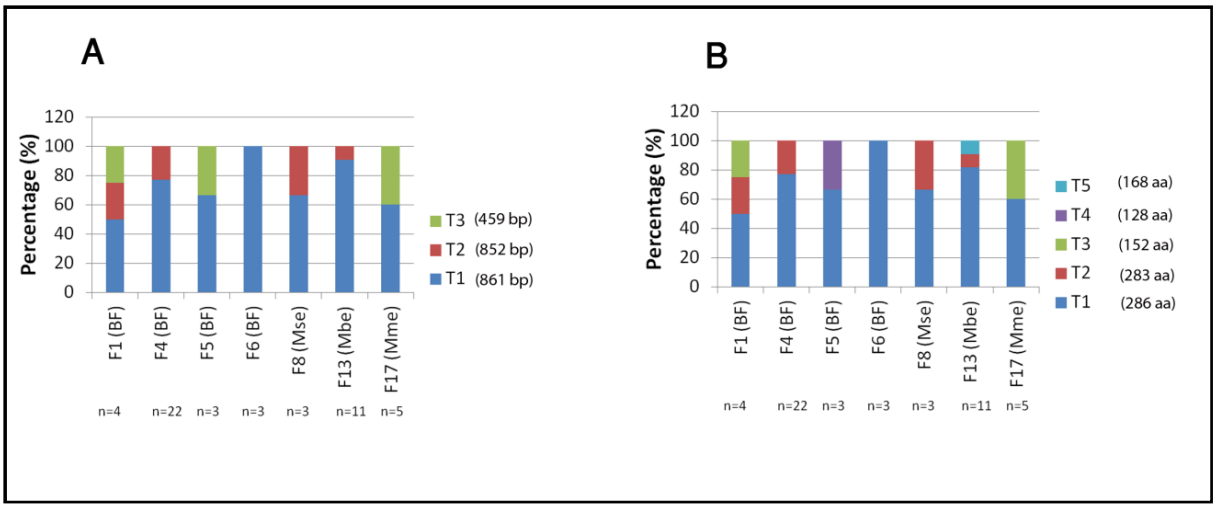

Fig. 4.5. Different types of *Distal-less* cDNA (**A**) and predicted *Distal-less* amino acid (**B**) sequences found in seven individuals of *J. orithya* from one side wing experiment. n is number of clones obtained experimentally per individual.

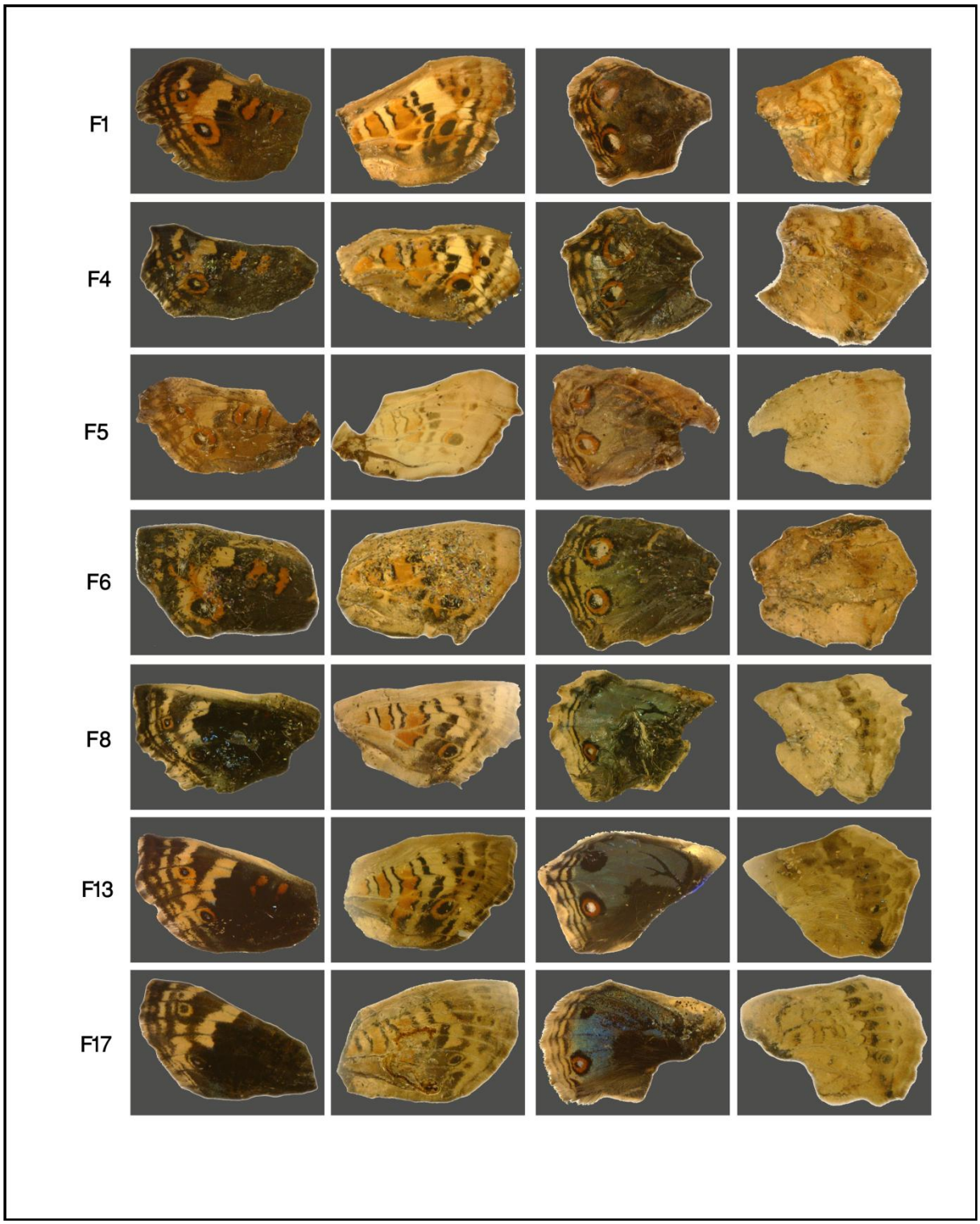

Fig. 4.6. The dorsal and ventral sides of forewings and hindwings of seven different individuals of *J. orithya* wings used for one side wing experiment.

Table 4.1. Polymerase chain reaction (PCR) primers for *Distal-less*.

Primer	PCR	Site	Sequences	Bases	Tm
DLL1up	RT-PCR	Up	5'-ATGACXACXCARGARCTXGAYCAYC-3'	25	75.0°C
DLL1down		Down	5'-TCARCTRTCRTARTTRTTYTGYTC-3'	24	65.0°C
Dll2up	nested PCR	Up	5'-ATHGARTTRCARCARCAYGGXTAYG-3'	25	71.7°C
Dll2down		Down	5'-AXCCYAARAAYTGRCTXCGYAAXCC-3'	25	74.0°C
Dll3up	RT-PCR	Up	5'-ATGACCACCCAGGAGCTAGATCACC-3'	25	78.0°C
Dll3down		Down	5'-AGGGTTGGCATCAGCCTGGTACCAG-3'	25	80.0°C
Dll4up	nested PCR	Up	5'-AAGTCTGCGTTCATAGAGTTACAGC-3'	25	72.0°C
Dll4down		Down	5'-TACTGCGGCACGTAGGGCGGGTGCG-3	25	86.0°C

Table 4.2. Recipes for reverse transcription polymerase chain reaction (RT-PCR).

Reagents	**Volume**
Access Quick Master Mix (Promega), 2X	25 µl
Upstream Primer, 10 µM	0.5 µl
Downstream Primer, 10 µM	0.5 µl
RNA Template	1pg-1µg

Table 4.3. Recipes for nested PCR.

Reagents	**Volume**
Tfl buffer, 10X	5 µl
dNTP Solution, 10mM	1 µl
Nested Upstream Primer, 10 µM	0.5 µl
Nested Downstream Primer, 10 µM	0.5 µl
$MgSO_4$, 50 mM	2 µl
Initial PCR product	4 µl
Tfl DNA Polymerase, 5U	0.5 µl
Sterile Water	36.5 µl
Total Volume	**50 µl**

Table 4.4. Cycling parameters for PCR.

RT-PCR

Temperature	Time	Cycles
45°C	45 minutes	1
95°C	2 minutes	1
95°C	1 minute	40
50°C	30 seconds	
72°C	1 minute and 20 seconds	
72°C	5 minutes	1

Nested PCR

Temperature	Time	Cycles
95°C	2 minutes	1
95°C	1 minute	40
50°C	1 minute	
72°C	1 minute and 20 seconds	
72°C	5 minutes	1

Table 4.5. PCR primers for 5' RACE for *Distal-less*.

Primer	PCR	Site	Sequences	Bases	Tm
RGSP1	PCR	Down	5'-GACCACCCGGGGACCCAAAGTGGTG-3'	25	84°C
RGSPN1	nested PCR	Down	5'-AAAGTGGTGGGGATGCTGGTAACCAC-3'	26	80°C
RGSP2	PCR	Down	5'-GATAGGCCGCACTTTTCATCTTTAG-3'	25	72°C
RGSPN2	nested PCR	Down	5'-ACTGAGGAGCATAGGAACCTAAATG-3'	25	72°C
RGSP3	PCR	Down	5'-TCGCACACTGAGGAGCATAGGAACC-3'	25	78°C
RGSPN3	nested PCR	Down	5'-TAAATGATAACCATACGTGTTCTGG-3'	25	68°C
RGSP4	PCR	Down	5'-TTCCTCATCTTCTTGCCTTTGCC-3'	23	68°C
RGSPN4	nested PCR	Down	5'-ACCTGGGTCGTCTGATAGGCCGCAC-3'	25	82°C
RGSP5	PCR	Down	5'-AGGCGCGCCACCAACTTGAGCAGCC-3'	25	84°C
RGSPN5	nested PCR	Down	5'-TGGAGGCTGGAGTATATCGTGCGCG-3'	25	80°C
RGSP6	PCR	Down	5'-TGCGTTAACCCTAAGCTGGCAGCG-3'	24	76°C
RGSPN6	nested PCR	Down	5'-TCGGGCTAGGAAACCCTGACGCC-3'	23	74°C
RGSP7	PCR	Down	5'-TAACCCTAAGCTGGCAGCGAGCTCAGCTCG-3'	30	96°C
RGSPN7	nested PCR	Down	5'-TTCTTGCCTTTGCCGTTCACGCGGAGACC-3'	29	92°C
RSP8	PCR	Down	5'-AACTGCTGGAGCTGGAGGCTGGAGTATATCG-3'	31	96°C
RGSPN8	nested PCR	Down	5'-TAGGCGGACTCGCACACTGAGGAGCATAGG-3'	30	96°C
GeneRacer5'Primer	PCR	Up	5'-CGACTGGAGCACGAGGACACTGA-3'	23	74°C
GeneRacer5' nested Primer	nested PCR	Up	5'-GGACACTGACATGGACTGAAGGAGTA-3'	26	78°C

Table 4.6. PCR primers for 3' RACE for *Distal-less.*

Primer	PCR	Site	Sequences	Bases	Tm
FGSP1	PCR	Up	5'-GCGCGCCACCCGGCCCTTGGGACATG-3'	26	92
FGSPN1	nested PCR	Up	5'-GACATGAAGGGCGCGCACCACGCGC-3'	25	86
FGSP2	PCR	Up	5'-CGCGCACCACGCGCTCCACCACCAG-3'	25	88
FGSPN2	nested PCR	Up	5'-CTCCACCACCAGGGGGCGCCGCAGC-3'	25	90
FGSP3	PCR	Up	5'-AGGTCGCTCGCCAGACGGCACCTCG-3'	25	86
FGSPN3	nested PCR	Up	5'-ACGTGAAGCCTCCACACCAGCAGTCG-3'	26	84
FGSP4	PCR	Up	5'-AGCAGCTGAACAGGAGGTTTCAAAGG-3'	26	78
FGSPN4	nested PCR	Up	5'-AGTACCTTGCGCTGCCGGAGCGGGCTG-3'	27	92
FGSP5	PCR	Up	5'-AGCGGTTCTCAACATTCACCGTCCG-3'	25	78
FGSPN5	nested PCR	Up	5'-ACGTGAAGCAGCCGCCGCAGCCGGC-3'	25	88
FGSP6	PCR	Up	5'-ACTCGCCCACGCCGAGTTCCACGCC-3'	25	86
FGSPN6	nested PCR	Up	5'-ATGTAAAGGTTGGATATCCGACGG-3'	24	70
FGSP7	PCR	Up	5'-AAGATGATGAAGGCTGCTCAAGTTGGTGGC-3'	30	90
FGSPN7	nested PCR	Up	5'-TCTGTCTCCGACTGGGACGCCGTGGGACG-3'	29	98
FGSP8	PCR	Up	5'-TTCCACGCCAGTATCAGAGCTATCGCCAGG-3'	30	94
FGSPN8	nested PCR	Up	5'-GCCGGCTTGGGATGTAAAGGTTGGATATCC-3'	30	92
GeneRacer3' Primer	PCR	Down	5'-GCTGTCAACGATACGCTACGTTAACG-3'	25	76
GeneRacer3' nested Primer	nested PCR	Down	5'-CGCTACGTAACGGCATGACAGTG-3'	23	72

Table 4.7. Recipes for 5’ and 3’ RACE PCR.

Reagents	**5' RACE PCR**	**3' RACE PCR**
GeneRacer 5' Primer, 10 µM	3 µl	NA
Reverse GSP, 10 µM	1 µl	NA
GeneRacer 3' Primer, 10 µM	NA	3 µl
Forward GSP, 10 µM	NA	1 µl
RT Template	1 µl	1 µl
Tfl Buffer, 10X	5 µl	5 µl
dNTP Solution, 10 mM	1 µl	1 µl
Tfl DNA Polymerase, 5U	0.5 µl	0.5 µl
$MgSO_4$, 50 mM	2 µl	2 µl
Sterile Water	36.5 µl	36.5 µl
Total Volume	**50 µl**	**50 µl**

Table 4.8. Recipes for 5’ and 3’ RACE Nested PCR.

Reagents	**5' RACE PCR**	**3' RACE PCR**
GeneRacer 5' Nested Primer, 10 µM	1 µl	NA
Reverse Nested GSP, 10 µM	1 µl	NA
GeneRacer 3' Nested Primer, 10 µM	NA	1 µl
Forward Nested GSP, 10 µM	NA	1 µl
Initial PCR	4 µl	4 µl
Tfl Buffer, 10X	5 µl	5 µl
dNTP Solution, 10 mM	1 µl	1 µl
Tfl DNA Polymerase, 5U	0.5 µl	0.5 µl
$MgSO_4$, 50 mM	2 µl	2 µl
Sterile Water	35.5 µl	35.5 µl
Total Volume	**50 µl**	**50 µl**

Table 4.9. Cycling parameters for 5' and 3' RACE PCR of *Distal-less*.

Temperature	Time	Cycles
94°C	2 minutes	1
94°C	30 seconds	5
72°C	3 minutes	
94°C	30 seconds	5
70°C	3 minutes	
94°C	30 seconds	35
65°C	30 seconds	
70°C	3 minutes	
70°C	10 min	1

Chapter 5

Morphometric analysis of nymphalid butterfly wings: number, size, and arrangement of scales, and their implications for tissue-size determination

5.1. Introduction

Animal body size is a species-specific quantitative trait that is genetically determined, but it is also a plastic trait that is strongly influenced by environmental factors. Within a tolerable range in a species, the size of an individual varies, but the developmental system is plastic enough to maintain overall isometric structures. This plastic ability to achieve a macroscopically isometric final construct irrespective of size variation is one of the remarkable features that characterize living organisms (Raff, 1996; Conlon and Raff, 1999). To achieve this, all macroscopic traits must be phenotypically coordinated. The question arises as to how individual cells contribute to the overall size variation. More concretely, is the overall size increase achieved by an increase of the number of cells or by larger cell size? Dynamically, this problem is directly translated into the problem of cell proliferation (i.e., an increase of the number of cells) and cell growth or differentiation (i.e., an increase of cell size in the course of functional maturation) during development (O'Farrell, 2004).

The *Drosophila* imaginal discs in larvae, which are set aside for adult tissues, increase in size through cell proliferation without differentiation (Weigmann et al., 1997; Neufeld et al., 1998). In contrast, in other systems, organismal growth does not accompany cell proliferation (Gatti and Baker, 1989; O'Farrell, 2004). An isometric structure can be achieved more easily if each cell expands or shrinks in size, and thus the size of the whole macroscopic structure changes. This strategy is employed in the larval growth of *Drosophila* (Gatti and Baker, 1989). Interestingly, rearing larvae at low temperature results in larger larvae and then larger adults (Powell, 1974; Partridge et al., 1994; de Moed et al., 1997). This temperature response is accompanied by an increase in cell size but not in the number of cells (Partridge et al., 1994; Azevedo et al., 2002). It has been known that in *Drosophila*, size control involves in insulin and Target of Rapamycin (TOR) pathways (Mirth and Riddiford, 2007). However, our knowledge on this problem in insects is mainly limited to *Drosophila* larvae (Edgar and Nijhout, 2004). Little is known about the size control mechanisms of tissues and organs in pupae and in other non-model insects.

To shed light on this fundamental biological problem associated with size, we focused on the wings of nymphalid butterflies. Wings of different individuals of a given butterfly species are likely geometrically proportional to one another irrespective of the whole wing size. Butterfly wings are a two-dimensional system on which scales are regularly arranged in anteroposterior rows at regular intervals (Süffert, 1937; Nijhout, 1991; Yoshida et al., 1983; Yoshida, 1988; Yoshida and Aoki, 1989).

It is thought that a scale arrangement pattern is not unique to a species and has no spatial correlation with scale color patterns (Yoshida, 1988). Each scale is produced by a single scale cell, and it has a distinct single color (Nijhout, 1991), although a single scale often has multiple physicochemical mechanisms to express a coherent color (Nijhout, 1991; Ghiradella, 1998; Vukusic et al., 2000; Kristensen and Simonsen, 2003). This fact may be dubbed the "one cell, one scale, and one color" rule. This rule allows us to examine the number of scale cells simply by counting scales on an adult wing.

These scales of various colors constitute macroscopic mosaic color patterns on a wing surface. The whole wing color pattern on a wing is composed of color-pattern elements. Each color-pattern element is thought to be equivalent to a three-dimensional anatomical structure of other body parts. Consistent with this notion, the whole color pattern is laid down based on the nymphalid groundplan (Nijhout, 1991, 2001; Otaki, 2009, 2012a). The nymphalid groundplan is an ideal positioning of dark-colored elements against a light-colored background, although a distinction between elements and background is sometimes difficult in real butterflies. The background is often colored in a position-dependent manner in many species (Nijhout, 1991). We have previously found that the wide blue background region of the blue pansy butterfly *Junonia orithya* (Linnaeus, 1758) (Lepidoptera, Nymphalidae, Nymphalinae) has some elemental characteristics (Kusaba and Otaki, 2009).

Because the body size, and hence the wing size, are strongly influenced by genetic factors and by environmental factors, including temperature and nutrition, there must be mechanisms that adjust the wing size and also the positions and sizes of color-pattern elements. Wing size adjustment can be carried out either by changing the number of cells (i.e., cell proliferation) or by changing cell size (i.e., cell growth). In either case, the elements must be positioned at correct locations relative to the rest of the wing. As one might expect, scale length and wing length among wings from many lepidopteran insects are correlated (Kristensen and Simonsen, 2003; Simonsen and Kristensen, 2003). However, a potential relationship between scale length and wing length within a single species has not been demonstrated. This can be realized by examining many wings of different sizes from a given species. Additionally, other aspects of wing structure such as a potential isometric relationship between wing size and compartment size may be investigated in a similar way.

Previously, we focused on *J. orithya* to elucidate the relationships among size, shape, and position of the scales on a wing (Kusaba and Otaki, 2009). We demonstrated that scales on a single wing vary in size and shape in a position-dependent manner in *J. orithya*. This result suggests that scale size and shape are influenced by positional information for color-pattern signals from the same organizing centers (Kusaba and Otaki, 2009). This position-dependent nature appears to be a general rule in butterflies, judging from a general trend of scale size change from the proximal to distal regions across Lepidoptera (Kristensen and Simonsen, 2003; Simonsen and Kristensen, 2003), but other

butterflies have not been rigorously examined for this trait, although a relationship between scale structure and scale color has been reported in a different species (Janssen et al., 2001).

In insects, genome amplification (i.e., polyploidy) contributes to cell size (Hayashi, 1996; Follette et al., 1998; Weiss et al., 1998). Because polyploidy is observed in butterfly scale cells (Nijhout, 1991), scale size likely reflects the degree of polyploidy in butterflies. As noted by Nijhout (1991), Henke (1946) and Henke and Pohley (1952) presented evidence that scale size is proportional to the degree of ploidy of scale cells on a wing. Recently, Cho and Nijhout (2012) confirmed this classical finding. However, the size variation of cover scales that is likely produced by morphogenic signals for color-pattern determination, discovered by Kusaba and Otaki (2009), has not been discussed.

In the present study, we used three nymphalid butterflies, *J. orithya*, *Vanessa cardui* (Linnaeus, 1758), and *Danaus chrysippus* (Linnaeus, 1758), to examine the relationships among the sizes of the wing, compartment, and element and the number and size of the scales. Theoretically, it would be ideal to count and measure all scales on an entire surface of a wing, but this would be labor-intensive and inaccurate due to physical overlaps of scales. We thus focused on a single compartment as a representative of the whole wing in these three species. Based on quantitative morphological analysis, which was made possible by a high-resolution digital microscope, we propose a model for how cells cope with the size problem, and we suggest the nature of morphogenic signals that determine the cell size, scale coloration, and scale shape on wings.

5.2. Materials and methods

5.2.1. Butterflies

We used three species of nymphalid butterflies: *J. orithya* (Nymphalinae), *V. cardui* (Nymphalinae), and *D. chrysippus* (Danainae). Adult females or larvae were collected in the Okinawa-jima Island or Ishigaki-jima Island, the Ryukyu Archipelago, Japan, during the summer of 2011 and 2012. Eggs were obtained from these females. Larvae were reared to adults at 27 ± 1 °C using their natural host plants: *Plantago major* for *J. orithya*, *Artemisia princeps* for *V. cardui*, and *Asclepias curassavica* for *D. chrysippus*. Immediately after eclosion, emerged adults were frozen to avoid damaging their wings. These three nymphalid species do not show any geographical variation in the Ryukyu Archipelago. In this sense, geographical variations within a species may be ignored.

We focused on specific dorsal hindwing compartments of these butterflies for measurements (Fig. 1A). These compartments were chosen to obtain a large background area. The *J. orithya* compartment R_s has a large blue region except for a parafocal element (PFE) and other marginal elements. The *V. cardui* compartment M_1 has a relatively large orange background region despite the fact that it contains a black spot, a PFE, and other marginal elements. The *D. chrysippus* compartment M_3 does

not contain any element except a marginal black and white (MBW) region. Due to sexual dimorphism, we used only males in *J. orithya*. For each species, we examined ten individuals (n = 10) unless otherwise indicated. These ten individuals were chosen to represent a high degree of variance in wing size.

5.2.2. Scale counting and size measurement

The surface of wings from the three nymphalid butterflies we used is entirely covered with neatly arranged cover scales, and no ground scales are visible without removing cover scales (Fig. 1B). This is why we focused only on cover scales. Each cover scale has a single color, which makes identification of elemental boundaries simple. Wing scales were examined using a Keyence digital microscope VHX-1000 (Osaka, Japan). We also used a Saitoh Kougaku digital microscope SKM-S30A-PC (Yokohama, Japan) for routine viewing.

To obtain a specific area in numerical values and to count the number of scales that constituted a specific pattern, we first obtained high-resolution, high-depth digital images of the whole compartment of interest. Using the built-in image analyzer, the area value for a specified region was calculated. To measure the orange area of *V. cardui*, only the orange area excluding the PFE and the most proximal black region but including the black spot was measured. To count the number of scales, check marks were placed on the screen images, and the number of check marks was automatically counted. To count the number of scales in the orange area of *V. cardui*, the most proximal black region and the most distal region from the PFE were excluded, but the black spot was included.

To measure the scale size, we focused on cover scales whose entire surface was observable so that we could easily measure their widths. Scale size, defined as the maximum width, was measured using the measurement function of the image analyzer. Three such scales were chosen randomly from each row, one from the anterior region, one from the middle region, and one from the posterior region of a compartment, and their measurements were averaged as the scale size of that row. When we encountered a row that was a part of the black spot in *V. cardui*, we chose one orange scale from the anterior region, one from the posterior region, and one from the vicinity of the black spot, avoiding the black scales entirely.

We also obtained the PFE area and MBW area in numerical values. Elemental boundaries were determined easily by scale colors. All measurable scales were measured, and the average size was then calculated for these structures.

We assigned the row numbers from proximal (basal) to distal (peripheral). A branched row was considered a single row when the forked parts were shorter than the non-forked part. When the forked parts were longer, they were considered two rows. Scale density was calculated by dividing the

number of scales in a row by the length of the row. The length of the row was measured using the built-in image analyzer of the Keyence digital microscope. Anterior branching was defined as a branching pattern that had two branching rows ending at the anterior side. Posterior branching was defined in the same way.

5.2.3. Statistics

We examined Pearson correlation coefficients together with *p*-values using IBM SPSS Statistics 19 (2010).

5.3. Results

5.3.1. A single compartment represents the whole wing size

We first examined if a given compartment area is proportional to the whole wing area. Whole wing area and wing compartment area were well correlated in *J. orithya* ($r = 0.98$, $p < 0.001$), in *V. cardui* ($r = 0.98$, $p < 0.001$), and in *D. chrysippus* ($r = 0.82$, $p = 0.004$) (Fig. 2A, left). Percentages of the compartment area to the whole wing area showed small standard deviations (Fig. 2A, right). Additionally, the wing compartment area was correlated with the blue area in *J. orithya* ($r = 0.97$, $p < 0.001$) and with the orange area in *V. cardui* ($r = 0.98$, $p < 0.001$) and in *D. chrysippus* ($r = 0.98$, $p < 0.001$) (Fig. 2B, left). Percentages of the blue or orange area to the compartment area showed small standard deviations (Fig. 2B, right). These results indicate that the compartments in small and large wings are isometric to one another in relation to the whole wing and that the blue or orange area can represent the compartment area in these butterflies.

5.3.2. Contribution of the number of scales and rows to background area

We next examined the blue or orange area in a compartment and the number of scales that were contained in that area (Fig. 3A). The blue area was well correlated with the number of scales in *J. orithya* ($r = 0.95$, $p < 0.001$). The orange area (including the black spot) in *V. cardui*, however, did not show a correlation ($r = 0.39$, $p = 0.25$), although a reasonable correlation was obtained when an outlier (which had the largest orange area shown in Fig. 3A) was excluded ($r = 0.73$, $p = 0.03$). In *D. chrysippus*, a weak correlation was detected ($r = 0.57$), but with a high *p*-value ($p = 0.08$).

In contrast, we obtained a reasonably high correlation between the blue or orange area and the number of rows in *J. orithya* ($r = 0.87$, $p = 0.001$) and in *D. chrysippus* ($r = 0.75$, $p = 0.01$) (Fig. 3B). In *V. cardui*, its correlation coefficient was not as high as those of the other species ($r = 0.69$, $p = 0.03$), but it became comparatively high when an outlier (which had the largest orange area in Fig. 3B) was excluded ($r = 0.88$, $p = 0.002$). These results suggest that variation of the background area accompanied the change in the number of scales through an increase of the number of rows.

5.3.3. Contribution of scale size to background area

We then examined the possible variation in scale size. The average scale size of the blue region was reasonably correlated with the blue area in *J. orithya* (r = 0.66, p = 0.04), but not at all with the orange area in *V. cardui* (r = 0.07) or in *D. chrysippus* (r = -0.18) (Fig. 3C). These results indicate that the variation of background area is not related to scale size in *V. cardui* and *D. chrysippus*. However, it is related to scale size, to a certain degree, in *J. orithya*.

5.3.4. PFE area versus scale number and size

We next examined if the elemental area is correlated with scale number and size (Fig. 4A, B). In *J. orithya*, the number of scales in the PFE was reasonably correlated with PFE area (r = 0.76, p = 0.01). In *V. cardui*, the number of scales in the PFE was not significantly correlated with PFE area at the level of $p < 0.05$ (r = 0.61, p = 0.06). In *D. chrysippus*, the number of scales was not correlated with the MBW area (r = 0.059). The correlation between scale size in the PFE and PFE area was not significant statistically in *J. orithya* (r = 0.56, $p > 0.05$) and in *V. cardui* (r = -0.05) (Fig. 4B). The average scale size appeared to have a weak correlation with the MBW area (r = 0.66, p = 0.04), but this may have been simply because of a single outlier of the largest MBW area (Fig. 4B). These results suggest that the PFE area of *J. orithya*, and not of the other two species, is related to the number of scales, as in the case of the blue area, and that in any species, the PEF or MBW area is not related to scale size of its own region.

5.3.5. Relationship between element and background

We next examined correlations between an element (i.e., PFE or MBW) and the blue or orange region to elucidate any possible heterochronic relationship between them during development. PFE area was reasonably correlated with the blue area (r = 0.70, p = 0.02) in *J. orithya*, but not with the orange area in *V. cardui* (r = 0.37, p = 0.20) (Fig. 5A). In *D. chrysippus*, the MBW area showed a weak correlation with the orange area (r = 0.51, p = 0.13) (Fig. 5A). Somewhat unexpectedly, the number of scales in the PFE or MBW did not show any correlation with compartmental blue or orange area in any of the three species, (r = 0.23 in *J. orithya*; r = -0.10 in *V. cardui*; r = 0.40 in *D. chrysippus*) (Fig. 5B).

In contrast, scale size in the PFE exhibited a reasonable correlation with the blue area in *J. orithya* (r = 0.73, p = 0.02), but not in *V. cardui* (r = 0.43, p = 0.21) or in *D. chrysippus* (r = -0.17) (Fig. 5C). Furthermore, the PFE area was weakly correlated with the number of scales in the blue region (r = 0.65, p = 0.04) but not with scale size (r = 0.52, p = 0.12) in the blue region in *J. orithya* (Fig. 5D).

5.3.6. Scale size and scale density

To investigate how scales are arranged in the blue or orange region of the compartment, we measured the average scale size of all rows in the compartments of at least three individuals of each species. An overall decreasing size change from the proximal to the distal portion was observed in all three species (Fig. 6A), as expected from our previous study (Kusaba and Otaki, 2009). However, in *J. orithya*, a scale size increase was found in the middle portion in four out of ten individuals examined, which may represent the influence of a near-by element, a border ocellus in the adjacent compartment. In *V. cardui*, a gradual decrease in scale size was observed throughout (n = 3), and in *D. chrysippus*, the proximal portion showed a brief increase and then an overall decrease (n = 3).

We next measured scale density (defined as the number of scales per row length) in these individuals (Fig. 6B). In *V. cardui*, in parallel with a consistently decreasing tendency of scale size, a consistent increasing tendency of scale density was observed (n = 3). In *J. orithya* and *D. chrysippus*, the density dropped where the size increased, and the density increased where the size decreased (n = 3). This general trend was also observed in *J. orithya* (n = 10).

5.3.7. Row branching patterns

We examined the row branching patterns in three individuals of each species. In all three species, a simple bifurcation pattern was found: anterior and posterior branching patterns (Fig. 7A). Additionally, there was at least one irregular branching pattern, a chiasmatic branching pattern, only in *J. orithya* (Fig. 7B). In this case, one large scale was found at the center of the branching. Posterior branching was more frequent than anterior branching in *J. orithya* and *V. cardui*, but not in *D. chrysippus* (n = 3 for each species) (Fig. 7C). Branching rows were found mostly in the middle portion of a compartment (Fig. 7D), although the distribution pattern was variable among individuals even in the same species (not shown).

5.4. Discussion

5.4.1. Compartment area in relation to the whole wing area

In the present study, we focused on the nymphalid butterfly wing systems to examine how scale cells contribute to wing size variation. In the butterfly wing system, scales are fixed on a two-dimensional plane with a definitive size and coloration. Thus, simple size measurement and counting of scales are technically feasible with a high-resolution digital microscope.

We first examined how wing size variation is related to the number and size of the scales. An entire wing area seems to be proportionally reduced to a wing compartment area in all three species, as suggested by the high correlation coefficient between these two areas, although this correlation was

higher in *J. orithya* than in the other two species. Furthermore, background area likely proportionally represents the whole compartment area in all three species. Therefore, we morphometrically demonstrated isometric nature of butterfly wing structures.

Compartments can be considered independent units of development in *Drosophila* (González-Gaitán et al., 1994; Dahmann and Basler, 1999; Milán and Cohen, 2000; Milán et al., 2002), which may also be true in butterflies, at least to some extent (Beldade et al., 2002; Beldade and Brakefield, 2003; Monteiro et al., 2003). However, the degree of independence in terms of area seems to vary from species to species, judging from the various degrees of correlation. We also note that color patterns beyond a single compartment are not uncommon in butterflies (Otaki, 2011a).

5.4.2. Sizes and numbers of scales and scale cells

Cell size variation in the pupal wing tissue is limited within a relatively narrow size window, in contrast to the addition or elimination of cells. Judging from our correlation coefficients, changes in the number of scales are likely the primary contribution to changes in the whole wing size. This is expected from our general knowledge on organismal size differences (Raff, 1996; Conlon and Raff, 1999; O'Farrell, 2004). This change in scale number appears to be accomplished by changes in the number of scale rows in a compartment. Additionally, changes in the scale size are most likely the second most important contributing factor to changes in the whole wing size, at least in *J. orithya*. Thus, we propose a two-step model for wing-size determination, in which the tissue size is largely determined by cell number but later fine-tuned by cell size. These relationships in *J. orithya* are much less obvious in *V. cardui* and in *D. chrysippus*.

5.4.3. PFE development

In *J. orithya*, PFE scale number but not scale size showed a reasonable correlation with PFE area. The PFE's strategy to cope with the size change is most likely similar to the blue or orange region in that the number of scales is the primary thing that changes, with scale size changes secondary.

The correlations between PFE area and background area were also interesting. In *J. orithya*, the PFE area was correlated with the blue area, which means that the PFE area and the blue area increase or decrease proportionally to each other. That is, their area changes seem synchronized at first glance. However, unexpectedly, the number of scales in the PFE had no correlation with the blue area. In contrast, scale size in the PFE showed a relatively weak but significant correlation with the blue area. Furthermore, the PFE area was weakly correlated with the number of scales, but not with the scale size, in the blue region in *J. orithya*. These results may suggest that when the blue region is in the cell proliferation stage, the PFE is already in the differentiation stage, in which cell size changes. That is, the two regions may be slightly desynchronized in developmental stages in *J. orithya*. This

interpretation is consistent with the developmental time difference among scales of different colorations (Nijhout, 1980a, 1991; Koch et al., 2000; Otaki, 2008; Dhungel and Otaki, 2009).

5.4.4. Size gradient and density gradient

We measured scale size in every row, focusing on a single compartment. In all three species, scale size tended to decrease from the proximal to the distal side. This result was not surprising because similar results were obtained by Kusaba and Otaki (2009) in both *J. orithya* and *J. oenone*. One possibility is that the background coloration and size are determined by a signal from an organizing center, as in the case of elements. The coloration in the background region is also graded in many species (Nijhout, 1991), as quantitatively demonstrated in *J. orithya* (Kusaba and Otaki, 2009). Relatively smooth size and color changes may suggest a simple morphogenic gradient model for the background coloration. However, it is important to note that the induction model for color-pattern elements (Otaki, 2011a,b,c, 2012a,b) can easily produce a gradient when only one type of signal to specify a single color is emitted continuously and an inhibitory signal is up-regulated in the regions away from the organizing center. That is, a classical gradient model is an approximation of the induction model, which is more widely applicable to various color patterns.

Together with the general trend of size decreases from the proximal to the distal side, scale density increased. That is, size and density changes appear to be spatially correlated especially in *V. cardui* and in *D. chrysippus*. In *J. orithya*, this correlation was less obvious. The size–density correlation may suggest that scale cells are packed tightly in every row and that cell size may be determined just before row arrangement. The reverse order, row arrangement first and size changes second, would be difficult to carry out because massive cell death would be required in the row of larger scales, and row arrangement would be more disorganized.

5.4.5. Row branching pattern

Additional information on scale organization was obtained from row branching patterns. Yoshida and Aoki (1989) documented the bifurcation branching pattern of scale arrangement, which we observed in all three species. We think that the branching patterns are produced to adjust arrangement gaps. Because the branching rows are frequently found in the middle portion of a compartment, scale cell arrangement may occur from both the distal and proximal sides. We do not know how to interpret the ratio of the anterior to posterior bifurcation patterns at this point, but it may be related to the arrangement process and could be incorporated into a mathematical model (Sekimura et al., 1999).

Interestingly, we found a chiasmatic branching pattern (a large scale at the center of branching) only in *J. orithya*. In the process of row arrangement, cells likely stop enlarging due to contact inhibition from adjacent cells. However, a physical vacancy may still exist after the row arrangement,

which could allow a cell to enlarge. Thus, it is likely that cell size can continue to change during and after row arrangement.

5.4.6. The possible nature of the morphogenic signal

During development, each immature scale cell has to obtain positional information on scale size and color to produce the scales. The positional information is in general thought to be supplied from organizing centers, usually located at the center of an element (French and Brakefield, 1995; Brakefield and French, 1995; Nijhout, 1980b; Otaki et al., 2005; Otaki, 2011c). Because there is a good spatial correlation between scale color and size and a reasonable correlation between the eyespot size and the maximal eyespot scale size in *J. orithya* (Kusaba and Otaki, 2009), color information and size information are likely supplied simultaneously by a single morphogenic signal. The present study is consistent with the idea that the putative morphogenic signal specifies not only the color of scales but also the size of scales by increasing the degree of ploidy of scale cells. Color-pattern and size information is most likely dissipated before the event of row arrangement. Indeed, color patterns have been considered unrelated to row arrangement (Yoshida, 1988).

An important clue into the nature of the morphogenic signal has been obtained from scale-size analysis (Kusaba and Otaki, 2009). Scale size in eyespots is not smoothly graded. Rather, there is a gap between the dark and light rings (Kusaba and Otaki, 2009), suggesting that the morphogenic signal for an eyespot is not smoothly graded. This then implies that the morphogenic signal could be emitted in a progressive wave or pulse. It appears that the putative morphogenic signal is a ploidy signal that is interpreted by receptor cells pleiotropically. Damage-induced ectopic eyespots also have relatively larger scales than the background (Kusaba and Otaki, 2009). Damage to wing tissue in the pupal stage causes developmental delay of the cells at the damaged region (Takayama and Yoshida, 1997). Thus, damage may give scale cells around the damaged site a longer time to synthesize genomic DNA. As a result, cell fate is determined dose-dependently by the number of gene copies. This fate determination depending on gene dose may explain the pleiotropic nature of the morphogenic signal.

5.4.7. Integrative model for wing development

Based on the present data alone, we are able to propose an integrative model for wing development, as follows. The wing tissue size is first determined by the number of constituent cells. At this point, cells are proliferating, and the cells are relatively small. The number of cells at this point determines the number of rows that are formed later. This proliferation process is immediately followed by cell enlargement in a position-dependent manner, governed by the morphogenic signals that induce polyploidy. This cell size change most likely takes place before row arrangement and contributes to a

small increase of wing size. This is the process of fate determination and differentiation. At this point, size, color, and shape are determined together. Then, scale cells are arranged most likely from both ends of a compartment. Gaps of rows are accommodated by row branching patterns. This model is largely consistent with other developmental observations (Nijhout, 1991; Cho and Nijhout, 2012). Allometric constraints (Frankino et al., 2005, 2007) may originate from the disruption of these coordinated processes. In the future, it is expected that the model presented above can further be integrated with cellular and molecular mechanisms of scale development (Greenstein, 1972; Ghiradella, 1998; Kristensen and Simonsen, 2003) and body-size regulations (Mirth and Riddiford, 2007).

5.5. References

Azevedo RBR, French V, Partridge L: Temperature modulates epidermal cell size in *Drosophila melanogaster*. Journal of Insect Physiology 2002, 48: 231-237.

Beldade P, Koops K, Brakefield PM: Modularity, individuality, and evo-devo in butterfly wings. Proceedings of the National Academy of Sciences USA 2002, 99: 14262-14267.

Beldade P, Brakefield PM: Concerted evolution and developmental integration in modular butterfly wing patterns. Evolution and Development 2003, 5: 169-179.

Brakefield PM, French V: Eyespot development on butterfly wings: the epidermal response to damage. Developmental Biology 1995, 168: 98-111.

Cho EH, Nijhout HF: Development of polyploidy of scale-building cells in the wings of Manduca sexta. Arthropod Structure and Development 2012, 42: 37-46.

Conlon I, Raff M: Size control in animal development. Cell 1999, 96: 235-244.

Dahmann C, Basler K: Compartment boundaries: At the edge of development. Trends in Genetics 1999, 15: 320-326.

de Moed GH, de Jong G, Scharloo W: Environmental effects on body size variation in *Drosophila melanogaster* and its cellular basis. Genetic Research 1997, 70: 35-43.

Dhungel B, Otaki JM: Local pharmacological effects of tungstate on the color-pattern determination of butterfly wings: a possible relationship between the eyespot and parafocal element. Zoological Science 2009, 26: 758-764.

Edgar BA, Nijhout HF: Growth and cell cycle control in *Drosophila*. In: Hall MN, Raff M, Thomas G (eds) Cell Growth: Control of Cell Size 2004, pp. 23-83. Cold Spring Harbor Laboratory Press, Cold Spring Harbor.

Follette PJ, Duronio RJ, O'Farrell PH: Fluctuations in cyclin E levels are required for multiple rounds of endocycle S phase in Drosophila. Current Biology1998, 8: 235-238.

Frankino WA, Zwaan BJ, Stern DL, Brakefield PM: Natural selection and developmental constraints in the evolution of allometries. Science 2005, 307: 718-720.

Frankino WA, Zwaan BJ, Stern DL, Brakefield PM: Internal and external constraints in the evolution of morphological allometries in a butterfly. Evolution 2007, 61: 2958-2970.

French V, Brakefield PM: Eyespot development on butterfly wings: the focal signal. Developmental Biology 1995, 168: 112-123.

Gatti M, Baker BS: Genes controlling essential cell-cycle functions in *Drosophila melanogaster*. Genes and Development 1989, 3: 438-453.

Ghiradella H: Hairs, bristles and scales. In: Harrison FW, Locke M (eds) Microscopic Anatomy of Invertebrates 1998, Volume 11: Insecta. pp. 257-287. John Wiley & Sons, New York.

González-Gaitán M, Capdevila MP, García-Bellido A: Cell proliferation patterns in the wing imaginal disc of *Drosophila*. Mechanisms of Development 1994, 46: 183-200.

Greenstein ME: The ultrastructure of developing wings in the giant silkmoth, *Hyalophora cecropia*. II. Scale-forming and socket-forming cells. Journal of Morphology 1972, 136: 23-52.

Hayashi S: A Cdc2 dependent checkpoint maintains diploidy in *Drosophila*. Development 1996, 122: 1051-1058.

Henke K: Über die verschiedenen Zellteilungsvorgange in der Entwicklung des beschuppten Flügelepithels der Mehlmotte Ephestia kühniella Z. Biologisches Zentralblatt 1946, 65: 120-135.

Henke K, Pohley H-J: Differentielle Zellteilungen und Polyploedie bei der Schuppenbildung der Mehlmotte Ephestia kühniella. Zeitschrift für Naturforschung Section B 1952, 7: 65-79.

Janssen JM, Monteiro A, Brakefield PM: Correlations between scale structure and pigmentation in butterfly wings. Evolution and Development 2001, 3: 415-423.

Kristensen NP, Simonsen TJ: Hairs and scales. In: Kristensen NP (ed) Lepidoptera, Moths and Butterflies: Morphology, Physiology, and Development. Handbook of Zoology 2003, Volume IV, Anthropoda: Insecta, pp. 9-22. Walter de Gruyter, Berlin.

Koch PB, Lorenz U, Brakefield PM, ffrench-Constant RH: Butterfly wing pattern mutants: developmental heterochrony and co-ordinately regulated phenotypes. Development Genes and Evolution 2000, 210: 536-544.

Kusaba K, Otaki JM: Positional dependence of scale size and shape in butterfly wings: Wing-wide phenotypic coordination of colour-pattern elements and background. Journal of Insect Physiology 2009, 55: 174-182.

Milán M, Cohen SM: Subdividing cell populations in the developing limbs of Drosophila: Do wing veins and leg segments define units of growth control? Developmental Biology 2000, 217: 1-9.

Milán M, Perez L, Cohen SM: Short-range cell interactions and cell survival in the *Drosophila* wing. Developmental Cell 2002, 2: 797-805.

Mirth CK, Riddiford LM: Size assessment and growth control: how adult size is determined in insects. BioEssays 2007, 29: 344-355.

Monteiro A, Prijs J, Bax M, Hakkaart T, Brakefield PM: Mutants highlight the modular control of butterfly eyespot patterns. Evolution and Development 2003, 5: 180-187.

Neufeld TP, de la Cruz AF, Johnston LA, Edgar BA: Coordination of growth and cell division in the *Drosophila* wing. Cell 1998, 93: 1183-1193.

Nijhout HF: Ontogeny of the color pattern on the wings of *Precis coenia*. Developmental Biology 1980a, 80: 275-288.

Nijhout HF: Pattern formation on lepidopteran wings: determination of an eyespot. Developmental Biology 1980b, 80: 267-274.

Nijhout HF: The Development and Evolution of Butterfly Wing Patterns 1991. Smithsonian Institution Press, Washington.

Nijhout HF: Elements of butterfly wing patterns. Journal of Experimental Zoology 2001, 291: 213-225.

O'Farrell PH: How metazoans reach their full size: the natural history of bigness. In: Hall MN, Raff M, Thomas G (eds) Cell Growth: Control of Cell Size 2004, pp. 1-22. Cold Spring Harbor Laboratory Press, Cold Spring Harbor.

Otaki JM: Physiologically induced colour-pattern changes in butterfly wings: Mechanistic and evolutionary implications. Journal of Insect Physiology 2008, 54: 1099-1112.

Otaki JM: Colour-pattern analysis of parafocal elements in butterfly wings. Entomological Science 2009, 12: 74-83.

Otaki JM: Colour-pattern analysis of eyespots in butterfly wings: a critical examination of morphogen gradient models. Zoological Science 2011a, 28: 403-413.

Otaki JM: Generation of butterfly wing eyespot patterns: a model for morphological determination of eyespot and parafocal element. Zoological Science 2011, 28: 817-827.

Otaki JM: Artificially induced changes of butterfly wing colour patterns: dynamic signal interactions in eyespot development. Scientific Reports 2011c, 1: 111.

Otaki JM: Colour pattern analysis of nymphalid butterfly wings: Revision of the nymphalid groundplan. Zoological Science 2012a, 29: 568-576.

Otaki JM: Structural analysis of eyespots: dynamics of morphogenic signals that govern elemental positions in butterfly wings. BMC Systems Biology 2012b, 6: 17.

Otaki JM, Ogasawara T, Yamamoto H: Morphological comparison of pupal wing cuticle patterns in butterflies. Zoological Science 2005, 22: 21-34.

Partridge L, Barrie B, Fowler K, French V: Evolution and development of body size and cell size in *Drosophila melanogaster* in response to temperature. Evolution 1994, 48 1269-1276.

Powell JR: Temperature related genetic divergence in *Drosophila* body size. Journal of Heredity 1974, 65: 257-258.

Raff MC: Size control: The regulation of cell numbers in animal development. Cell 1996, 86: 173-175.

Sekimura T, Zhu M, Cook J, Maini PK, Murray JD: Pattern formation of scale cells in lepidoptera by differential origin-dependent cell adhesion. Bulletin of Mathematical Biology 1999, 61: 807-828.

Simonsen TJ, Kristensen NP: Scale length/wing length correlation in Lepidoptera (Insecta). Journal of Natural History 2003, 37: 673-679.

Süffert F: Die Geschichte der Bildungs zellen im Puppen-flügelepithel bei einem Tagschmetterling. Biologisches Zentralblatt 1937, 57: 615-628.

Takayama E, Yoshida A: Color pattern formation on the wing of the butterfly *Pieris rapae*. 1. Cautery induced alteration of scale color and delay of arrangement formation. Development Growth and Differentiation 1997, 39: 23-31.

Vukusic P, Sambles JR, Lawrence CR: Colour mixing in wing scales of a butterfly. Nature 2000, 404: 457.

Weigmann K, Cohen SM, Lehner CF: Cell-cycle progression, growth and patterning in imaginal discs despite inhibition of cell division after inactivation of *Drosophila* Cdc2 kinase. Development 1997, 124: 3555-3563.

Weiss A, Herzig A, Jacobs H, Lehner CF: Continuous cyclin E expression inhibits progression through endoreduplication cycles in Drosophila. Current Biology 1998, 8: 239-242.

Yoshida A: Scale arrangement on lepidopteran wings. Special Bulletin of the Lepidopterological Society of Japan 1988, 6: 447-464. (In Japanese)

Yoshida A, Shinkawa T, Aoki K: Periodical arrangement on lepidopteran (butterfly and moth) wings. Proceedings of the Japan Academy 1983, 59B: 236-239.

Yoshida A, Aoki K: Scale arrangement pattern in a lepidopteran wing. 1. Periodic cellular pattern in the pupal wing of *Pieris rapae*. Development Growth and Differentiation 1989, 31: 601-609.

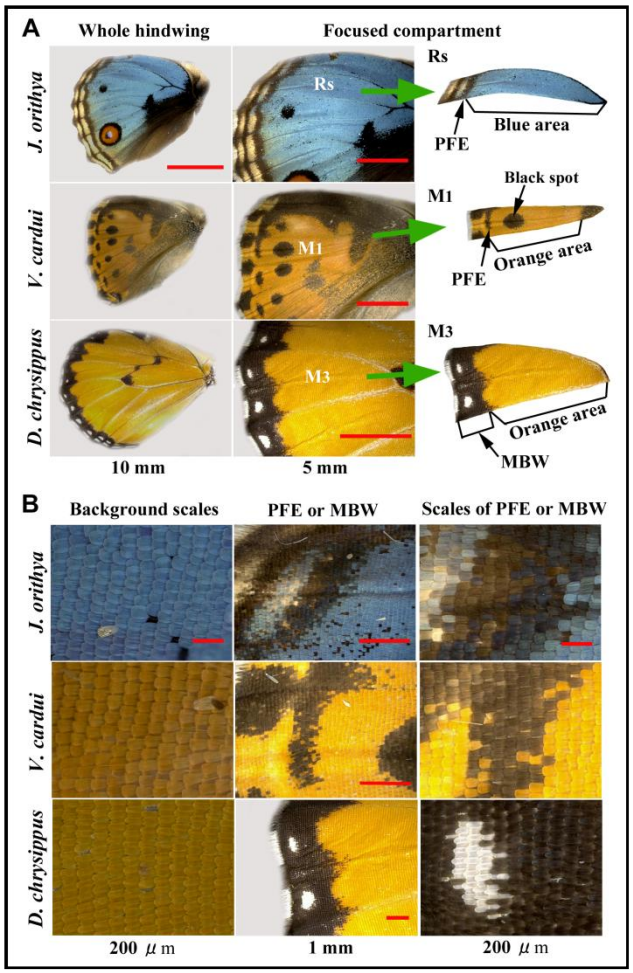

Fig. 5.1 Wings, compartments, and scales of the three nymphalid species studied in this paper. Scale bar size is shown at the bottom of each column. If a single bar is shown in a column, that bar applies to all panels of the column. PFE: parafocal element. MBW: marginal black and white region. (**A**) The compartments focused on in this study (R_s in *J. orithya*, M_1 in *V. cardu*i, and M_3 in *D. chrysippus*). In the third column, these compartments are isolated**.** (**B**) Background scales and PFE or MBW scales. Only cover scales are visible.

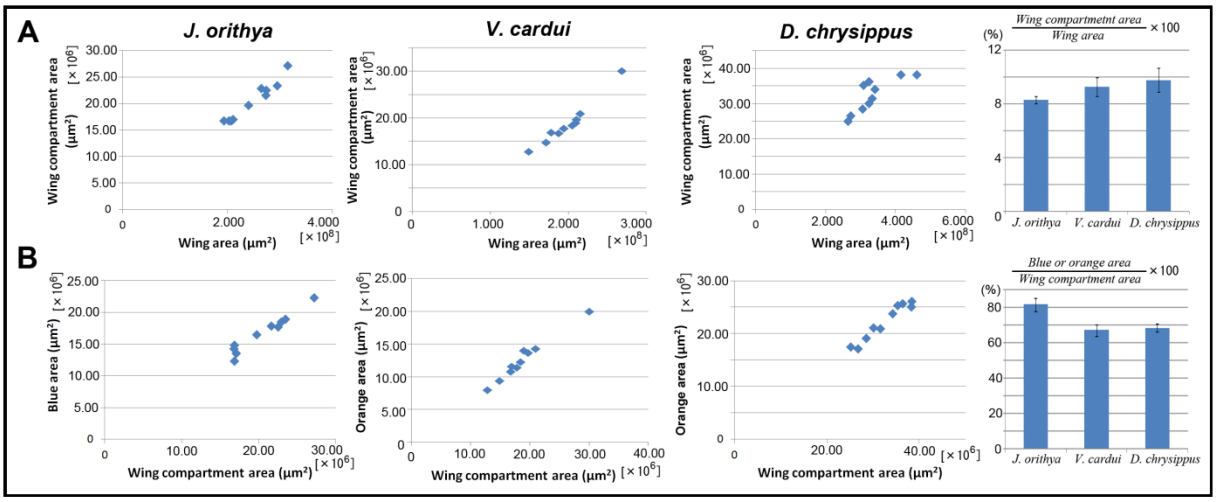

Fig 5.2 Relationships among wing area, wing compartment area, and background (blue or orange) area in three nymphalid species. (**A**) Scatter plots showing relationships between wing area versus compartment area (left), and percentages of the compartment area to the whole wing area, showing small standard deviations (right). (**B**) Scatter plots showing relationships between wing compartment area versus blue or orange area (left), and percentages of the blue or orange area to the compartment area, showing small standard deviations (right).

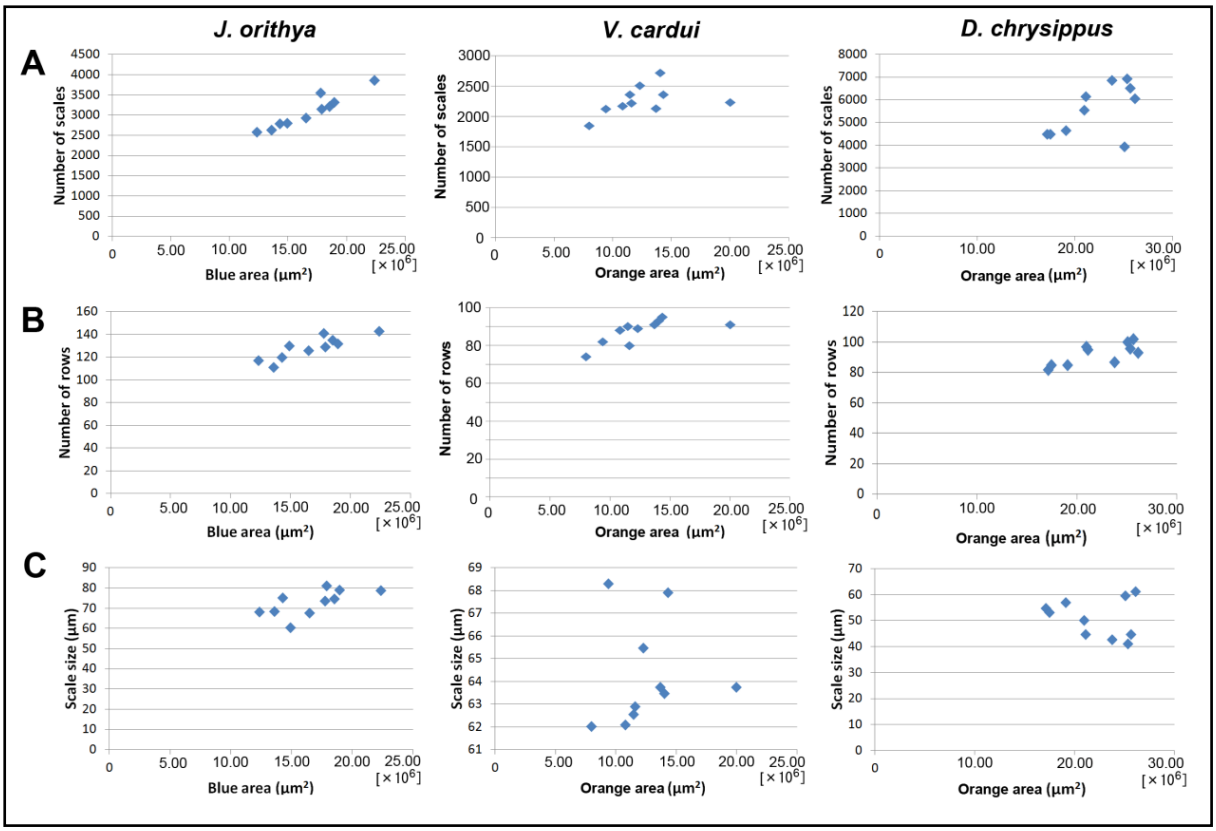

Fig. 5.3 Scatter plots showing relationships among background (blue or orange) area, number of scales, number of rows, and scale size in three nymphalid species. (**A**) Blue or orange area versus the number of scales. (**B**) Blue or orange area versus the number of rows. (**C**) Blue or orange area versus scale size.

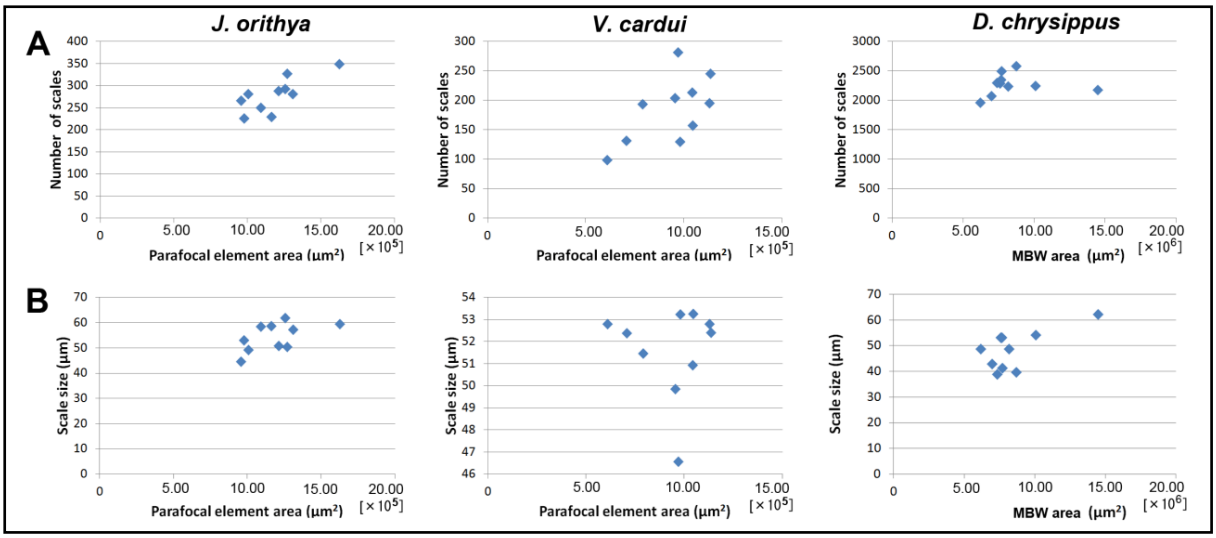

Fig. 5.4 Scatter plots showing relationships among PFE or MBW area, number of scales, and scale size in three nymphalid species. (**A**) PFE or MBW area versus the number of scales. (**B**) PFE or MBW area versus scale size.

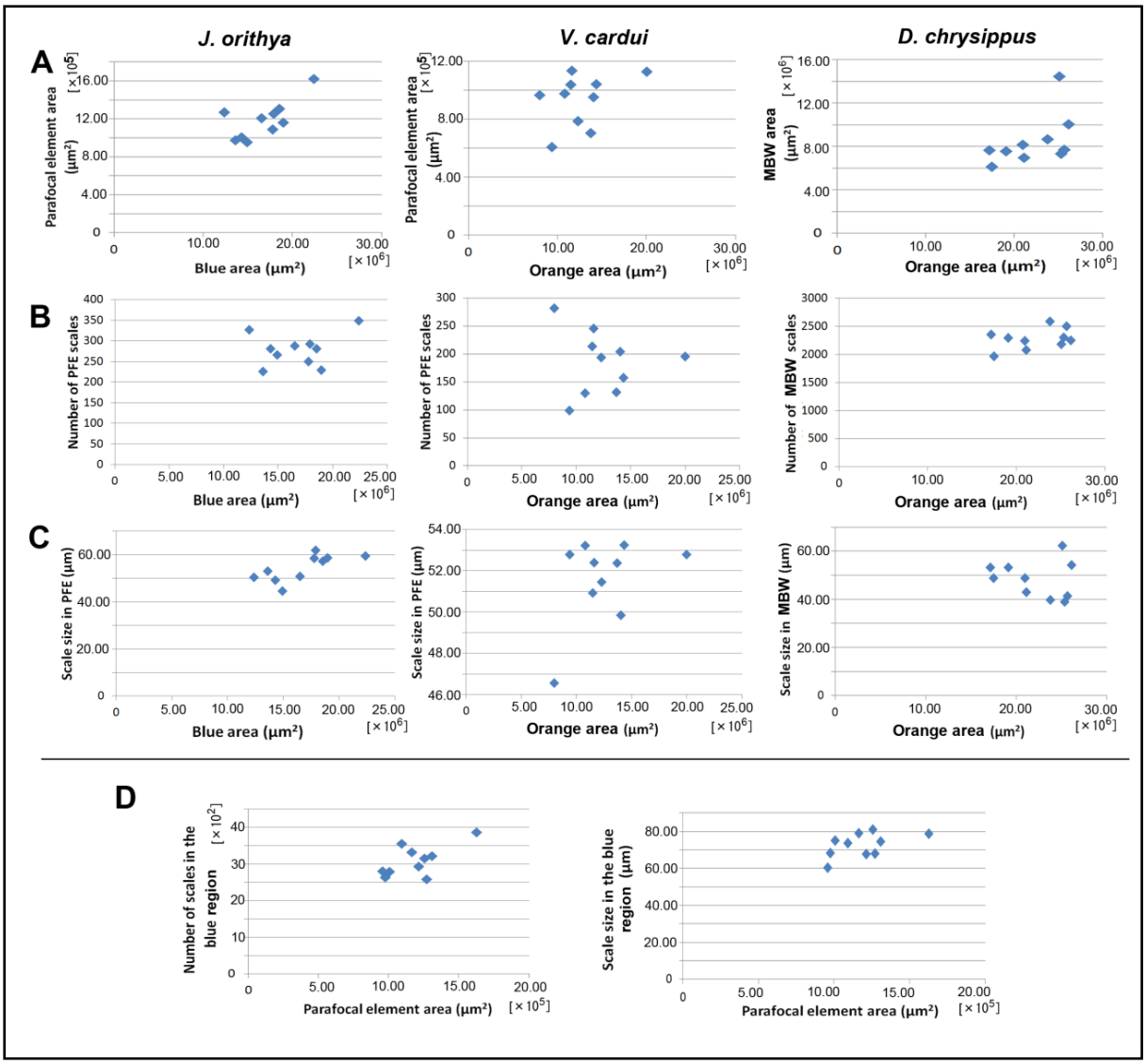

Fig. 5.5 Scatter plots showing relationships among PFE or MBW area, background (blue or orange) area, the number of PFE or MBW scales, and scale size in the PFE or MBW in three nymphalid species. (**A**) Blue or orange area versus PFE or MBW area. (**B**) Blue or orange area versus scale size in the PFE of MBW. (**C**) Blue or orange area versus scale size in the PFE or MBW. (**D**) PFE area versus the number of scales or scale size in the blue region in *J. orithya*.

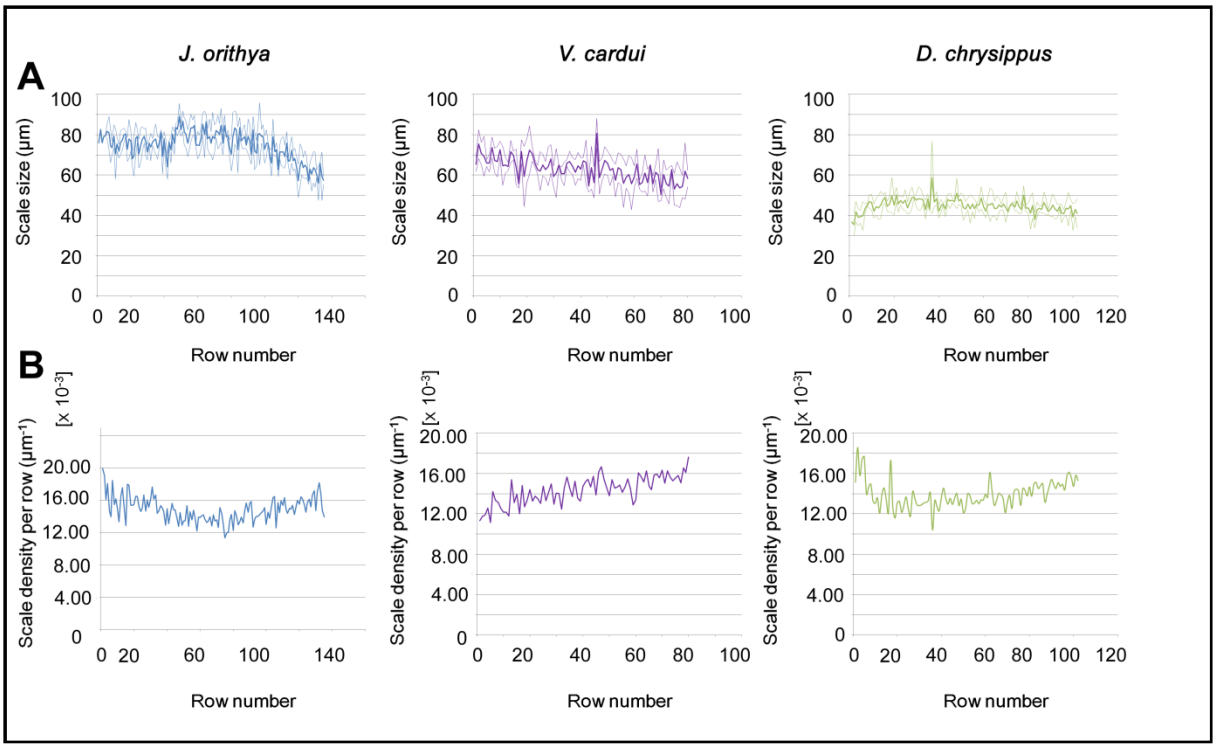

Fig. 5.6 Position-dependent changes of scale size and scale density in the blue or orange region in three nymphalid species. Rows are numbered from proximal to distal. Scale size and density data were recorded from the same individual. (**A**) Scale size distribution. (**B**) Scale density distribution.

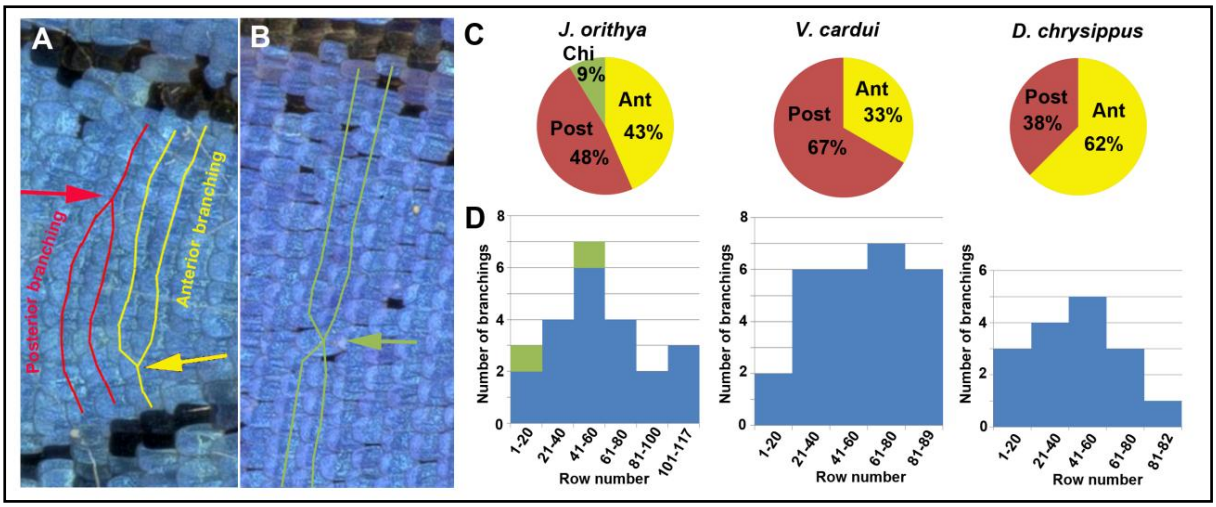

Fig. 5.7 Row branching patterns in the blue or orange region in three nymphalid species. (**A**) Anterior and posterior branching patterns in *J. orithya*. Arrows indicate branching points. (**B**) Chiasmatic branching pattern. An arrow indicates a large scale located at the chiasmatic branching point. (**C**) Proportion of the anterior, posterior, and chiasmatic branching patterns. (**D**) Positional distributions of branching patterns. Data for C and D were obtained from the same individual.

Chapter 6

Artificial diets for rearing blue pansy butterfly *Junonia orithya*

6.1. Introduction

Nymphalid groundplan is an idealized color-pattern of butterfly wings proposed by Nijhout (1990, 1991, and 2001) and applies strictly to the family Nymphalidae butterfly but is still useful for understanding color-patterns of other butterflies and moths.

Pattern formation and variation in butterflies are a good model for evo-devo study (Beldade and Brakefield 2002; Joron *et al*., 2006, Brakefield 2007; Parchem *et al*., 2007; Beldade *et al*., 2008; Otaki 2008). The genes, development and evolution have integrated roles in phenotypic variations of butterfly (Nijhout1991, Monteiro *et al*., 1994; Brakefield *et al*., 1996; Brunetti *et al*., 2001; Beldade and Brakefield, 2002). The fruit fly has been intensively used and somewhat successful in deciphering the molecular events behind these phenotypic variations (Carroll *et al*., 2001). Molecular and cellular basis of pattern formation study in butterfly is difficult compared to the model organism *Drosophila melanogaster*, as we are still lacking molecular genetic techniques for butterflies. Alternately, aberrant forms of wing color pattern can be achieved by artificial means such as temperature shock as shown by Nijhout 1984, 1985 using Nymphalidae butterfly *Vanessa cardui, Vanessa virginiensis, and Junonia coenia* or systemic injection of some protein-tyrosine phosphatase (PTPase) inhibitors specially sodium tungstate (ST) shown by Otaki (1998, 2005) using *C. cardui, and J. orithya.* These studies help in understanding underlying developmental mechanism and color-pattern diversity. Temperature shock and sodium tungstate treatment are similar in nature in terms of pattern modifications they induce in butterfly wings. However, another way of obtaining modified wing color pattern and understanding underlying mechanism is feeding larvae with mutagens at the early stage. However, for this approach, artificial diet for a particular species is required.

Junonia coenia (Nymphalidae: Nymphalinae) has been used for the study of wing color pattern development and has distinctive eyespots on its wings (Nijhout 1980a, 1980b, 1984, 1985, 1991). Eyespots on butterfly wings have been used for mechanistic studies. An African butterfly *Bicyclus anynana* (Nymphalidae: Satyrinae) has also been widely used for eyespot study with the help of surgery and cautery, expression and genetic studies (French and Brakefield, 1992, 1995; Brakefield and French 1995; Brakefield *et al* 1996; Keys *et al* 1999; Brunetti *et al*. 2001). *J. orithya* also has distinctive eyespots on its wings and a simple color pattern (Figure 6.1). *J. orithya* is actually Japanese version of *J. coenia*. We have been using *J. orithya* for wing color-pattern studies.

In our study, we are using an artificial diet not only to standardize the rearing condition of the butterfly in the laboratory but also to study wing color pattern by feeding experiments with mutagens

that can alter wing color patterns. An artificial diet for another species *Z. maha* (Hiyama *et al*. 2010) has already been reported. Based on the diet for *Z.maha*, we are trying to prepare an artificial diet for *J. orithya*. The main component of the artificial diet for *Z. maha* is the leaves of the host plant *Oxalis*. We made diet similar to the one made for *Z. maha* but only host plant *Oxalis* was replaced by host plant *Plantago major* for *J.orithya*. The growth of the larvae was completely halted when we used this modified diet. Later, we improved the diet by the addition of many other ingredients from the diet for *J. coenia* (Browers, 1984) and *B. anynana* (Holloway, 1991).

The main purpose of this chapter is to make an artificial diet for *J. orithya* and increase experimental use of this butterfly in the wing color pattern formation and diversity.

6.2. Materials and methods

6.2.1. Insects

Female adult individuals of the blue pansy butterfly *J. orithya* Linnaeus, 1758 (Nymphalidae, Lepidoptera) were caught in Okinawa-jima island or Ishigaki-jima island in the Ryukyu Archipelago, Japan. Eggs were collected from these females. Alternatively, larvae were field-caught in these islands. This species shows sexual dimorphism and high color-pattern variation among individuals.

6.2.2. Rearing larvae

The first instar larvae were left untouched in the host plant until second instar to minimize larval death. Larvae were fed on a natural host plant *Plantago major* or an artificial diet. The larvae were divided into two groups, the second and the fourth instar groups. Larvae were fed with artificial diets from the second instar and in another from the fourth instar. The second instar larvae were transferred directly to artificial diet with the help of a wet fine paint brush. We kept six larvae in each plastic container (21 cm W × 15 cm D × 6 cm H) and an artificial diet was replaced daily, until these larvae became pupae. The eclosed adults were readily frozen not to damage their wings.

6.2.3. Artificial diets

Artificial diets were made mostly based on *Z. maha* diet (Hiyama *et al*, 2010) and we also referred to diet for *J. coenia* (Bowers, 1984) and *Bicyclus anynana* (Holloway *et al*, 1991).

In this chapter, seven different artificial diets were used for rearing larvae of *J. orithya* in search of suitable artificial diet for *J. orithya*. The artificial diet AD-FZMUV was very similar to artificial diet used for rearing *Z. maha* larvae, in which the host plant *Oxalis* leaves were replaced with *Plantago* leaves and no vitamin complex was used. For the artificial diet AD-FZM, only the host plant leaves were replaced. In order to improve the artificial diet made for *Z. maha* larvae, we added Brewer's

yeast in AD-FY, Brewer's yeast, cholesterol, and casein in AD-FYCC; Brewer's yeast, cholesterol, casein, starch, and wheat germ in AD-FYCCSW. Insecta F-II diet was bought, mixed with dried leaves of *Plantago* and used some preservatives for longer use of the prepared artificial diet. In order to make a diet similar to Insecta F-II, *Z. maha* diet was further modified by using a lesser amount of dried host plant leaves and increasing other ingredients. We used the same amount of dried leaves required to make Insecta F-II artificial diet. The ingredients of all the diets are shown in Table 6.1.

6.3. Results

6.3.1. Rearing *J. orithya* second instar larvae with artificial diets

J. orithya larvae were fed with artificial diet from the second instar stage. Very high larval mortality was seen in all the artificial diets used, when larvae from the second instar were used. The larval mortality rate was more than 30% in all the artificial diets, and larvae fed with the natural host plant leaves were healthy and no larval mortality (n = 29) was seen. The larval mortality rate was highest of (100%, n = 30) with AD-FYCCSW and lowest with Insecta F-II (33.3%, n = 45). The failure rate was the highest with artificial diet AD-DYCCSW (53.3%, n = 15, Table 6.2). Regarding the wing color pattern, the modification rate was highest in diet AD-DYCCSW (57.1%, n = 7, Table 6.2). Various kinds of modifications (Fig. 6.2) and homeotic transformation associated with diets are shown in Fig. 6.3. However, homeotic transformation was found only with diet AD-FZMUV. The homeotic transformation was 5.8% (n = 17, Table 6.2) in the diet with no vitamins added to the *Z. maha* diet.

The performance of each artificial diet was compared based on larval period, pupal weight, pupal period, and left-forewing length of adults reared with artificial diets, or natural fresh leaves (Fig. 6.4). Only in the artificial diet AD-FBY larval period was significantly longer than ND (n = 13, $p < 0.001$, Fig. 6.4A). Pupal period was significantly longer only in one artificial diet AD-FZMUV (n = 17, $p < 0.001$, Fig. 6.4B). The pupal weight was also significantly lower than in three artificial diets AD-FZMUV (n = 17, $p < 0.001$), AD-FBY (n = 13, $p < 0.01$) and AD-DYCCSW (n = 7, $p < 0.001$) when compared with ND (Figure 6.4C). However, left-forewing length was significantly different in groups fed with artificial diets AD-FZMUV (n = 17, $p < 0.01$) and AD-DYCCSW (n = 7, $p < 0.001$) (Fig. 6.4D).

Two artificial diets AD-FZM and AD-FYCC were ignored in this statistic analysis because both of them had only 1 case each.

In addition, the diet AD-FZM was able to keep larvae in the second instar phase for 30 days (n = 30) and when were given normal host plant leaves, the growth was normal and healthy pupae and adults without any color pattern modifications (n = 1, Table 6.2) were obtained.

Based on above data, Insecta F-II is a suitable artificial diet to rear *J. orithya* larvae from the second instar in laboratory.

6.3.2. Rearing with artificial diets from the fourth instar

The larval mortality was less than 10 % in the case of all artificial diets (Table 6.1). Insecta F-II diet (n = 30) and natural host plant (ND) (n = 30) had 0% mortality rate. The artificial diet AD-FYCCSW had the highest larval mortality rate of 6.7% (n = 30). Regarding the wing color pattern, the modification rate was highest in the diet AD-FBY (78.9%, n = 15), and no modification was observed in control group ND (n = 28). However, homeotic transformation was found only in three diets AD-FZMUV (4.7%, n = 42), AD-FZM (57%, n = 28), and AD-FBY (63.1%, n = 15) (Table 6.3).

Similarly, the performance of each artificial diet was compared based on pupal period, pupal weight, and left-forewing length of adults reared with artificial diets with control group (ND). Pupal period was significantly different in three artificial diets (Fig. 6.5): longer in AD-FZMUV (n = 42, p < 0.001, Fig. 6.5A), longer in AD-FZM (n = 28, p < 0.001, Fig. 6.5A), and shorter in the case of Insecta F-II (n = 27, p < 0.001, Fig. 6.5A). The pupal weight was significantly smaller in two artificial diets AD-FZMUV (n = 42, p < 0.001, Fig. 6.5B) and AD-FBY (n = 15, p < 0.01, Fig. 6.5B) when compared with ND. Left-forewing length was significantly shorter in two groups AD-FZMUV (n = 42, p < 0.01, Fig. 6.5C) and AD-FBY (n = 15, p < 0.001, Fig. 6.5C).

When larvae are reared from the fourth instar on artificial diets, the mortality rate, failure rate and modification rate were smaller than the second instar group.

6.3.3. Modified wing color pattern with artificial diets

With the artificial diets, normal (Fig. 6.1) as well as modified color patterns (Fig. 6.2) were achieved. In Fig. 6.2, some unusual color patterns in the wings of *J. orithya* were seen when larvae were fed with artificial diets. Most of them had underdeveloped scales (Figs. 6.2A-I). In another case, an eyespot was reduced to black spot (Figs. 6.2J-L). Yet another case, black smear black band was seen on the ventral side of the forewing (Figs. 6.2M-O). Wings with some black spots (Figs. 6.2P-R) and white spots (Figs. 6.2S-U) were also found. In one more case, extended black region with white at the end on the dorsal side of the hindwing (Figs. 6.2V-X) was seen.

The variety of the modified wing color pattern was seen, and they clearly indicate a lack of the key ingredients in the artificial diets.

6.3.4. Artificial diet and homeotic transformation

With three artificial diets, AD-FZMUV (4.7%, *n* = 42, Table 3, Fig. 6.6A), AD-FZM (57%, *n* = 28, Table 3, Fig. 6.6A), and AD-FBY (63.1, *n* = 15, Table 3, Fig. 6.6A), homeotically, transformed individuals were found, that is, some part of the ventral wing had the dorsal wing features (Figs. 6.3A-L). However, reversed type was never found. A small portion of ventral hindwing had dorsal hindwing identity (Figs. 6.3A-C). In Figs. 6.3D-F, a ventral forewing had almost 40% dorsal-forewing-like characteristic and resembles dorsal forewing scales. A ventral hindwing had around 30% dorsal hindwing feature (Figs. 6.3G-I). We also found a ventral forewing where it had more than 90% dorsal-forewing-like character (Figs. 6.3J-K). The scales were clearly seen in highly magnified images (Figs. 6.3C, F, I, L).

The homeotic transformation was found with three diets AD-FZMUV, AD-FZM, and AD-FBY. The AD-FBY had the highest rate of this transformation. In terms of sex, more females were homeotically transformed than males (Fig. 6.6B).

6.3.5. Comparison between groups fed with artificial diets from the second and the fourth instar larvae

The larval mortality was more than 30% (Table 6.2) when larvae were fed from the second instar compared to the fourth instar where larval mortality was less than 10% (Table 6.3). In the second instar group, homeotic transformation was found only with diet AD-FZMUV (Table 6.2). However, with the fourth instar group, the transformation was found with diets, AD-FZM and AD-FBY (Table 6.3) in addition to AD-FZMUV. Pupal period, pupal weight, and left-forewing length in two groups the second and the fourth instar fed with artificial diets were compared. No significant difference was found in pupal period whether larvae were fed with artificial diet from the second or the fourth instar (Fig. 6.7A). When pupal weight and left forewing length were compared in three groups AD-FZMUV, AD-FBY, and AD-DYCCSW, they were significantly different. AD-FZMUV and AD-FBY had lighter pupae with shorter forewing, when artificial diets were given from the fourth instar instead of the second instar. AD-DYCCSW had heavier pupae and adults with longer left forewing when diets were given from the fourth instar instead of the second instar larvae (Fig. 6.7B, C)

The feeding experiment should be started from the fourth instar to insure healthy pupae and healthy adults with wing color-pattern modification.

6.4. Discussion

In this study, six artificial diets based on already published *Z. maha* (Hiyama *et al*., 2010), *J. coenia* (Bowers, 1984), and *B. anynana* (Holloway, 1991) diets were prepared. The diet AD-FZM made for

J. orithya based on *Z. maha* must be missing some key ingredients essential for growth so the growth of larvae could not take place. Nevertheless, diet AD-FZM can be used to keep larvae in earlier stage for a long time and when needed can be fed to normal host plant leaves and get healthy larvae, pupae, and adults at the time of need. The diet AD-FZM might be lacking key ingredients that are responsible for growth and metamorphosis. Before this diet, to delay larval growth or to keep the larvae in the same stage for longer time we used to keep larvae at cold temperature. The diet AD-FZM also has similar effects and could be used for keeping the larvae at the earlier stage for longer time. Once they were again fed with normal leaves, healthy pupae and adults were obtained.

We added many ingredients to the original *Z. maha* diet and finally obtained reasonable diets for *J. orithya*. Larvae were fed with one of the AD-FYCC diet and healthy pupae and adults were obtained. The adults from this diet had 15% wing color pattern modifications (Table 6.3). The diet AD-FYCC was comparable to the control group (ND). The diet AD-FYCC can be used for rearing *J. orithya* larvae in the laboratory, but slightly modified wing color patterns are inevitable. The diet AD-FYCC can be improved in the future for laboratory purpose by adding more ingredients

Furthermore, homeotic transformation where a portion of ventral hindwing had the dorsal identity was achieved with certain diets, AD-FZMUV, AD-FZM, and AD-FBY. When larval group was fed with these diets from the fourth instar we obtained highest modification with AD-FBY. However, no modification was seen when fed from the second instar. After a month, those second instar larvae were fed with normal leaves and thus they might have acquired all the key ingredients form leaves and less homeotic mutation was observed. Homeotic transformation with AD-FZMUV was found only when larvae were fed from the second instar stage. Homeotic transformation such as *hindsight* has been associated with functional loss of gene *Ultrabithorax* (*Ubx*) (Weatherbee *et al*, 1998). Furthermore, ectopic expression of gene *Ubx* in the forewing of butterfly *J.coenia* via recombinant SIN virus resulted in hindwing identity (Lewis *et al*., 1999). But in the *hindsight* mutant, hindwing had forewing identity not the kind of mutant we found. In the mutant we encountered, the ventral wing had the dorsal wing identity. Furthermore in *Drosophila*, the group of cells expressing gene *apterous* becomes dorsal side and non-expressing cells becoming ventral side (Kim *et al*., 1995). So, in the mutant we got, the same gene *apterous* might be responsible for the dorsal identity in the ventral wing. The mutant might be one of the phenocopy due to a lack of some nutrient in the diets. The loss of functionality of the protein that represses *apterous* activation might have caused this kind of modification. But at this stage, we are not able to identify which ingredients in the diet or a lack of some key ingredients are responsible for this homeotic transformation in these modified individuals.

Insecta F-II diet for *J. orithya* has already been reported (Hirai *et al*., 2011). However, the diet could be used for a week only. We slightly modified the diet with the addition of few preservatives (Table 6.1) and now can be used for at least more than a week without any problems. Among all the

artificial diets tested, modified Insecta F-II diet was comparable to natural diet. So for physiological assay, and wing color pattern formation and diversity study, this diet can be used.

6.5. Conclusions

Modified Insecta F-II diet was a very useful artificial diet to rear *J. orithya* larvae in laboratory. Three diets AD-FZMUV, AD-FZM, and AD-FBY produced adults with homeotic transformation with the ventral wing having the dorsal sight identity. Furthermore, an artificial diet AD-FBY can keep larvae in younger stage for longer time; later when fed with normal leaves, they grew normally without any wing color-pattern modifications.

6.6. References

Beldade P, Brakefield PM: The genetics and evo-devo of butterfly wing patterns. Nature Reviews Genetics2002, 3: 442-452.

Bowers MD: Iridoid glycosides and host-plant specificity in larvae of the buckeye butterfly, *Junonia coenia* (Nymphalidae). Journal of Chemical Ecology 1984, 10: 11.

Brakefield PM, French V: Eyespot development on butterfly wings: the epidermal response to damage. Developmental Biology1995, 168: 98-111.

Brakefield PM, Gates J, Keys D, Kesbeke F, Wijngaarden PJ, Monteiro A, French V, Carroll SB: Development, plasticity and evolution of butterfly eyespot patterns. Nature 1996, 384:236-242.

Beldade P, McMillan WO, Papanicolaou A: Butterfly genomics eclosing. Heredity 2008, 100: 150-157.

Brakefield PM: Butterfly eyespot patterns and how evolutionary tinkering yields diversity. Novartis Foundation Symposia 2007, 284: 90-115.

Brunetti CR, Selegue JE, Monteiro, A, French V, Brakefield PM, Carroll SB: The generation and diversification of butterfly eyespot color patterns. Current Biology2001, 11:1578-1585.

Carroll SB, Grenier JK, Weatherbee SD: *From DNA to Diversity: molecular genetics and the evolution of animal design* Malden, USA: Wiley-Blackwell; 2001.

French V, Brakefield PM: The development of eyespot patterns on butterfly wings: morphogen sources or sink? Development 1992, 116: 103-109.

Hirai N, Tanikawa T, Ishii M: Development, seasonal polyphenism and cold hardiness of the blue pansy, *Junonia orithya orithya* (Lepidoptera, Nymphalidae). Lepidoptera Science 2011, 62: 57-63.

Hiyama A, Iwata M, Otaki JM: Rearing the pale blue *Zizeeria maha* (Lepidoptera, Lycaenidae): Toward the establishment of a lycaenid model system for butterfly physiology and genetics. Entomological Science 2010, 13: 293-302.

Holloway GJ, Brakefield PM, Kofman S, Windig JJ: An artificial diet for butterflies, including *Bicyclus* species, and its effects on development period, weight and wing pattern. The Journal of Research on the Lepidoptera 1991, 30: 121-128.

Joron M, Jiggins CD, Papanicolaou A, McMillan WO: *Heliconous* wing patterns: an evo-devo model for understanding phenotypic diversity. Heredity 2006, 97: 157-167.

Kim J, Irvine KD, Carroll SB: Cell recognition, signal induction, and symmetrical gene activation at the dorsal-ventral boundary of the developing *Drosophila* wing. Cell 1995, 82: 795-802.

Keys DN, Lewis DL, Selegue JE, Pearson BJ, Goodrich LV, Johnson RL, Gates J, Scott MP, Carroll SB: Recruitment of a hedgehog regulatory circuit in butterfly eyespots evolution. Science 1999, 283:532-534.

Lewis DL, DeCamillis MA, Brunetti CR, Halder G, Kassner VA, Selegue JE, Higgs S and Carroll SB: Ectopic gene expression and homeotic transformation in arthropods using recombinant Sindbis viruses. Current Biology1999, 9:1279-1287.

Monteiro AF, Brakefield PM, French V: The evolutionary genetics and developmental basis of wing pattern variation in the butterfly *Bicyclus anynana*. Evolution 1994, 48: 1147-1157.

Nijhout HF: Pattern formation in Lepidoptera: determination of an eyespot. Developmental Biology1980a, 80: 267-274.

Nijhout HF: Ontogeny of the colour pattern on the wings of *Precis coenia* (Lepidoptera: Nymphalidae). Developmental Biology1980b, 81: 275-288.

Nijhout HF: Colour pattern modification by coldshock in Lepidoptera. Journal of Embryology and Experimantal Morphology 1984, 81: 287-305.

Nijhout HF: Cautery-induced colour patterns in *Precis coenia* (Lepidoptera: Nymphalidae). Journal of Embryology and Experimantal Morphology 1985, 86: 191-203.

Nijhout HF: A comprehensive model for colour pattern formation in butterflies. Proceedings of Royal Society B 1990, 239: 81-239.

Nijhout HF: The developmental and evolution of butterfly wing patterns Washington, USA: Smithsonian Institution Press; 1991.

Nijhout HF: Elements of butterfly wing patterns. Journal of Experimental Zoology 2001, 291: 213-225.

Otaki JM: Color pattern modifications of butterfly wings induced by transfusion and oxyanions. Journal of Insect Physiology1998, 44: 1181-1190.

Otaki JM: Physiologically induced color-pattern changes in butterfly wings: mechanistic and evolutionary implications. Journal of Insect Physiology2008, 54:1099-1112.

Otaki JM, Ogasawara T, Yamamoto H: Tungstate-induced color-pattern modifications of butterfly wings are independent of stress response and ecdysteriod effect. Zoological Science 2005, 22: 635-644.

Parchem RJ, Perry MW, Patel NH: Patterns on the insect wing. Current Opinion in Genetics and Development 2007, 17: 300-308.

Weatherbee SD, Nijhout HF, Grunert LW, Halder G, Galant R, Selegue J, Carroll, S: *Ultrabithorax* function in butterfly wings and the evolution of insect wing patterns. Current Biology1999, 9:109-115.

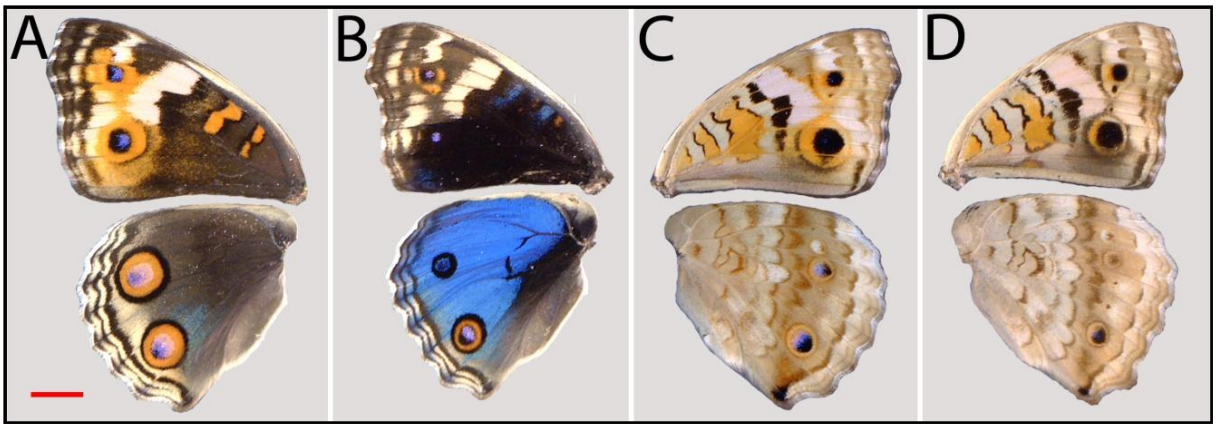

Fig. 6.1. Normal wings of *J. orithya*. (**A**) Dorsal forewing and hindwing of the female. Scale bar, 5.0 mm. This bar is applicable to all the panels in this figure. (**B**) Dorsal forewing and hindwing of the male. (**C**) Ventral forewing and hindwing of the female. (**D**) Ventral forewing and hindwing of the male.

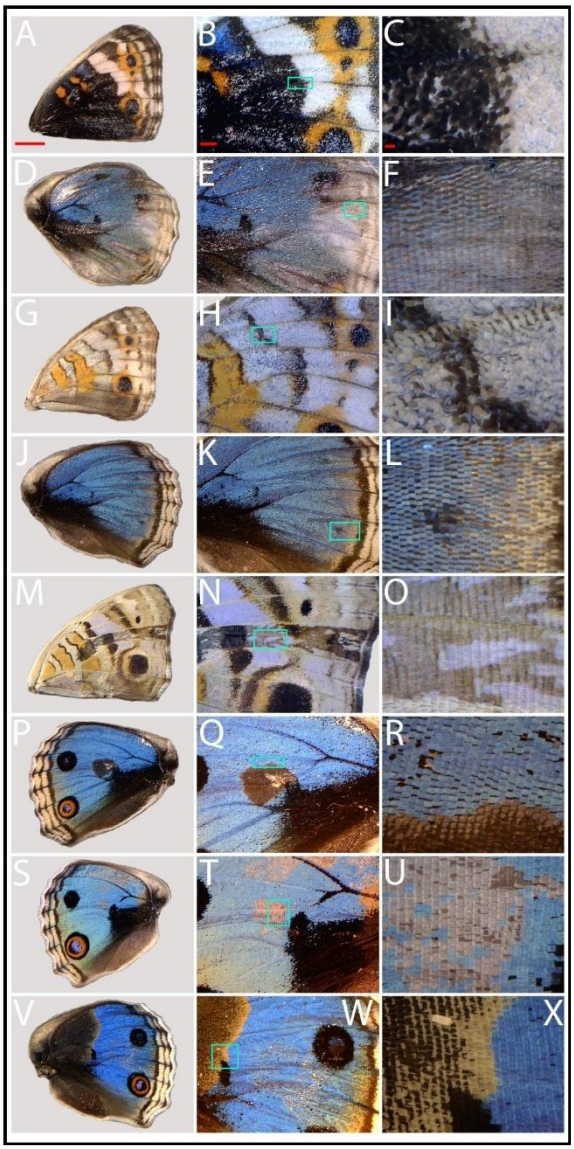

Fig. 6.2. Artificial diet induced color patterns of *J. orithya*. Except, panel P and V, all wings are from larval group fed with artificial diet from fourth instar. P and V are from larval group fed with artificial diet from second instar. (**A**) Diet AD-FYCCSW induced color pattern in dorsal forewing. Scale bar, 5.0 mm and is applicable to all the vertical panels to A. (**B**) is identical to A, only small modified portion is amplified. Boxed region is enlarged in C. Scale bar, 1 mm and is applicable to all the panels vertical to B. (**C**) High magnification identical to B. Scale bar, 0.1 mm and is applicable to all the panels vertical to C. (**D**) AD-DYCCSW induced modified dorsal hind wing. (**E**) is modified portion identical to D. Boxed region is amplified in F. (**F**) is identical to E but magnified. (**G**) Modified ventral forewing with diet AD-DYCCSW. (**H**) Modified portion is amplified, identical to G. (H). Highly magnified picture of H. Boxed region is enlarged in I. (**I**) Identical to H but magnified .(**J**) Modified dorsal hindwing associated with diet AD-FZMWV. (**K**) A small portion of J, is amplified. (L) Highly magnified picture of K. The boxed region is enlarged in L. (**L**) is identical to K and highly magnified. (**M**) AD-ADFZM induced modified ventral forewing. (**N**) is identical to M only a small

portion is amplified. Boxed region is amplified in O. (**O**) is identical to N but highly magnified. (**P**) Modified dorsal hindwing from diet AD-FZMWV. (**Q**) is identical to P, modified portion is amplified. Boxed region is magnified in R. (**R**) is identical to Q, modified portion is highly magnified. (**S**) Modified dorsal hindwing with diet AD-FZM. (**T**) Modified portion in S is amplified. Boxed region is magnified in U. (**U**) Modified portion in T is magnified. (**V**) Modified dorsal hind wing due to diet Insecta F-II. (**W**) Modified portion in V is focused. Boxed region is enlarged in X. (**X**) is identical to W but modified portion is magnified.

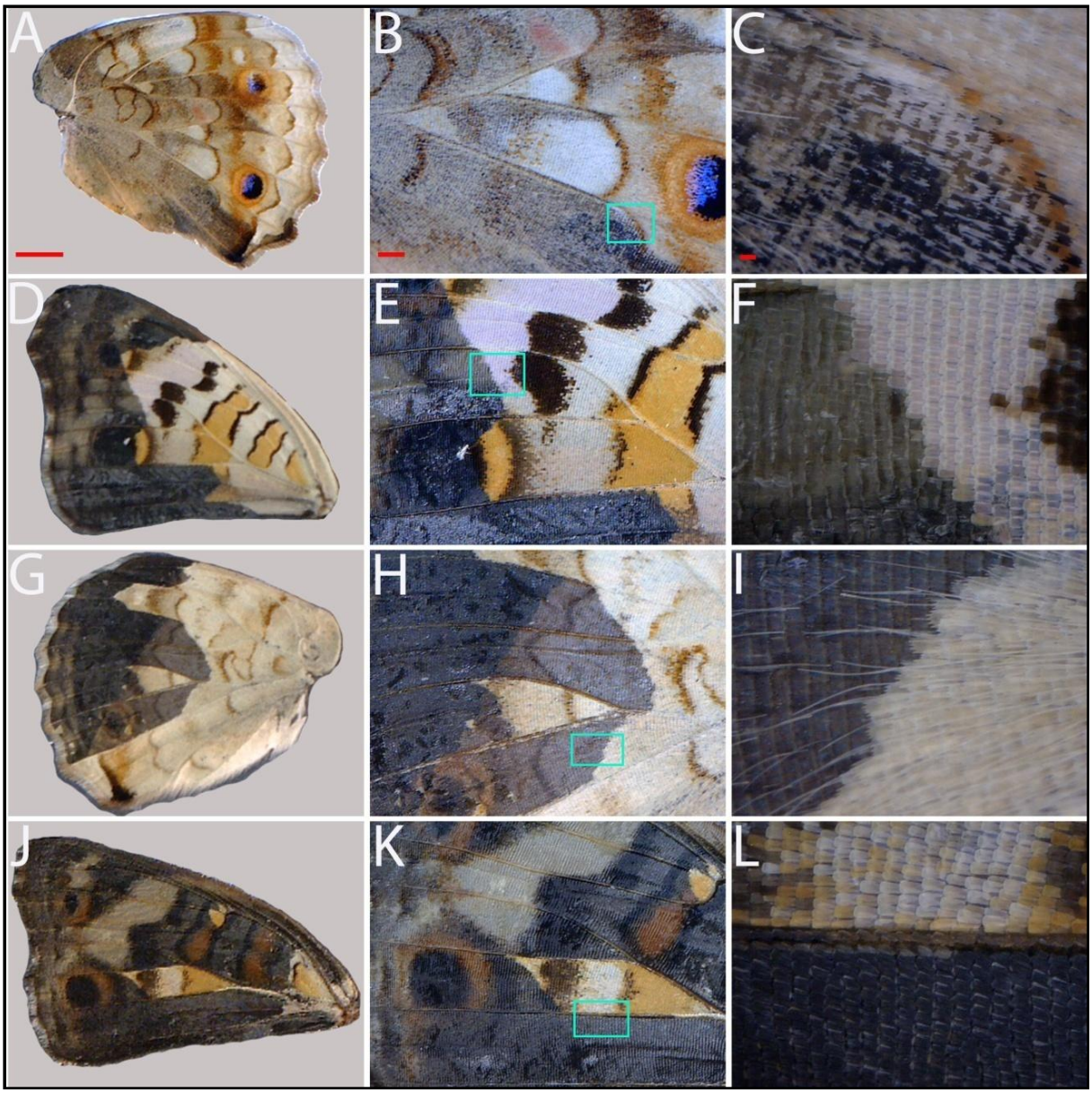

Fig. 6.3. Artificial diet-induced homeotic transformed wings of *J. orithya*. Except A, all larval groups were fed with artificial diet from fourth-instar. A is fed with artificial diet from second-instar. (**A**) Homeotic transformed ventral hind wing due to AD-FZMWV. Scale bar, 5mm and is applicable to all the panels vertical to A. (**B**) is identical to A. Transformed portion is focused. Boxed region is enlarged in C. Scale bar, 1 mm and is applicable to all the panels vertical to B. (**C**) is identical to B but transformed portion is highly magnified. Scale bar, 0.1 mm and is applicable to all the panels vertical to C. (**D**) AD-FZM induced transformed ventral forewing. (**E**) Portion of D is magnified. Boxed region is enlarged in F. (**F**) is identical to E, transformed region is highly magnified. (**G**) AD-FZM induced transformed ventral hindwing. (**H**) is identical to G, only transformed portion is focused. Boxed region is enlarged in I. (**I**) is highly magnified portion of H. (**J**) Homeotic transformed ventral forewing associated with diet AD-FBY. (**K**) is identical to J. Boxed region is enlarged in L. (**L**) highly magnified picture of K.

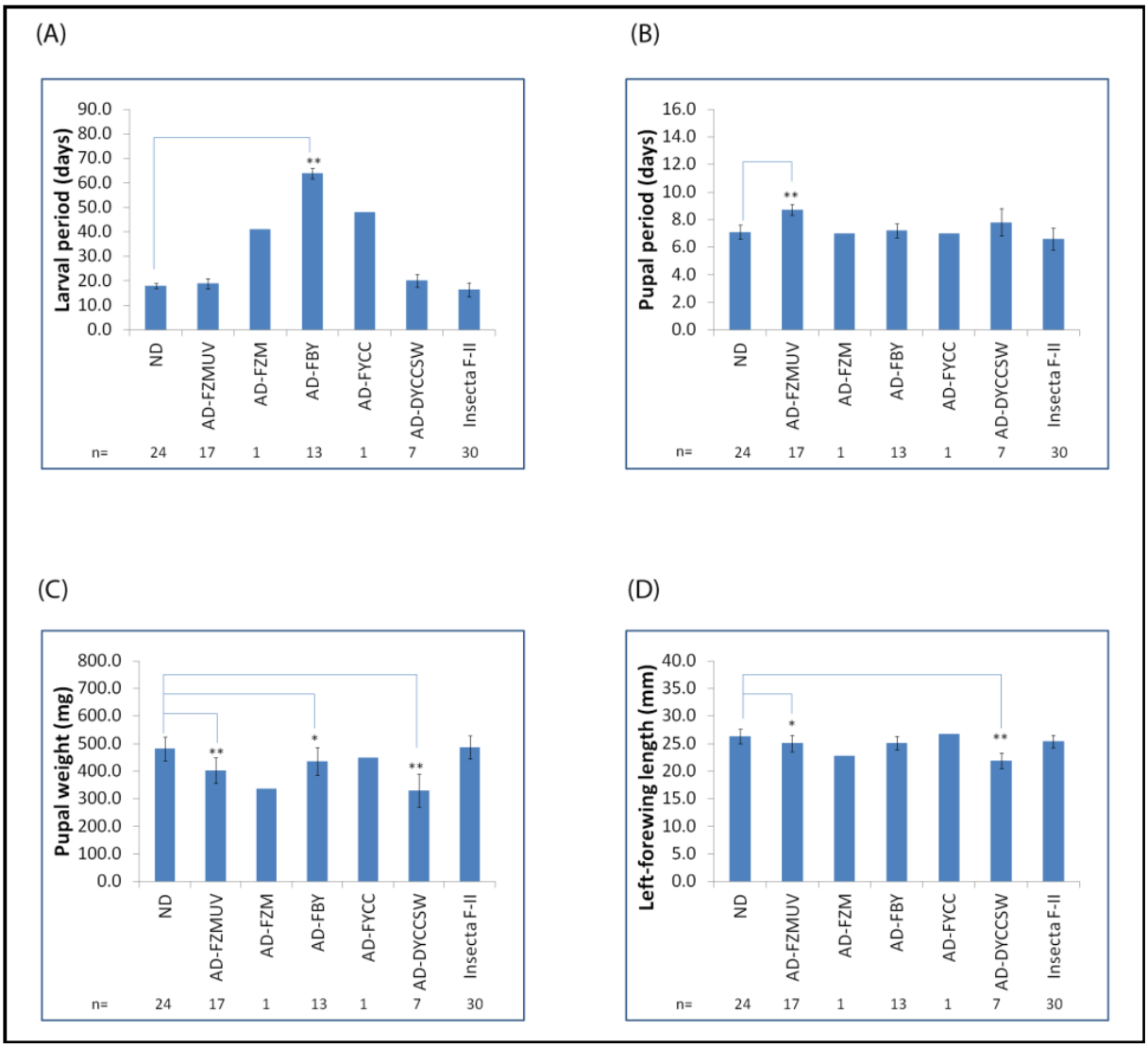

Fig. 6.4. Performance of artificial diets used for rearing *J. orithya* larvae from second instar. (**A**) Larval period. The artificial diet AD-FBY is significantly different than control group (ND). (**B**) Pupal period. The artificial diet AD-FZMUV is significantly different than control group (ND). (**C**) Pupal weight. The artificial diet AD-FZMUV, AD-FBY, and AD-DYCCSW are significantly different than control group (ND). (**D**) Left-forewing length. The artificial diets AD-FZMUV and AD-DYCCSW are significantly different than control group (ND). * $p < 0.01$, ** $p < 0.001$.

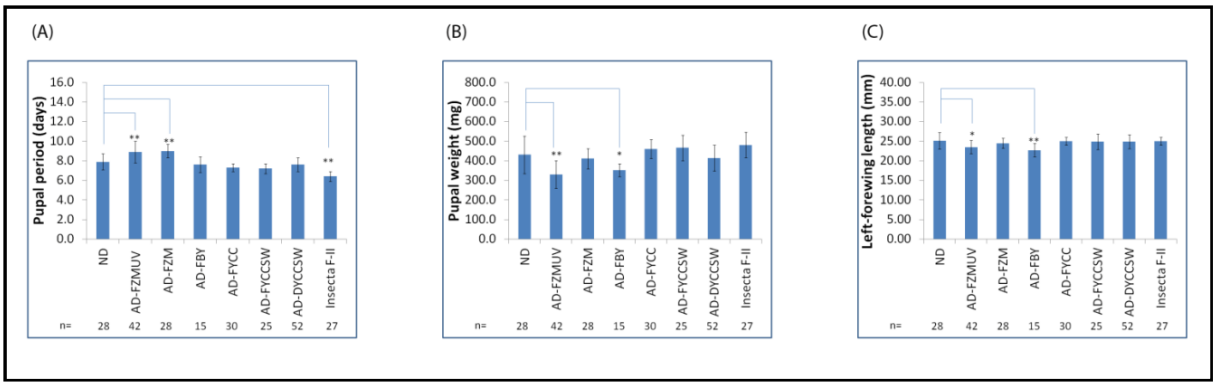

Fig. 6.5. Performance of artificial diets used for rearing *J. orithya* larvae form fourth instar. (**A**) Pupal period. The artificial diet AD-FZMUV, AD-FZM, and Insecta F-II are significantly different than control group (ND). (**B**) Pupal weight. The artificial diet AD-FZMUV and AD-FBY are significantly different than control group (ND). (**C**) Left-forewing length. The artificial diet AD-FZMUV and AD-FBY are significantly different than the control group. * $p < 0.01$, ** $p < 0.001$

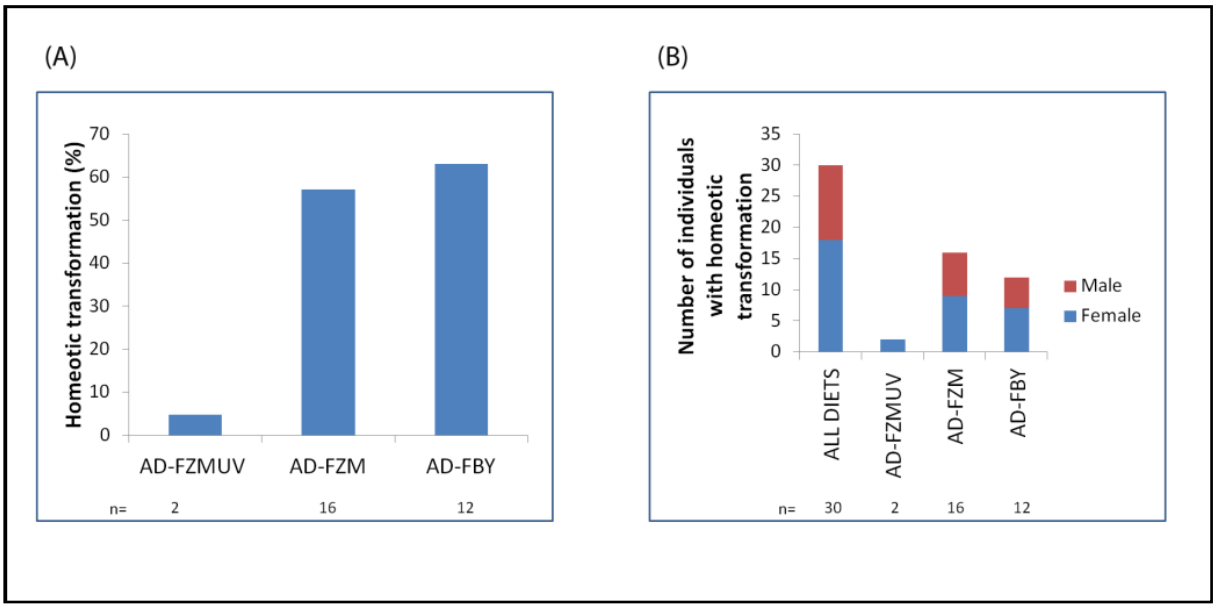

Fig. 6.6. Homeotic transformation associated with artificial diets. (**A**) Homeotic transformation percentage in three different diets. (**B**) The total number of individuals with homeotic transformation and classification according to sex in three different diets.

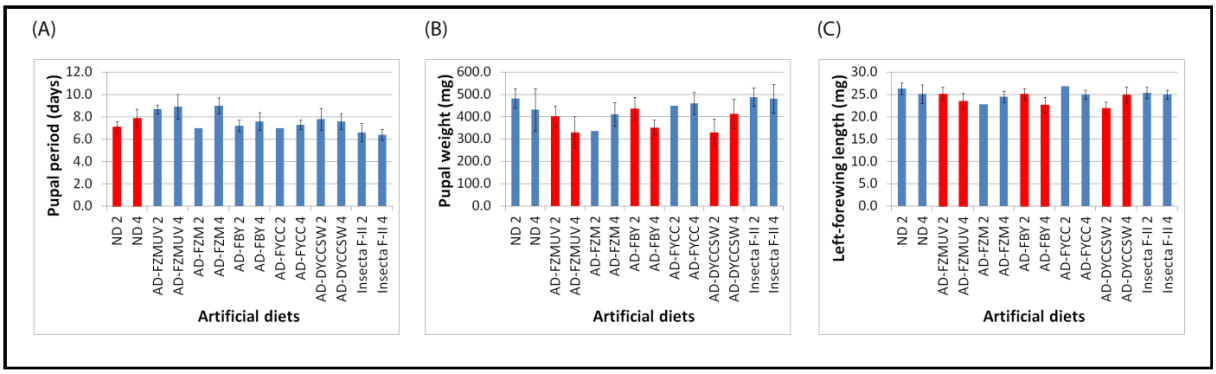

Fig. 6.7. Performance of artificial diets used for *J. orithya* larvae compared between second instar and fourth instar groups. The diets with significant difference are shown in red bars. The numbers after name of the diet stand for second or fourth instar groups. (**A**) Pupal period. No significant difference is seen. (**B**) Pupal weight. Three diets AD-FZMUV, AD-FBY, and AD-DYCCSW are significantly different. (**C**) Left-forewing length. Similarly, three diets AD-FZMUV, AD-FBY, and AD-DYCCSW are significantly different.

Table 6.1. Artificial diets ingredients for *Junonia orithya*.

Group	Ingredient	Weight or Volume AD-FZMWV	Weight or Volume AD-FZM	Weight or Volume AD-FBY	Weight or Volume AD-FYCC	Weight or Volume AD-FYCCSW	Weight or Volume AD-DYCCSW	Weight or Volume Insecta F-II
A	Processed leaves of *Plantago* (Wild harvested)	80 g	80 g	80 g	80 g	80 g	30 g	30 g
B	Insecta F-II (Nihon-Nosan-Kogyo, Japan)	NA	NA	NA	NA	NA	NA	70g
B	Bacteriological agar (Sigma)	2.15 g	2.15 g	2.15 g	2.15 g	2.15 g	14.084 g	NA
B	Choline chloride (Kanto)	0.07 g	0.07 g	0.07 g	0.07 g	0.07 g	0.0825 g	NA
B	Sorbic acid (Kanto)	0.165 g	0.165 g	0.165 g	0.165 g	0.165 g	0.195 g	0.194 g
B	Potassium phosphate, Monobasic (Sigma)	0.145 g	0.145 g	0.145 g	0.145 g	0.145 g	0.171 g	0.17 g
B	Potassium phosphate, Dibasic (Sigma)	0.235 g	0.235 g	0.235 g	0.235 g	0.235 g	0.277 g	NA
B	Distilled water	51 mL	51 mL	51 mL	51 mL	51 mL	298.361 mL	260 mL
C	Sucrose (Kanto)	0.85 g	0.85 g	0.85 g	0.85 g	0.85 g	17.429 g	NA
C	Myo-inositol (Kanto)	0.21 g	0.21 g	0.21 g	0.21 g	0.21 g	0.248 g	NA
C	Streptomycin (Sigma)	0.021 g	0.021 g	0.021 g	0.021 g	0.021 g	0.024 g	0.024 g
C	Gallic acid (Kanto)	0.21 g	0.21 g	0.21 g	0.21 g	0.21 g	0.248 g	0.24 g
C	L-Ascorbic acid (Kanto)	0.415 g	0.415 g	0.415 g	0.415 g	0.415 g	0.490 g	0.492 g
C	Brewers yeast (Asahi, Tokyo, Japan)	NA	NA	0.456g	1.785 g	1.785 g	2.112 g	NA
C	Cholesterol (Kanto)	NA	NA	NA	0.267 g	0.267 g	0.316 g	NA
C	Casein (Nacalai tesque, Kyoto, Japan)	NA	NA	NA	21.698 g	21.698 g	25.669 g	NA
C	Starch (Sigma)	NA	NA	NA	NA	8.929 g	10.563g	NA
C	Wheat germ (Kaneyoshi, Okinawa, Japan)	NA	NA	NA	NA	7.14 g	8.450 g	NA
D	Vitamin complex*	NA	0.0625 g	0.0625 g	0.0625 g	0.0625 g	0.0739 g	NA
E	Linseed oil (Flaxeed oil; Sabo Italia)	0.65 mL	0.65 mL	0.65 mL	0.65 mL	0.65 mL	0.768 mL	NA

*Vitamin complex is made by adding corn starch (Sigma, 122.9 mg) and the following vitamins: D-biotin (Kanto, 0.05 mg), D-pantotenic acid hemicalcium salt (Sigma, 0.5 mg), folic acid (Sigma, 0.05 mg), nicotinamide (Kanto, 0.5mg), phridoxine hydrochloride (Vitamin B_6-HCl, Sigma, 0.25 mg), riboflavin 5'-monophosphate salt dihydrate (FMN-Na, Sigma, 0.25 mg), thiamine hydrochloride (Vitamin B_1-HCl, Kanto, 0.25) and L-carnitine inner salt (Vitamin B_T, Sigma, 0.25 mg). AD-FZM, artificial diet with fresh leaves similar to *Zizeeria maha* diet; AD-FBY, artificial diet with fresh leaves and brewers yeast; AD-FYCC, artificial diet with fresh leaves, yeast, cholesterol and casein; AD-FYCCSW, artificial diet with fresh leaves, yeast, cholesterol, casein, starch and wheat germ; AD-DYCCSW, artificial diet with dried leaves, yeast, cholesterol, casein, starch and wheat germ; Insecta F-II, artificial diet with dried leaves and insect F-II Sigma, Tokyo, Japan; Kanto, Tokyo, Japan.

Table 6.2. Rearing *Junonia orithya* second instar larvae with artificial diets.

Diet	Larvae (n)	Pupae (n)	Adults (n)	Larval mortality (%)	Failure rate (%)	Modification rate (%)	Pupal period (days)	Pupal weight (mg)	Left-forewing length (mm)	Homeotic transformation (%)	Larval period (days)
AD-FZMUV	30	18	17	40.0	5.5	5.8	8.7±0.4	402.2±46.8	25.1±1.5	5.8	18.9±2.1
AD-FZM	30	1	1	96.7	0.0	0.0	7.0	336.6	22.8	0.0	41.0
AD-FBY	30	13	13	56.7	0.0	7.6	7.2± 0.5	435.7±50.7	25.1±1.2	0.0	63.9±2.1
AD-FYCC	30	1	1	96.7	0.0	0.0	7.0	449.7	26.8	0.0	48.0
AD-FYCCSW	30	0	NA	100.0	NA	NA	NA	NA	NA	NA	NA
AD-DYCCSW	30	15	7	50.0	53.3	57.1	7.8±1.0	329.5±60.0	21.9±1.4	0.0	20.1±2.7
Insecta F-II	45	30	30	33.3	0.0	3.3	6.6±0.8	487.6±41.8	25.4±1.2	0.0	16.4±2.9
ND	29	29	24	0.0	17.2	16.6	7.1±0.5	481.3±43.5	26.3±1.3	0.0	17.9±1.0

Table 6.3. Rearing *Junonia orithya* fourth instar larvae with artificial diets.

Diet	Larvae (n)	Pupae (n)	Adults (n)	Larval mortality (%)	Failure rate (%)	Modification rate (%)	Pupal period (days)	Pupal weight (mg)	Left-forewing length (mm)	Homeotic transformation (%)
AD-FZMUV	43	42	42	2.3	0.0	11.9	8.9±1.1	330.1±71.4	23.5±1.7	4.7
AD-FZM	33	33	28	0.0	15.2	71.4	9.0±0.7	410.6±52.5	24.5±1.3	57.0
AD-FBY	37	37	15	0.0	59.5	78.9	7.6±0.8	351.5±32.9	22.7±1.7	63.1
AD-FYCC	31	31	30	0.0	3.2	10.0	7.3±0.4	459.7±48.5	25.0±1.0	0.0
AD-FYCCSW	30	28	25	6.7	10.7	36.0	7.2±0.5	466.0±65.8	24.9±2.0	0.0
AD-DYCCSW	61	60	52	1.6	13.3	19.2	7.6±0.7	413.4±66.0	24.9±1.8	0.0
Insecta F-II	30	30	27	0.0	10.0	3.7	6.4±0.5	481.1±64.8	25.0±1.0	0.0
ND	30	30	28	0.0	6.7	0.0	7.9±0.8	430.8±95.4	25.1±2.1	0.0

Chapter 7

Larval temperature experience determines sensitivity to cold-shock-induced wing color pattern changes in the blue pansy butterfly *Junonia orithya*

7.1. Introduction

Butterfly wing color patterns are highly diverse, and the mechanisms by which this diversity evolved and is achieved during development constitute interesting questions in biology (Nijhout, 1991). Butterfly wing color patterns are delineated based on the so-called nymphalid groundplan, which is a basic blueprint for how elements are positioned against a plain background canvas (Nijhout, 1991, 2001; Otaki, 2009, 2012). Within the framework of the nymphalid groundplan, elements (and also background coloration) are elaborated independently and coordinately, yielding a species-specific color pattern.

To investigate how these elemental elaborations occur, we have been studying the color pattern changes induced by physiological means, such as applications of temperatures and chemicals, including sodium tungstate (Nijhout, 1984; Otaki, 1998, 2008a; Otaki and Yamamoto, 2004; Hiyama et al., 2012), using several nymphalid butterflies, including *Junonia orithya* (Otaki et al., 2005a; Dhungel and Otaki, 2010; Mahdi et al., 2010, 2011) and *J. almana* (Otaki, 2007, 2011), and a few lycaenid butteflies, including *Zizeeria maha* (Otaki et al., 2010). Upon cold-shock or tungstate treatment, many species of butterfly produce unique temperature shock-type (TS-type) modifications in a dose-dependent manner (Nijhout, 1984; Otaki, 1998, 2008a; Otaki and Yamamoto, 2004). Furthermore, one can change not only the position of an element but also its shape and size wing-wide in a species-specific fashion through these physiological means (Nijhout, 1984; Otaki, 1998, 2008a; Otaki and Yamamoto, 2004). Based on these changes and the changes induced by physical damage (Nijhout, 1985; Brakefield and French, 1995; French and Brakefield, 1995; Otaki et al., 2005b; Otaki, 2011), developmental mechanisms and evolutionary mechanisms for color pattern diversification may be deciphered (Hiyama et al., 2012).

Previously, we focused on *J. orithya* to investigate the physiological mechanisms of TS-type color pattern changes (Otaki et al., 2005a; Dhungel and Otaki, 2010; Mahdi et al., 2010, 2011). We demonstrated that the cold-shock-inducing property, which is attributed to cold-shock hormone (CSH), can be transferred via hemolymph (Otaki et al., 2005a; Dhungel and Otaki, 2010; Mahdi et al., 2010, 2011). We also found that the brain-retrocerebral neuroendocrine complex is not responsible for the secretion of CSH, that CSH may be secreted from trachea-associated cells, and that CSH may be related to biogenic amines (Mahdi et al., 2010). On the other hand, many *Junonia* and other nymphalid butterflies, including *J. orithya*, exhibit distinct seasonal polyphenism (McLeod, 1968;

James, 1987; Smith, 1991; Nijhout, 1991, 1994; Nobayashi, 2002; Hirai et al., 2011). In *J. orithya*, the ventral color patterns are different between the summer and fall morphs, although the dorsal patterns are not. More concretely, in the summer morph, the ventral eyespots are relatively large with a clear boundary on a light orange background, whereas in the fall morph, they are relatively small or even dot-like (but without positional changes) on a dark gray background. The fall morph is most likely a dead-leaf mimic widely observed in nymphalid butterflies (Nijhout, 1991). In contrast, the dorsal patterns of this species are sexually dimorphic.

Seasonal polyphenism in *Araschnia levana* and *J. coenia* is regulated by the timing of ecdysteroid release (Koch and Bückmann, 1987; Rountree and Nijhout, 1995a; Nijhout, 1991, 1994). A similar effect of ecdysteroid has also been reported in *Bicyclus anynana* (Koch et al., 1996). In addition to ecdysteroid, summer morph-producing hormone (SMPH) controls seasonal polyphenism in *Polygonia c-aureum* and is likely a peptide secreted by the brain (Endo et al., 1988, 1990; Tanaka et al., 1997). Recently, SMPH activity has also been discovered in other non-polyphenic butterflies (Tanaka et al., 2009). The TS phenotypes are different from the seasonal morph phenotypes, and furthermore, CSH appears to be different from ecdysteroid and SMPH with regard to its physiological characteristics (Otaki et al., 2005a). Nonetheless, seasonal morphs are dependent on environmental temperatures (and also photoperiod). Therefore, there must be a physiological and developmental relationship between the TS phenotype and the seasonal morph phenotypes; however, their possible relationship has not been investigated to date.

In this study, we examined whether color pattern changes in response to cold-shock and tungstate treatments at the pupal stage are dependent on the larval temperature conditions that induce the summer or fall morph. We hypothesized that the larvae that experienced relatively low temperatures develop hardiness against cold shock at the pupal stage, because these larvae may "expect" that the fall or winter season is coming. Without this hardiness, much more TS-type individuals might be expected in the fall. Based on previous reports on the observations and the experimental production of seasonal morphs in *Junonia* (McLeod, 1968; James, 1987; Smith, 1991; Nijhout, 1991, 1994; Rountree and Nijhout, 1995a, b; Nobayashi, 2002; Hirai et al., 2011), we chose two clearly different larval rearing conditions: a high-temperature condition for producing the summer morph and a low-temperature condition for producing the fall morph. We then examined the differences in the color patterns between these larval rearing conditions in response to cold-shock and tungstate treatments at the pupal stage. Tungstate injection to pupae is an established method for producing TS-type modifications in adult wings (Otaki, 1998, 2008a; Otaki and Yamamoto, 2004; Hiyama et al., 2012). However, an effect of tungstate on larvae is not known. We thus fed larvae an artificial diet containing tungstate, in addition to injecting pupae with tungstate, to examine whether this compound causes effects that are similar to those of the low-temperature larval rearing condition. In this paper, we

describe a new physiological phenomenon, cold-shock hardiness, which was induced by rearing larvae under the low-temperature condition but not by feeding them an artificial diet containing tungstate.

7.2. Materials and methods

7.2.1. Butterflies

Female adults of the blue pansy butterfly *Junonia orithya* (Linnaeus, 1758) (Nymphalidae, Lepidoptera) were routinely caught on Okinawa-jima Island or Ishigaki-jima Island in the Ryukyu Archipelago, Japan, during the summer. Eggs were later collected from these females. Alternatively, larvae were field-caught on these islands during the summer. Unless otherwise specified, the larvae were fed their natural host plant *Plantago major* (wild harvested at the Nishihara campus of the University of the Ryukyus). The eclosed adults were immediately frozen so as not to damage their wings.

This species of butterfly is sexually dimorphic. Typically, a hindwing of the males is blue with one large and one small eyespot on the dorsal side. A hindwing of the females is either blue or orange with two eyespots of similar sizes on the dorsal side. However, the ventral side of the fore- and hindwings is not sexually dimorphic. Seasonal changes are observed only on the ventral side of the hindwings.

7.2.2. Cold-shock and tungstate treatments

The pupae were cold-shocked at −2°C for 2 days within 3-6 hours of pupation. An aqueous solution of sodium tungstate (1.0 M; Sigma, St. Louis, MO, USA) was prepared, and 1.0 μL of this solution was injected into the abdomen of pupae using a microsyringe (Ito, Fuji, Shizuoka, Japan) within 3-6 hours of pupation.

7.2.3. High- temperature condition and experimental treatments

Larvae were reared at ambient temperature with a long-day photoperiod (27°C, 16L-8D; defined as the high-temperature condition) under which summer-morph adults (wet-season form) were frequently produced (see Results for the statistical analysis). Under the high-temperature condition, 95 larvae were fed their natural host plant. Of the 90 pupae that developed, 59 pupae were subjected to no subsequent treatment, resulting in 52 adults (24 males and 28 females), and 15 pupae were cold-shocked, resulting in 11 adults (7 males and 4 females). An aqueous solution of sodium tungstate was injected into the abdomen of 16 pupae, resulting in 11 adults (4 males and 7 females).

7.2.4. Low temperature condition and experimental treatments

In the low-temperature condition, larvae were kept in an incubator at 16°C in complete darkness (0L-24D) from the third-instar stage, which frequently produced fall-morph adults (dry-season form) (see Results for the statistical analysis). A total of 160 larvae were reared under the low-temperature condition. Once pupated, the insects were returned to the summer-morph condition to eliminate differences in the rearing conditions at the pupal stage. Out of 76 pupae, 25 pupae were subjected to no subsequent treatment, resulting in 19 adults (11 males and 8 females), and 30 pupae were cold-shocked, resulting in 24 adults (8 males and 16 females). In addition, 21 pupae were injected with the tungstate solution, resulting in 21 adults (11 males and 10 females).

7.2.5. Rearing larvae with an artificial diet

Similar to Hirai et al. (2011), we employed Insecta F-II (Nihon Nosan Kogyo, Yokohama, Japan), a mixture of nutrients required for many lepidopteran and coleopteran insect species but lacking a vital ingredient, the specific host plant, as a major ingredient of our artificial diet. Dried leaves of the natural host plant *P. major* and some preservatives (see below) were added to the original nutrient mixture, as follows: processed dried leaves of *P. major* (wild harvested at the Nishihara campus of the University of the Ryukyus) [30 g]; Insecta F-II mixture (Nihon Nosan Kogyo) [70 g]; sorbic acid (Kanto Chemical, Tokyo, Japan) [0.194 g]; potassium phosphate, monobasic (Sigma) [0.17 g]; distilled water [260 mL]; streptomycin (Sigma) [0.024 g]; gallic acid (Kanto) [0.24 g]; and L-ascorbic acid (Kanto) [0.492 g]. We followed Hiyama et al. (2010) for the preparation of this artificial diet. When necessary, sodium tungstate solution (1.0 M) was placed on the surface of the artificial diet so that it spontaneously seeped into the diet (13 μL solution per 1 g diet), which was fed to larvae from the fourth-instar stage. We housed six larvae in each plastic container (21 cm W × 15 cm D × 6 cm H), and the artificial diet was replaced daily until the larvae pupated.

We fed 30 larvae our standard artificial diet (which did not contain tungstate) under the high-temperature condition without any subsequent treatment, producing 27 pupae and 27 adults (14 males and 13 females). We fed 90 larvae the diet containing tungstate under the high temperature condition. Out of 82 pupae, 25 pupae were subjected to no subsequent treatment, resulting in 13 adults (9 males and 4 females), and 29 pupae were exposed to cold shock, resulting in 21 adults (14 males and 7 females). In addition, 28 pupae were subjected to the tungstate injection, resulting in 20 adults (11 males and 9 females).

7.2.6. Color pattern evaluation

We evaluated the degrees of global TS-type color pattern modifications using the induction rate (*IR*), modification-inducing index (*MI*), and the survival rate (*SR*), as defined in Otaki (1998, 2007) and Otaki and Yamamoto (2004). The *IR* is a percentage of the modified individuals among the successfully eclosed individuals given a particular treatment as larvae or pupae; however, the *IR* does not consider the degree of modification in an individual. Therefore, we established modification degrees (*MD*), from *MD0* (no modification) to *MD3* (extreme modification), according to Otaki et al. (2005) (Figure 1). An *MD* score was assigned to each individual after visual inspection. The *MI* was defined for a particular treatment mode as the percentage of the average degree of modification relative to the extreme degree of modification, i.e., *MD3*. Thus, the *MI* can be expressed as *MI* (%) = [*m*/3] × 100, where *m* is the mean *MD* score for a particular treatment mode. The survival rate (*SR*) was used to evaluate the possible harmful effect of a given treatment and to confirm that the pupae we used for a given treatment were sufficiently healthy. The *SR* is the percentage of successfully eclosed individuals among the treated pupae.

To evaluate the color patterns of the seasonal morphs, we examined the number of eyespots on the ventral hindwings, according to Hirai et al. (2011), with a large number of eyespots being indicative of the summer morph (Figure 2). Similar to the *MD* score and the *MI*, we defined the eyespot score on a scale of *ES0* (no eyespot) to *ES2* (two eyespots), and the eyespot-score index for the summer morph, *EI(S)*, as *EI(S)* (%) = [*m*/2] × 100, where *m* is the mean *EI(S)* score for a particular treatment mode. We defined the eyespot-score index for the fall morph, *EI(F)*, as *EI(F)* = 100 – *EI(S)*. The dorsal hindwing coloration of the females was also examined, whereby blue coloration is an indication of the fall morph (Hirai et al., 2011) (Figure 1). We calculated the blue rate (*BR*, %) among all the females examined as an indication of the fall morph. The *BR* was defined as *BR* (%) = [*b*/*n*] × 100, where *b* is the number of blue females and *n* is the total number of females for a particular treatment mode. It should be noted that, due to genetic differences, fluctuation in the responses among individuals in producing seasonal morphs was unavoidable (Rountree and Nijhout, 1995b).

7.2.7. Statistics

We analyzed the data using the χ^2 test and Fisher's exact test using IBM SPSS Statistics 19 (2010) and JSTAT 13.0 (2012) software. The results were reported with the χ^2, *df*, and *p*-values that were obtained after applying the Yates correction. In performing the χ^2 test, we checked if there were any cells with an expected count of less than 5 in a contingency table. If an expected count was less than 5, Fisher's exact test was performed and a two-sided *p*-value was reported.

7.3. Results

7.3.1. Cold-shock hardiness against the TS-type modifications

We first confirmed that the high-temperature condition for larval rearing without any subsequent treatment did not induce TS-type modifications (*IR* = 0 and *MI* = 0) (*n* = 52); similarly, no TS-type modifications were induced by the low-temperature larval rearing condition without any subsequent treatment (*n* = 19) (Table 1, Figure 3A, B). To confirm the previously reported results regarding the TS-type color pattern changes in *J. orithya* (Otaki et al., 2005a; Mahdi et al., 2010), larvae reared under the high-temperature condition were cold-shocked (*n* = 11) or injected with sodium tungstate (*n* =11). Both treatments induced TS-type color pattern changes, with reasonably high *IR* (100% for cold shock and 91% for tungstate) and *MI* (64% for cold shock and 36% for tungstate) values (Table 1, Figure 3A, B).

To examine the effect of low-temperature exposure at the larval stage, larvae were reared under the low-temperature condition, and when they had pupated, the pupae were treated with cold shock (*n* = 24) or tungstate (*n* = 21). For both treatments, the *IR* (33% for cold shock and 19% for tungstate) and *MI* (25% for cold shock and 6% for tungstate) values were considerably lower than those attained using the high-temperature larval rearing condition with subsequent cold-shock or tungstate treatment as pupae, as described above (Table 1, Figure 3A, B). A χ^2 test was performed on the number of modified and non-modified individuals obtained, based on the null hypothesis that low-temperature has no effect on color pattern changes, and we obtained $\chi^2 = 11$, $df = 1$, and $p = 0.009$ for the cold shock treatment and $\chi^2 = 12$, $df = 1$, and $p = 0.004$ for the tungstate treatment. These results demonstrated that the low-temperature condition at the larval stage induced hardiness against the TS-type color pattern changes imposed by cold-shock or tungstate treatment at the pupal stage.

We then tested whether tungstate exposure during the larval stage induces a similar hardiness. We first confirmed that no TS-type color pattern modification was observed (*IR* = 0% and *MI* = 0%) (*n* = 27) when the larvae were fed our standard artificial diet (which did not contain tungstate) under the high-temperature condition without any subsequent treatment (Table 1, Figure 3A, B). Adding tungstate to the diet without any subsequent treatment also did not produce any modification (*IR* = 0% and *MI* = 0%) (*n* = 13) (Table 1, Figure 3A, B).

When larvae that were fed the tungstate-containing diet were exposed to cold shock (*n* = 21) or subjected to tungstate injection (*n* = 20) at the pupal stage, we observed reasonably high *IR* (100% for cold shock and 85% for tungstate) and *MI* (78% for cold shock and 35% for tungstate) values (Table 1, Figure 3A, B). These values were similar to those obtained using the high-temperature condition. Hardiness against the TS-type changes imposed by the cold-shock and tungstate treatments at the

pupal stage was not induced by consuming tungstate at the larval stage in comparison to the high-temperature condition with subsequent cold-shock (p = 1.00; Fisher's exact test) or tungstate treatment (p = 1.00; Fisher's exact test).

The modification degrees of the eclosed modified adults (excluding the non-modified adults) showed that cold shock produced *MD1*, *MD2*, and *MD3*, whereas tungstate treatment produced *MD1* and *MD2*, irrespective of the temperature and dietary conditions (Table 1, Figure 3B), suggesting that there may be a threshold-like response to cold-shock and tungstate treatments with regard to survivorship and wing color pattern modification.

7.3.2. Cold-shock hardiness against the fall-morph eyespot trait

The *EI(F)* (Table 2, Figure 3C) and *BR* (Table 3, Figure 3D) values associated with the different rearing conditions followed a similar trend. We first confirmed that the high-temperature condition without any subsequent treatment produced low *EI(F)* and *BR* values, indicating that this condition mostly produced the summer morph. When the larvae were reared under the low-temperature condition without subsequent cold-shock or tungstate treatment, the *EI(F)* and *BR* values of the resulting adults were larger than the values of those raised under the high-temperature condition (Tables 2 and 3 and Figure 3C, D), indicating that the low-temperature condition induced the fall-morph traits. We combined the data for *ES0* and *ES1* as opposed to *ES2* and performed a χ^2 test based on the null hypothesis that the high- and low-temperature larval rearing conditions did not produce any difference in these two groups. We obtained values of χ^2 = 7.15, df = 1, and p = 0.0075, indicating that two rearing conditions have significantly different effects in terms of the ventral eyespot patterns. In contrast, the number of brown and blue female adults resulting from the larvae reared under the two rearing conditions was not statistically different by Fisher's exact test (p = 0.66).

When larvae reared under the high temperature condition were treated with cold shock at the pupal stage, the *EI(F)* and *BR* values increased to 100% (Tables 2 and 3, Figure 3C, D), indicating that the fall-morph traits, in addition to TS-type changes, were induced by cold shock. We detected no difference between the males and females in their eyespot scores or *EI(F)* values (data not shown). Interestingly, when the larvae reared under the low-temperature condition were treated with cold shock or tungstate at the pupal stage, the *EI(F)* and *BR* values increased in comparison to those of non-treated individuals reared under the same low-temperature condition. However, these *EI(F)* and *BR* values obtained from the larvae reared under the low-temperature condition with subsequent cold-shock or tungstate treatment were still lower than those of larvae reared under the high-temperature condition with subsequent cold-shock or tungstate treatment (except the *EI(F)* value for tungstate treatment) (Tables 2 and 3, Figure 3C, D). After combining the *ES1* and *ES2* data as opposed to the *ES0* data, we performed Fisher's exact test based on the null hypothesis that no hardiness to cold

shock or tungstate treatment developed under the low-temperature rearing condition in comparison to the high-temperature rearing condition. We obtained $p = 0.015$ for cold shock and $p = 0.029$ for tungstate treatment. These results demonstrated that hardiness against the fall-morph eyespot traits developing in response to cold-shock and tungstate treatments at the pupal stage was induced by the low-temperature condition at the larval stage.

When the artificial diet containing tungstate was fed to larvae with subsequent cold-shock or tungstate treatment at the pupal stage, the *EI(F)* and *BR* values of the adults were largely similar to those resulting from larvae fed the natural diet under the high-temperature condition (Tables 2 and 3, Figure 3C, D). Using the same morphological categories as above, it appeared that no hardiness developed when tungstate was fed to larvae in comparison to the larvae raised under the high-temperature condition with subsequent cold shock ($p = 0.53$) or with the tungstate treatment ($p = 1.00$), according to Fisher's exact test.

Although the dorsal blue coloration in females is considered an indication of the fall morph (Hirai et al., 2011), no statistically significant difference was observed in the number of blue and brown females between individuals raised under the high- and low-temperature conditions with subsequent cold shock ($p = 0.12$) or tungstate treatment ($p = 0.64$), according to Fisher's exact test. When larvae fed tungstate were subsequently subjected to cold shock or tungstate injection, we detected no statistically significant difference in terms of the dorsal coloration of the females' wings, in comparison to the results obtained using the high-temperature larval rearing condition with subsequent cold shock ($p = 1.00$) or the tungstate treatment ($p = 0.60$) at the pupal stage, according to Fisher's exact test.

7.4. Discussion

In this study, we demonstrated that a low-temperature condition at the larval stage induced physiological hardiness against cold-shock induction of TS-type color pattern changes at the pupal stage. This hardiness is biologically relevant in that it contributes to the consistent production of a normal color pattern in adult wings throughout the year, except for the seasonal morphs. Feeding tungstate to the larvae did not induce the development of hardiness against cold-shock-induced TS-type color pattern changes, suggesting that tungstate cannot substitute for low temperature in the development of hardiness. This finding is understandable when considering that, in pupae, tungstate acts as a molecular mimic of CSH, a hormone that is produced during the pupal stage, and is unlikely to function in the larval stage (Otaki, 1998, 2008a; Otaki et al., 2005a; Mahdi et al., 2010). However, to efficiently obtain specific seasonal morphs, we manipulated not only the temperature but also the light cycle. Although the induction stimulus at the pupal stage was the temperature, we cannot

exclude the possibility that the light cycle at the larval stage may affect the cold-shock hardiness of pupae. The possible effect of light on cold-shock hardiness may be resolved in the future.

The cold-shock hardiness considered in this paper is restricted to color patterns and, thus, is different from the general cold hardiness widely reported in insects (Zachariassen, 1985; Bale, 1993; Duman, 2001; Sinclair and Chown, 2005). However, there must be some similarities between these processes. Hirai et al. (2011) investigated the cold hardiness of *J. orithya*, based on the mean supercooling points of fourth-instar larvae, pupae, and adults, in which two rearing conditions, a high-temperature, long-photoperiod condition (25°C, 16L-8D) and a low-temperature, short-photoperiod condition (20°C, 12L-12D), were employed. No statistically significant differences in the supercooling points between individuals subjected to these two conditions were observed for any of the developmental stages. However, the individuals used in the study of Hirai et al. (2011) were habituated to the short-day 15°C condition for at least 3 days prior to the determination of their supercooling points, and this habituation process might have nullified the differences.

We showed for the first time that cold-shock and tungstate treatments at the pupal stage induce fall-morph traits in addition to TS-type changes. Hirai et al. (2011) also proposed that the blue coloration of the dorsal wing surface is an indication of the fall morph. However, the blue coloration, as represented by the *BR* value, was not significantly different between the summer morph (reared under the high-temperature condition) and fall morph (reared under the low-temperature condition) in our study. The blue coloration in females may also be regulated genetically because it has been reported that the blue form can be obtained during the summer (Nobayashi, 2002).

Interestingly, hardiness against the cold-shock induction of the fall-morph color pattern (i.e., a small number of eyespots on the ventral hindwings) was also observed when the larvae were reared under the low-temperature condition, even though this tendency was not apparent when tungstate treatment was employed at the pupal stage. The fact that hardiness developed for both the TS-type and fall-morph eyespot traits suggest that these two types of color pattern changes are related to each other developmentally and physiologically. It is somewhat surprising to find that hardiness developed against the induction of the fall-morph trait because the fall morph is one of the normal phenotypes. Indeed, this hardiness may explain why intermediate phenotypes between the summer and fall morphs are rare in nymphalid butterflies in nature (McLeod, 1968; Nijhout, 1991).

Although the mechanism of hardiness against cold-shock-induced TS-type changes remains unclear, one possibility is that the endocrine secretion of the cold-shock hormone (CSH) may not be triggered in individuals that are already habituated to low or cold temperatures. However, the individuals reared under the low-temperature condition also developed hardiness to tungstate treatment at the pupal stage. Considering that tungstate is thought to act via the same molecular

pathway as CSH (Otaki, 1998, 2008a), a more likely explanation is that, even if the endocrine secretion of CSH is triggered, cells in the pupal wing tissues are no longer receptive to CSH after a low-temperature experience at the larval stage.

The TS-type modifications are phenocopies that can be physiologically produced in a laboratory and occur in the field as aberrant forms, although the TS-type changes are within a range of phenotypic plasticity of wing color patterns (Hiyama et al., 2012). The TS-type modifications do not seem to have biological roles in signaling for mate choice and in survival (Otaki, 2008b). That is, the TS-type changes are neutral or non-functional in term of successful mating and the survival of an individual. In some species of butterflies, however, it appears that such plastic phenotypes are genetically fixed as a wing color pattern of a given species (Otaki, 2008b, Otaki *et al*., 2010; Hiyama *et al*., 2012). The neutral or non-functional developmental changes in the TS-type modification pathways can thus contribute to evolutionary changes of wing color patterns in butterflies. Similar cases have been found in other organisms (Gilbert, 2012). The present study suggests that there may be a molecular pathway for resistance against these physiological and evolutionary changes. By the same token, this pathway may have a role in the development and evolution of species-specific butterfly wing color patterns.

In contrast, the fall morph most likely has an important role in survival because it appears to be a dead-leaf mimic that would function in the fall. The hardiness detected in this study is also relevant for survival because an individual that has experience at low temperatures can adapt to future cold temperatures more efficiently. Because both the TS-type and fall-morph color patterns can be induced by temperature shock, our results suggest that the molecular pathways for these two color patterns may influence each other or utilize some of the same molecules. For example, heat-shock proteins may play a role in both pathways.

In this study, we employed an artificial diet to administer a chemical to the larvae. Artificial diets have been developed for *J. coenia* (Bowers, 1984), *Bicyclus anynana* (Holloway et al., 1991), and *Z. maha* (Hiyama et al., 2010); indeed, the establishment of an artificial diet widens the experimental utility of a given insect species. The present study demonstrated that feeding an artificial diet is a useful technique to chemically modify the physiological state of larvae.

7.5. Conclusions

We demonstrated that larvae that experienced low temperatures develop cold-shock hardiness against the induction of TS-type color pattern changes at the pupal stage. The observed hardiness at the pupal stage was not induced by consuming tungstate at the larval stage. We also showed that cold-shock and tungstate treatments induce not only TS-type traits but also fall-morph traits and that the cold-shock

induction of fall-morph traits was repressed by a low-temperature condition at the larval stage. Apparently, the cold-shock-induced or tungstate-induced color pattern modification pathway has a physiological relationship with the fall-morph-inducing pathway.

7.6. References

Brakefield PM, French V: Eyespot development on butterfly wings: the epidermal response to damage. Developmental Biology1995, 168: 98-111.

Bale JS: Classes of Insect Cold Hardiness. Functional Ecology 1993, 7: 751-753.

Dhungel B, Otaki JM: Local pharmacological effects of tungstate on the color-pattern determination of butterfly wings: a possible relationship between the eyespot and parafocal element. Zoological Science2010, 26: 758-74.

Duman JG: Antifreeze and ice nucleator proteins in terrestrial arthropods. Annual Review of Physiology 2001, 63: 327-357.

Endo K, Masaki T, Kumagai K: Neuroendocrine regulation of the development of seasonal morphs in the Asian comma butterfly, *Polygonia c-aureum* L.: Difference in activity of summer-morph-producing hormone from brain extracts of the long-day and short-day pupae. Zoological Science1998, 5: 145-152.

Endo K, Fujimoto Y, Masaki T, Kumagai K: Stage-dependent changes in the activity of the prothoracicotropic hormone (PTTH) in the brain of the Asian comma butterfly, *Polygonia c-aureum* L. Zoological Science1990, 7: 697-704.

French V, Brakefield PM: Eyespot development on butterfly wings: the focal signal. Developmental Biology1995, 168: 112-123.

Gilbert, S. F., 2012. Ecological developmental biology: environmental signals for normal animal development. Evol. Dev. 14, 20-28.

Hirai N, Tanikawa T, Ishii M: Development, seasonal polyphenism and cold hardiness of the blue pansy, *Junonia orithya orithya* (Lepidoptera, Nymphalidae). Lepidoptera Science 2011, 62: 57-63.

Hiyama A, Iwata M, Otaki JM: Rearing the pale blue *Zizeeria maha* (Lepidoptera, Lycaenidae): Toward the establishment of a lycaenid model system for butterfly physiology and genetics. Entomological Science 2010, 13: 293-302.

Hiyama A, Taira W, Otaki JM: Color-pattern evolution in response to environmental stress in butterflies. Frontiers in Genetics 2012, 3: 15.

James DG: Effects of temperature and photoperiod on the development of *Vanessa kershawi McCoy* and *Junonia villida Godart* (Lepidoptera: Nymphalidae). Australian Journal of Entomolology 1987, 26: 289-292.

Koch PB, Bückmann D: Hormonal control of seasonal morphs by the timing of ecdysteroid release in *Araschnia levana L*. (Nymphalidae: Lepidoptera). Journal of Insect Physiology1987, 33: 823-829.

Koch PB, Brakefield, PM, Kesbeke F: Ecdysteroids control eyespot size and wing color pattern in the polyphonic butterfly *Bicyclus anynana* (Lepidoptera: Satyridae). Journal of Insect Physiology1996, 42: 223-230.

Mahdi SHA, Gima S, Tomita Y, Yamasaki H, Otaki JM: Physiological characterization of the cold-shock-induced humoral factor for wing color-pattern changes in butterflies. Journal of Insect Physiology2010, 56: 1022-1031.

Mahdi SHA, Yamasaki H, Otaki JM: Heat-shock-induced color-pattern changes of the blue pansy butterfly *Junonia orithya*: Physiological and evolutionary implications. Journal of Thermal Biology2011, 36: 312-321.

McLeod L: Controlled environmental experiments with Precis octavia cram. The Journal of the Research on the Lepidoptera 1968, 7: 1-18.

Neven LG, Duman JG, Beals JM, Castellino FJ: Overwintering adaptations of the stag bettle, Ceruchus piceus: removal of ice nucleators in the winter to promote supercooling. Journal of Comparative Physiology B 1986, 156: 707-716.

Nijhout, HF: Color pattern modification by cold shock in Lepidoptera. Journal of Embryology and Experimental Morphology 1984, 81: 287-305.

Nijhout HF: Cautery-induced colour patterns in *Precis coenia* (Lepidoptera: Nymphalidae). Journal of Embryology and Experimental Morphology 1985, 86: 191-203.

Nijhout HF: The developmental and evolution of butterfly wing patterns Washington, USA: Smithsonian Institution Press; 1991.

Nijhout HF: Insect hormones Princeton, USA: Princeton University Press; 1994.

Nijhout HF: Elements of butterfly wing patterns. Journal of Experimental Zoology 2001, 291: 213-225.

Nobayashi S: Color pattern variation of the blue pansy butterfly in Okinawa Island. Chouken Field 2002, 17(11): 18-20. (In Japanese)

Olsen TM, Duman JG: Maintenance of the supercooled state in overwintering pyrochroid beetle larvae, Dendroides Canadensis: role of hemolymph ice nucleators and antifreeze proteins. Journal of Comparative Physiology B 1997, 167: 105-113.

Otaki JM: Color-pattern modifications of butterfly wings induced by transfusion and oxyanions. Journal of Insect Physiology1998, 44: 1181-1190.

Otaki JM: Stress-induced color-pattern modifications and evolution of the Painted Lady butterflies *Vanessa cardui* and *Vanessa kershawi*. Zoological Science 2007a, 24: 811-819.

Otaki JM: Reversed type of color-pattern modifications of butterfly wings: A physiological mechanism of wing-wide color-pattern determination. Journal of Insect Physiology2007, 53: 526-537.

Otaki JM: Phenotypic plasticity of wing color patterns revealed by temperature and chemical applications in a nymphalid butterfly *Vanessa indica*. Journal of Thermal Biology 2008a, 33: 128-139.

Otaki JM: Physiological side-effect model for diversification of non-functional or neutral traits: a possible evolutionary history of *Vanessa* butterflies (Lepidoptera, Nymphalidae). Transactions of the Lepidopterological Society of Japan 2008b, 59: 87-102.

Otaki JM: Physiologically induced color-pattern changes in butterfly wings: mechanistic and evolutionary implications. Journal of Insect Physiology2008c, 54:1099-1112.

Otaki JM: Colour-pattern analysis of parafocal elements in butterfly wings. Entomological Science 2009, 12: 74-83.

Otaki JM: Artificially induced changes of butterfly wing colour patterns: dynamic signal interactions in eyespot development. Scientific Reports 2011a, 1:111.

Otaki JM: Colour pattern analysis of nymphalid butterfly wings: Revision of the nymphalid groundplan. Zoological Science2012, 29: 568-576.

Otaki JM, Yamamoto H: Color-pattern modifications and speciation in lycaenid butterflies. Transactions of the Lepidopterological Society of Japan 2003, 54: 197-205.

Otaki JM, Yamamoto H: Species-specific color-pattern modifications of butterfly wings. Development, Growth and Differentiation 2004a, 46: 1-14.

Otaki JM, Yamamoto H: Color-pattern modifications and speciation in butterflies of the genus *Vanessa* and its related genera *Cynthia* and *Bassaris*. Zoological Science 2004b, 21: 967-976.

Otaki JM, Ogasawara T, Yamamoto H: Tungstate-induced color-pattern modifications of butterfly wings are independent of stress response and ecdysteriod effect. Zoological Science2005a, 22: 635-644.

Otaki JM, Ogasawara T, Yamamoto H: Morphological comparison of pupal wing cuticle patterns in butterflies. Zoological Science2005b, 22: 21-34.

Otaki JM, Kimura Y, Yamamoto H: Molecular phylogeny and color-pattern evolution of *Vanessa* butterflies (Lepidoptera, Nymphalidae). Transactions of the Lepidopterological Society of Japan 2006, 57: 359-370.

Otaki JM, Hiyama A, Iwata M, Kudo T: Phenotypic plasticity in the range-margin population of the lycaenid butterfly *Zizeeria maha*. BMC Evolutionary Biology 2010, 10: 252.

Pfister, TD, Storey KB: Responses of protein phosphatases and cAMP-dependent protein kinase in a freeze-avoiding insect, Epiblema scudderiana. Archives of Insect Biochemistry 2006, 62: 43-54.

Rountree DB, Nijhout HF: Hormonal control of a seasonal polyphenism in *Precis coenia* (Lepidoptera: Nymphalidae). Journal of Insect Physiology1995a, 41: 987-992.

Rountree DB, Nijhout HF: Genetic control of a seasonal morph in *Precis coenia* (Lepidoptera: Nymphalidae). Journal of Insect Physiology1995b 41, 1141-1145.

Smith, K. C., 1991. The effects of temperature and daylength on the rosa polyphenism in the buckeye butterfly, *Precis coenia* (Lepidoptera: Nymphalidae). The Journal of the Research on the Lepidoptera 1991, 30: 225-236.

Sinclair BJ, Chown SL: Climatic variability and hemispheric differences in insect cold tolerance: support from Sothern Africa. Functional Ecology 2005, 19: 214-221.

Tanaka D, Sakurama T, Mitsumasu, K, Yamanaka A, Endo K: Separation of bombyxin from a neuropeptide of Bombyx mori showing summer-morph-producing hormone (SMPH) activity in

the Asian comma butterfly, *Polygonia c-aureum L*. Journal of Insect Physiology1997, 43: 197-201.

Tanaka A, Inoue M, Endo K, Kitazawa C, Yamanaka A: Presence of a cerebral factor showing summer-morph-producing hormone activity in the brain of the seasonal non-polyphenic butterflies *Vanessa cardui*, *Vanessa indica* and *Nymphalis xanthomelas japonica* (Lepidoptera: Nymphalidae). Journal of Insect Science 2009, 16: 125-130.

Zachariassen KE: Physiology of cold tolerance in insects. Physiological Reviews 1985, 65: 799-832.

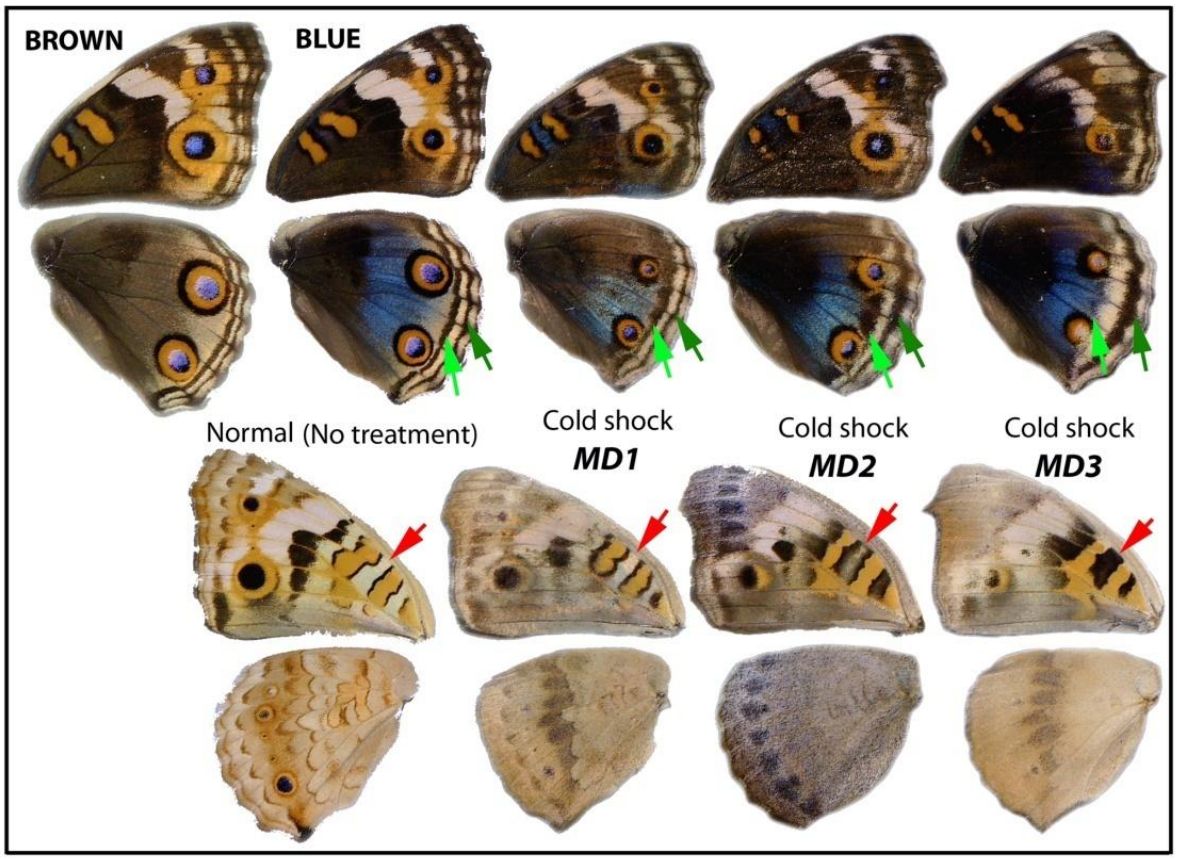

Fig. 7.1. Dorsal (top) and ventral (bottom) wing color patterns of *J. orithya* females reared under the high-temperature condition. Normal brown and blue wings are shown on the left side of the figure, and modified wings (*MD1*, *MD2*, and *MD3*) are shown on the right side. The light green and dark green arrows indicate the dislocation of parafocal elements and the submarginal line, respectively, toward the wing base in the dorsal hindwings in response to cold shock. The red arrows indicate the disappearance of the white gaps in response to cold shock in the ventral forewings.

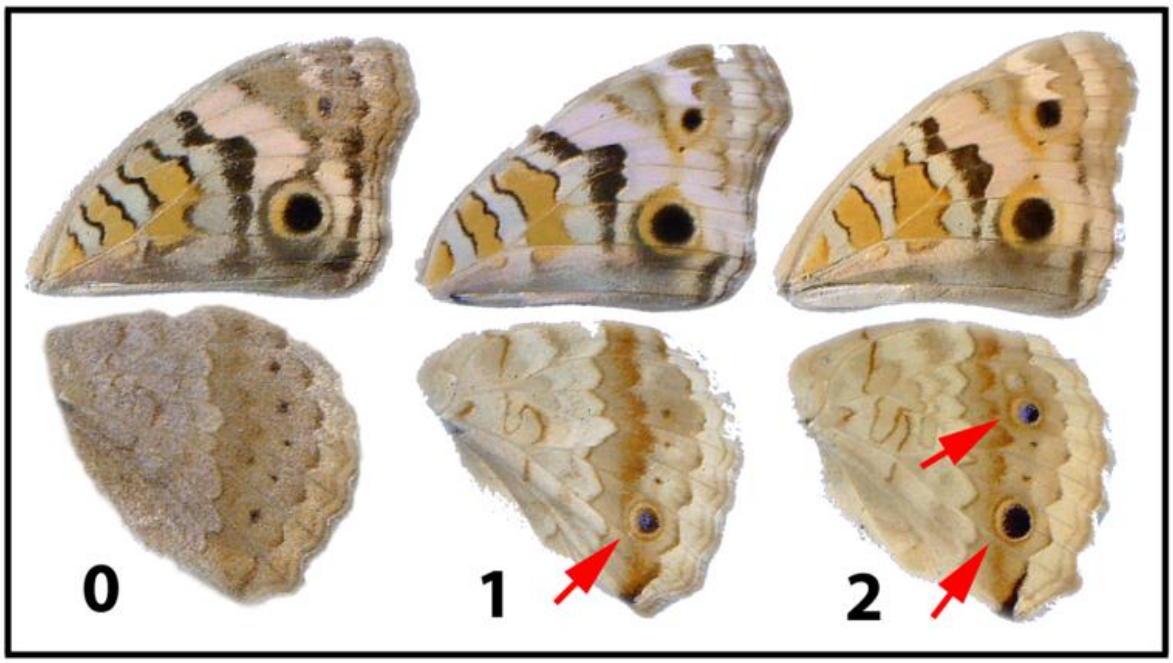

Fig. 7.2. Number of eyespots (red arrows) on *J. orithya* ventral hindwings. Shown from the left to the right are female wings that have no eyespot (0), one eyespot (1), and two eyespots (2). Note that there is no sexual dimorphism on the ventral side of the wings.

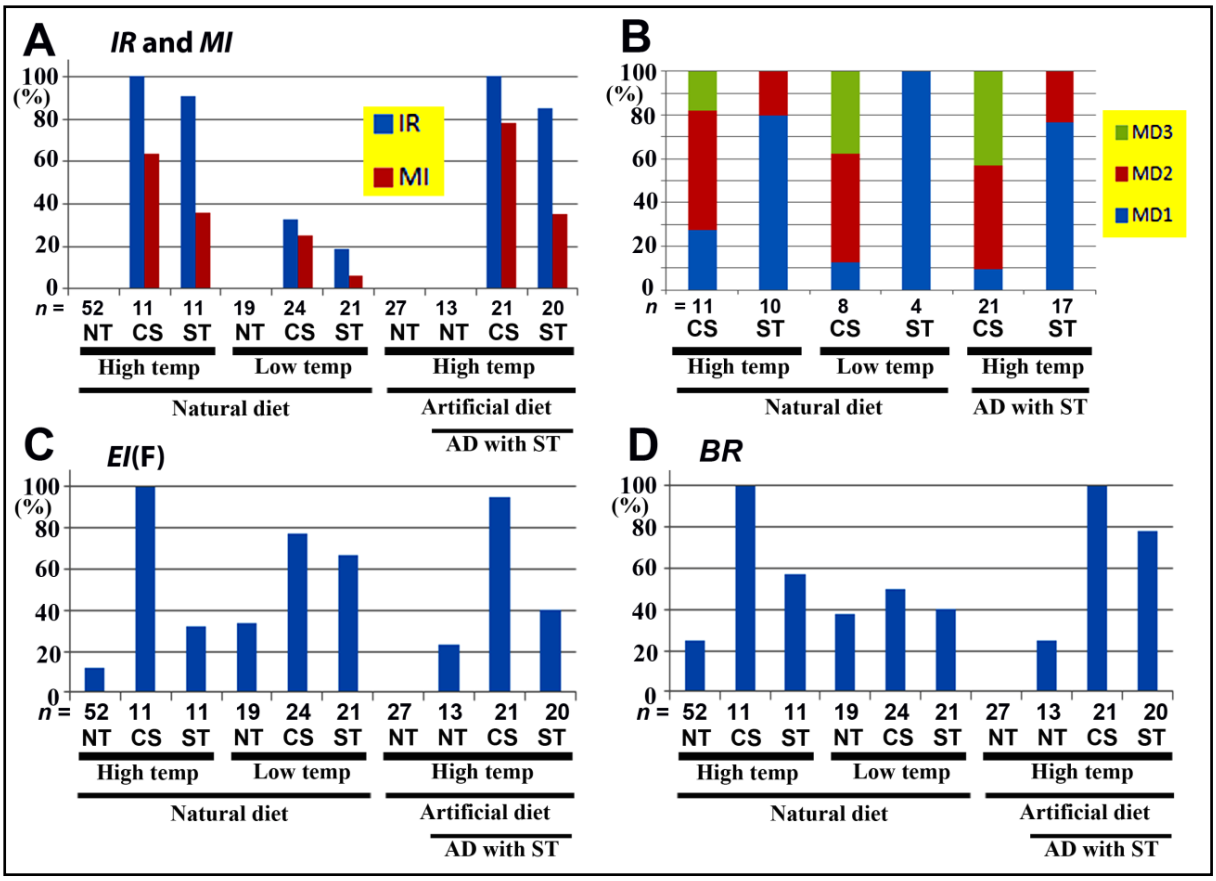

Fig. 7.3. Evaluation scores for the color pattern changes in *J. orithya* reared under different conditions and treatments. *IR*, induction rate; *MI*, modification-inducing index; *EI(F)*, eyespot-score index for the fall morph; *BR*, blue rate; NT, no treatment; CS, cold shock; ST, sodium tungstate; and AD, artificial diet. (**A**) *IR* (blue bar) and *MI* (red bar). Here, *n* indicates the total number of eclosed adults in each treatment group. (**B**) Proportions of *MD1*, *MD2*, and *MD3* wings among the successfully eclosed individuals. Here, *n* indicates the total number of modified individuals in each treatment group. (**C**) *EI(F)*. (**D**) *BR*.

Chapter 8

General Discussion

8.1 Molecular basis of wing color-pattern formation

Local ectopic gene expression via the genetic manipulation techniques was used in butterfly wing color pattern formation study. A new foreign gene delivery system was developed using baculovirus followed by anti-gp64 antibody injection to provide immunity against baculovirus infection. The success of the delivery system was verified with a reporter gene GFP expression on the wings of a butterfly. Gene expression studies have shown a number of genes in the prospective eyespot region (Carroll *et al*., 1994; Brakefield *et al*., 1996; Keys *et al*., 1999; Weatherbee *et al*., 1999; Brunetti *et al*., 2001; Reed *et al*., 2004; Monteiro *et al*., 2006; Saenko *et al*., 2011). The candidate gene functions can be studied with this tool.

With the recently developed baculovirus tool, we ectopically expressed one of the candidate genes in eyespot formation, *Dll*, whose function has been implicated in eyespot formation. But *Dll* expression was not able to induce any ectopic eyespot when infected with baculovirus construct with *Dll* and *GFP*. Some color pattern modification with minor spots and few elongated structures were observed but no major eyespot-like structures were induced. *Dll* might be responsible but not the sufficient gene for eyespot development. As a similar kind of modifications were also found with another candidate gene *in*.

The expression pattern of the genes in the prospective eyespot region during morphogenesis is different in two species butterfly *B. anynana* and *J. coenia*. *Antp* expression is found exclusively at the eyespot organizer in case of *B. anynana* but not in *J. coenia* (Saenko *et al*., 2011) Although, *J. orithya* is very close to *J. coenia* and assumed that gene expression pattern is similar between *J. orithya* and *J. coenia*. But, it might be possible that *Dll* in *J. orithya* has nothing to do with the eyespot organizers. In *J. orithya*, different genes might be responsible for eyespot organizer and no eyespot was induced with the *Dll* gene. The eyespot in different butterfly could have different gene expression patterns.

A series of genes *Distal-less*, *engrailed*, *spalt*, *wingless*, *cubitus interruptus*, *patched*, *hedgehog*, *decapentaplegic* have been associated with eyespot development. The molecular nature of putative morphogens from the prospective focus is also not characterized. Wingless and TGF-β are believed to be the putative morphogens secreted from a prospective focus and might determine eyespot rings and fate determination of other cells during morphogenesis (Carroll *et al*., 1994, 2001; Brakefield *et al*., 1996; Brunetti *et al*., 2001; Monteiro *et al*., 2006).

However, candidate genes in eyespot development as well as in wing color patterning can be studied with this baculovirus tool originally developed in *J. orithya* but can also be used for other butterflies and insects. This functional analysis tool will help bridging the gap between gene expression data and their direct involvement in pattern formation.

Ultimately, we will understand how these genes of developmental pathway interact with pigment biosynthesis pathway and lead to vast diversity seen in butterfly wing pattern in response to various environments. The findings from surgical experiments, gene expression studies, gene function studies, pigment synthesis, and the molecular nature of the morphogens should be integrated for better understanding the mechanism of eyespot development and pattern formation.

8.2. Cellular basis of wing color-pattern formation

Three nymphalid butterflies species *J. orithya*, *V. cardui*, and *D. chrysippus* were used for studying the underlying mechanism of tissue size determination during morphogenesis by counting and measuring all the scales in a wing compartment that represents the whole wing. As expected the overall size increase is contributed primarily by cell proliferation (an increase of the number of cells), and to lesser extents, by cell growth or cell differentiation (an increase of cell size). Initially, the group of cells is homogenous and undifferentiated until the cells receive the signals that determine their fate. The putative morphogen signal is a ploidy signal that determines cell size, scale size and most likely scale coloration and scale shape. We also speculate that the coloration of scales might have co-evolved with size adjustment of scale cells and overall wing structure.

However, the molecular nature of the putative morphogen is not known. TGF-β ligands (Monteiro *et al*., 2006), Hedgehog (Keys *et al*., 1999), and Wingless or Wnt (Monteiro *et al*., 2006; Martin *et al*., 2012) are some proposed morphogens that might determine fate of the developing cells.

In the future, population ecology, combined with developmental biology techniques and endocrinology will shed more light on the underlying mechanism of tissue-size determination.

8.3. Molecular basis of morphological variation

Different eyespots have different expression patterns of genes, but their actual contribution in phenotypic variation is not fully understood. More specifically, the actual gene contributing the eyespot morphology variation is not known. However, variation in *Dll* has been linked in individual variation in terms of eyespot size in *B.anynana* (Beldade *et al*., 2002).

In this thesis, to study the molecular basis of morphological variation, we chose *J. orithya* for our study. Three different types of *Dll* variants were observed in *J. orithya*. DNA polymorphism in *Dll* has been associated with eyespot size variation in *B. anynana* (Beldade *et al*., 2002). *Dll* sequence

variation was compared with phenotype but no clear relation could be established. Without knowing the function of *Dll* in butterfly wing color-pattern formation it is difficult to determine whether *Dll* is responsible for eyespot variation. At this point, the possible role of other candidate genes *decapentaplegic* (Carroll *et al*., 1994), *engrailed* (Keys *et al*., 1999; Brunetti *et al*., 2001), *spalt* (Brunetti *et al*., 2001), and *Ultrabithorax* (Weatherbee *et al*., 1999) also cannot be neglected.

8.4. TS-type modification and seasonal polyphenism

Butterfly wings are vulnerable to cold shock and tungstate treatment and produce a specific type of color pattern modification known as TS-type (Nijhout, 1984; Otaki and Yamamoto, 2004; Otaki, 2005, 2008; Dhungel and Otaki, 2010; Mahdi *et al*., 2010, 2011; Hiyama *et al*., 2012) which is different from general stress change or seasonal polyphenism (McLeod, 1968; James, 1987; Smith, 1991; Nijhout, 1991, 1994; Hirai *et al*., 2011). Depending upon the rearing temperature (and also photeperiod) of the earlier stage of larvae, the adult morphology can be different. At low rearing temperature, the butterfly will mostly be in the fall-morphology and vice versa (Hirai *et al*., 2011)

Previously, in *J. orithya* it was shown that cold shock and tungstate treatment produce TS-type modification (Otaki *et al*., 2005; Dhungel and Otaki, 2010; Mahdi *et al*., 2010, 2011), but they also produced fall-morphology traits. But rearing at low temperature, the resistance is built and they are immune to cold shock or tungstate treatment and the changes is minimum compared to organism raised at normal or higher temperature. The resistance in this thesis is termed as cold-shock hardiness.

We propose that cold shock-induced or tungstate-induced color-pattern modification pathway (or TS-type modification) has a link with the fall-morph inducing pathway. The TS-type pattern changes are observed in seasonal polyphenism in *Chilades pandava* and *Zizeeria maha* (Otaki, 2008a). This provides further evidence that these two pathways for TS-type modification and seasonal morph are physiologically related.

Both TS-type modification and seasonal morph are cases of phenotypic plasticity. They might or might not have a significant function. For development purpose they are important cases for studying the interconnection among hormone titer, genes for development and pigment synthesis. These plastic phenotypes can be sorted out by nature and play an important role in pattern evolution as well.

8.5. Study tools for butterfly wing color-pattern formation

Methodologically, this thesis includes four different tools used for butterfly wing color pattern study, namely genetic (baculovirus) tool, pharmacological (tungstate) tool, temperature (cold-shock) conditions, and artificial diet. Any modified color pattern produced with these tools might have developmental or evolutionary implications.

In this thesis, we showed the successful introduction of foreign genes with the help of baculovirus tool. Other virus had been used for this purpose but with minimum success; we chose baculovirus, a natural virus of butterfly, for infection. Furthermore, the double injection of baculovirus followed by antibody injection is a novel technique used in this thesis.

Tungstate and cold-shock are already established tools in the wing color pattern study. They induce characteristic TS-type modifications (Nijhout, 1984; Otaki and Yamamoto, 2004; Otaki *et al*., 2005, 2008; Dhungel and Otaki, 2010; Mahdi *et al*., 2010, 2011; Hiyama *et al*., 2012). But in this thesis, with these two tools, tungstate and cold-shock, we studied resistance against TS-type modification and fall morph, termed as cold-shock hardiness in *J. orithya*. Artificial diets have been reported for other butterfly but not from *J. orithya*. This thesis showed the use of artificial diet in the wing color pattern study. Use of artificial diet can increase a chance that a particular butterfly species could be used for experimental purpose. Together, tungstate, cold-shock and artificial diet were used in the study and the findings implicate that TS type modification pathway and seasonal polyphenism pathway might share a similar physiological relationship.

In the future, the baculovirus, tungstate, cold-shock, and artificial diet, if used wisely, can generate a vast amount of information on wing color pattern formation and evolution. This thesis did not only addressed the development of widely studied element (eyespot development), but also addressed other important wing color-pattern studies such as genotype-phenotype relation, seasonal polyphenism, TS-type color pattern modification, cold-shock hardiness and overall color pattern development in the whole wing.

8.6. Integrative model for wing color-pattern development and modification

During morphogenesis, the wing tissue size is determined by the number of constituent cells. At this point, cells are proliferating and relatively small. The number of cells at this point determines the number of rows that are formed later. This proliferation process is immediately followed by cell enlargement in a position-dependent manner, governed by the morphogenic signals that induce polyploidy. The morphogenic signal might be long range signals that cover a large wing area that could be explained by a ball rolling on a plane proposed by Otaki (2012). TGF-β ligands (Monteiro *et al*., 2006), Hedgehog (Keys *et al*., 1999), and Wingless or Wnt (Monteiro *et al*., 2006; Martin *et al*., 2012) are some of the proposed morphogenic molecules. The polyploidy signal is released from organizing center or prospective focus, whose identity is determined at the late larval stage. It is believed that the expression of *Dll* and wing veins determines the prospective focus but our result was not consistent with that. Not only the *Dll* but also expression of other genes such as *sal, eng, Antp* might be equally important. However, the sizes of the eyespot might depend on the expression of the particular variants of *Dll*. The cell size change most likely takes place before row arrangement and

contributes to a small increase of wing size. This is the process of fate determination and differentiation. At this point, size, color, and shape are determined together. Furthermore, the TS-type modification could be described with the heterochronic uncoupling model. TS-type modification is produced when there is an alteration in the normal way of wing color pattern development such as delaying of the signaling step with respect to reception step (Otaki, 2008). The cold-shock hardiness might be due to no production of putative cold shock hormone (CSH) or cells are already immune to CSH due to low temperature rearing conditions. However, the seasonal polyphenism might be regulated by ecdysteroid or summer-morph-producing hormone (SMPH). Then, scale cells are arranged most likely from both ends of a compartment. Gaps of rows are accommodated by row branching patterns. Finally, the adult wing with color pattern is produced. Final color-patterns might have behavioral or ecological functions such as mimicry, camouflage, mate selection or species recognition but some color-patterns might not have any significant function and might be produced in response to environmental stress as seen in *Vanessa indica*, *Vanessa cardui* and *Zizeeria maha* (Hiyama *et al., 2011)*. These non functional color-patterns can be considered as extreme cases of phenotypic plasticity, and when genetically assimilated in a population, they can play a vital role in butterfly wing pattern evolution.

8.7. References

Beldade P, Brakefield PM, Long AD: Contribution of *Distal-less* to quantitative variation in butterfly eyespots. Nature 2002, 315-318.

Brakefield PM, Gates J, Keys D, Kesbeke F, Wijngaarden PJ, Monteiro A, French V, Carroll SB: Development, plasticity and evolution of butterfly eyespot patterns. Nature 1996, 384:236-242.

Brunetti CR, Selegue JE, Monteiro, A, French V, Brakefield PM, Carroll SB: The generation and diversification of butterfly eyespot color patterns. Current Biology 2001, 11:1578-1585.

Carroll SB, Gates J, Keys DN, Paddock SW, Panganiban GE, Selegue JE, Williams JA: Pattern formation and eyespots determination in butterfly wings. Science 1994, 265:109-114.

Dhungel B, Otaki JM: Local pharmacological effects of tungstate on the color-pattern determination of butterfly wings: a possible relationship between the eyespot and parafocal element. Zoological Science 2010, 26: 758-74.

Hirai N, Tanikawa T, Ishii M: Development, seasonal polyphenism and cold hardiness of the blue pansy, *Junonia orithya orithya* (Lepidoptera, Nymphalidae). Lepidoptera Science 2011, 62: 57-63.

Hiyama A, Taira W, Otaki JM: Color-pattern evolution in response to environmental stress in butterflies. Frontiers in Genetics 2012, 3: 15.

James DG: Effects of temperature and photoperiod on the development of *Vanessa kershawi McCoy* and *Junonia villida Godart* (Lepidoptera: Nymphalidae). Journal of the Australian Entomological Society 1987, 26: 289-292.

Keys DN, Lewis DL, Selegue JE, Pearson BJ, Goodrich LV, Johnson RL, Gates J, Scott MP, Carroll SB: Recruitment of a hedgehog regulatory circuit in butterfly eyespots evolution. Science 1999, 283:532-534.

Mahdi SHA, Gima S, Tomita Y, Yamasaki H, Otaki JM: Physiological characterization of the cold-shock-induced humoral factor for wing color-pattern changes in butterflies. Journal of Insect Physiology 2010, 56: 1022-1031.

Mahdi SHA, Yamasaki H, Otaki JM: Heat-shock-induced color-pattern changes of the blue pansy butterfly *Junonia orithya*: Physiological and evolutionary implications. Journal Thermal Biology 2011, 36: 312-321.

Martin A, Papa R, Nadeau NJ, Hill RI, Counterman BA, Halder G, Jiggins CD, Kronforst MR, Long AD, McMillan WO, Reed RD: Diversification of complex butterfly wing patterns by repeated regulatory evolution of a *Wnt* ligand. Proceedings of the National Academy of Science USA 2012, 109: 12632-12637.

McLeod L: Controlled environmental experiments with *Precis octavia cram*. Journal of the Research on the Lepidoptera 1968, 7: 1-18.

Monteiro A, Glaser G, Stockslager S, Glansdrops N, Ramos D: Comparative insights into questions of lepidopteran wing pattern homology. BMC Developmental Biology 2006, 6:52.

Nijhout, HF: Color pattern modification by cold shock in Lepidoptera. Journal of Embryology and Experimental Morphology 1984, 81: 287-305.

Nijhout HF: *The developmental and evolution of butterfly wing patterns* Washington, USA: Smithsonian Institution Press; 1991.

Nijhout HF: *Insect hormones* Princeton, USA: Princeton University Press; 1994.

Otaki JM: Colour pattern analysis of nymphalid butterfly wings: Revision of the nymphalid groundplan. Zoological Science 2012, 29: 568-576.

Otaki JM: Phenotypic plasticity of wing color patterns revealed by temperature and chemical applications in a nymphalid butterfly *Vanessa indica*. Journal of Thermal Biology 2008a, 33: 128-139.

Otaki JM: Physiological side-effect model for diversification of non-functional or neutral traits: a possible evolutionary history of *Vanessa* butterflies (Lepidoptera, Nymphalidae). Transactions of the Lepidopterological Society of Japan 2008b, 59: 87-102.

Otaki JM: Physiologically induced color-pattern changes in butterfly wings: mechanistic and evolutionary implications. Journal of Insect Physiology 2008c, 54: 1099–1112.

Otaki JM, Yamamoto H: Species-specific color-pattern modifications of butterfly wings. Development, Growth and Differentiation 2004a, 46: 1-14.

Otaki JM, Yamamoto H: Color-pattern modifications and speciation in butterflies of the genus *Vanessa* and its related genera *Cynthia* and *Bassaris*. Zoological Science 2004b, 21: 967-976.

Otaki JM, Ogasawara T, Yamamoto H: Tungstate-induced color-pattern modifications of butterfly wings are independent of stress response and ecdysteriod effect. Zoological Science 2005a, 22: 635-644.

Otaki JM, Ogasawara T, Yamamoto H: Morphological comparison of pupal wing cuticle patterns in butterflies. Zoological Science 2005b, 22: 21-34.

Reed RD, Serfas MS: Butterfly wing pattern evolution is associated with changes in a *Notch/Distal-less* temporal pattern formation process. Current Biology 2004, 14:1159-1166.

Saenko SV, Marialva MS, Beldade P: Involvement of the conserved Hox gene *Antennapedia* in the development and evolution of a novel trait. Evo Devo 2011, 2:9.

Smith KC: The effects of temperature and daylength on the rosa polyphenism in the buckeye butterfly, *Precis coenia* (Lepidoptera: Nymphalidae). The Journal of Research on the Lepidoptera 1991, 30: 225-236.

Weatherbee SD, Nijhout HF, Grunert LW, Halder G, Galant R, Selegue J, Carroll, S: *Ultrabithorax* function in butterfly wings and the evolution of insect wing patterns. Current Biology 1999, 9:109-115.